MODAL ANALYSIS OF CONTINUOUS STRUCTURAL SYSTEM

WITH TAPERED CANTILEVERED MEMBERS

A Thesis

by

YOON MO KIM

Submitted to the Office of Graduate Studies of
Texas A&M University
in partial fulfillment of the requirements for the degree of

MASTER OF SCIENCE

December 2011

Major Subject: Civil Engineering

Modal Analysis of Continuous Structural System

with Tapered Cantilevered Members

MODAL ANALYSIS OF CONTINUOUS STRUCTURAL SYSTEM WITH TAPERED CANTILEVERED MEMBERS

A Thesis

by

YOON MO KIM

Submitted to the Office of Graduate Studies of
Texas A&M University
in partial fulfillment of the requirements for the degree of

MASTER OF SCIENCE

Approved by:

Chair of Committee,	John B. Mander
Committee Members,	Stefan Hurlebaus
	Reza Langari
	Monique Head
Head of Department,	John Niedzwecki

December 2011

Major Subject: Civil Engineering

ABSTRACT

Modal Analysis of Continuous Structural System with Tapered Cantilevered Members.

(December 2011)

Yoon Mo Kim, B.S., Myong-ji University, Yong-in, Republic of Korea

Chair of Advisory Committee: Dr. John B. Mander

Analytical Model of Traffic Signal Structures (TSS) is developed based on a continuous system method to observe dynamic characteristics of the structures. Conventional and basic continuous system method can show the approximate dynamic characteristics of the TSS, but the discretized continuous analytical model is proposed to get more accurate and realistic results of the TSS. In addition, the discretized continuous model can alternatively analyze the effect of the tapered cross-sectional members which are real model of TSS. For the verification of the analytical model, the dynamic characteristics of the numerical solutions by modal analysis in ABAQUS and the results of experimental measurements are provided. Compared with the numerical solutions and the experimental results, the analytical solution for each member shows its considerable accuracy. In addition, it will be also able to accurately express the effects of the linearly tapered cross-sectional member with more discretized continuous structural system. Moreover, the discretized analytical model of the TSS has the usability to observe the effects of boundary flexibility.

DEDICATION

To my family

ACKNOWLEDGMENTS

I would like to express my appreciation to Dr. John B. Mander and Dr. Stefan Hurlebaus for technical guidance and great interest during the research period. In the period, I could have overcome all of difficulties with your great advice and continuous interest. I also thank a committee member, Dr. Reza Langari for your interest of my research. In addition, I also would like to thank all of my friends, especially Teasun You and Kyle Wieghaus. Finally, I really thank my lovely wife, Tze-Chi Chen, and my family in my country for your great support.

TABLE OF CONTENTS

Page

Page

Page

Page

LIST OF FIGURES

Page

Page

Page

LIST OF TABLES

Page

Page

1. INTRODUCTION

1.1. Problem Statement

Traffic signal structures, as part of the basic infrastructure of modern society, are located throughout United States for controlling of traffic flow. They are exposed to various excitation effects like ambient natural wind, vehicle induced gust, wind induced galloping, and vortex shedding. For these reasons, cantilevered traffic signal structure often exhibit large amplitude vibrations which result in reduced fatigue life of the arm-to-pole connection of the structures. According to the survey in 1993 by 36 states Department of Transportation, there were a total of 80 occurrences of fatigue damage of cantilevered traffic signal structure by wind effects (Kaczinski et al. 1998). Since then, the number of the complete failures of cantilevered traffic signal structures has been increased due to the increasing length of the mast arm and its increased flexibility (Dexter et al. 2002), As a result, several efforts to understand vibrations in cantilevered traffic signal structures and attempts to develop mitigation strategies for the structures have been made.

This thesis follows the style of *Journal of Structural Engineering.*

Large amplitude vibrations of traffic signal structures have been attributed to wind-induced galloping of signal lights (McDonald et al. 1995). Various types of aero-dynamical mitigation devices damper plates or airfoil, configurations of signal lights, and measures have been developed and tested. That research indicated the limited effectiveness of an aero-dynamical mitigation strategy. However, large amplitude vibrations of traffic signal structures also can occur due to vortex shedding in a certain signal configuration (Letchford et al. 2008). They revealed that vortex shedding also needs to be considered for the fatigue design of cantilevered traffic signal structures. Contrary to previous studies, the attachment of traffic signals decreased the rate of vortex-induced vibration at low wind speeds and also inhibited large amplitude vibration in vertical direction, which occurred without signal heads (Zuo and Letchford 2010).

For the investigation of the fatigue behavior of cantilevered traffic signal structures, researchers have determined the vibration characteristics of the systems as numerical solutions from finite element method (FEM), and the solutions are verified in comparing with experimental measurements. However, the comparison of the results between numerical solution and experimental measurement often showed considerable differences. Clearly, the numerical modeling requires modification to capture real conditions including the tapered section of the members and possibly the foundation structure interaction.

In this thesis, an analytical approach with modal analysis of continuous system theory is proposed for vibration characteristics of a traffic signal structure. Modal

sensitivities are explored by introducing a measure of foundation flexibility. The modal analysis of a continuous system provided a closed-form solution for the eigenfrequencies and the corresponding modal responses of a traffic signal structures. Therefore, contrary to the finite element method, the motion of the given system with the suggested method should strictly be more exact. Moreover, although it may take considerable time for mathematical derivations and computation time in some cases, it leads to a more complete understanding of behavior and what parameters affect a quick design. Furthermore, through modifying the boundary conditions for vibration characteristics, the theoretical validation of the analytical model can be simultaneously ensured, and direct insight into the vibration problem can be provided.

1.2. Literature Review

The analytical modeling of the traffic signal structure herein implements the distributed parameter method using continuous system theory. Since the discovery of the law of elasticity which is well-known as Hooke's law in 1660, the second law of motion by Issac Newton in 1687, and the principles of differential calculus by Leibniz in 1684, the precise approach for vibration of a continuous system have been enabled. The equation of motion for the transverse vibration of thin beam was derived by Bernoulli in 1735, while solutions with various boundary conditions were developed by Euler in 1744. This is referred to as the Euler-Bernoulli thin beam theory. The improved theory of beam transverse vibration was presented by Timoshenko in 1921; this is the well-known

thick beam theory.

In past decades many researchers have developed analytical solutions for vibrations of continuous system, and have discussed issues arising from various types of boundary conditions. Since the closed-form expression for the solutions of vibrations of a beam with spring hinged and free ends (Chun 1972) and the analytical solutions for eigenfrequency and mode shape for a beam with continuously distributed mass and concentrated mass with rotational inertia were discussed (Jacquot and Gibson 1972), the analytical solutions for the vibrations of beams carrying a concentrated mass with free and hinged by rotational spring (Goel 1973) and for the free vibrations of the continuous beam with elastically restrained both ends against rotation carrying concentrated mass at arbitrary location (Goel 1976) have been proposed. That research provided the effects of eigenfrequencies of the given system with variation of parameters, the ratio of concentrated mass to beam mass, end stiffness to beam stiffness, and the location of a concentrated mass. Likewise, the analytical solution for transverse vibrations of elastically restrained free beams with a tip mass was studied by varying the ratio of the tip mass to the beam mass (Laura et al. 1974). A fundamental but comprehensive approach to an exact solution of mode shapes and frequency was obtained (Low 1991). In that study, the eigenvalue problem of transverse vibration of a beam was solved using various shape and boundary condition considerations. The system frequency equation was determined by incorporating the boundary conditions, and then the equation was symbolically solved using the secant method. The algorithm of the analytical approach

was validated with three case studies. The following research presented analytical and experimental comparisons study by using eigenfunctions of a transverse freely vibrating beam with various boundary conditions and multiple masses (Low 1997). The comparison of the analytical and experimental results verified the validity of the proposed analytical model.

In previous researches, investigators attempted to express their analytical solutions in a closed-form for eigenfrequencies and eigenfunctions of beams with additional parameters such as attached mass and spring, and with a relatively simple system configuration. On the other hand, the approximate approaches for the analytical solutions for eigenfrequency of a system have been studied with various methods, which can apply more complex parameters. The transverse vibration of continuous beam applied axial force and carrying concentrated masses was considered with the simple algorithm procedure taken into account approximate solutions by classical Ritz method (Laura et al. 1983). In addition, the fundamental mode shape function considering multiple concentrated masses is approximated using a polynomial coordinate equation. In following year, the study for vibration of restrained beams and rods with multiple point masses were conducted (Gürgöze 1984). The fundamental frequencies and the first mode shape of the system were mainly concerned with the approximate determination of analytical results which were approximate without solving characteristic equation. The approximate solutions for the first two eigenfrequencies and corresponding mode shapes with any number of point masses were obtained. Later, Gürgöze presented the effects of

the heavy masses on the same system (Gürgöze 1985).

The investigation into the vibration of a continuous beam carrying elastically mounted masses was conducted with comparison against experimental results (Ercoli and Laura 1987). The solutions were determined using different variation approach which can deal straightforwardly with additional complexities in the given system. In that study, the exact solutions and the corresponding eigenfrequency coefficients were compared not only with experimental results, but also with approximated solutions from Rayleigh-Schmidt procedure and Rayleigh-Ritz approach.

Since the early 1990s, due to the rapid developments of computer technology, computations of analytical solutions for dynamic problems have increased greatly. The analytical solutions for the free vibration problem of a uniform cantilever beam attached point masses were considered with the derivation of closed-form solution and its numerical computation (Wu and Lin 1990). The frequency equation of a cantilever beam with tip mass and spring-mass system was also derived using the Lagrange multiplier method and solved through numerical computation considering various boundary conditions (Gürgöze 1996). The effects of the multiple point masses along spans were taken into account for the transverse vibrations of an Euler-Bernoulli uniform beam (Naguleswaran 2001). There, only two particle parameters were considered in the resulting analytical eigenfrequencies and corresponding mode shapes. Following the research, an approach to apply an arbitrary number of particles on the same system was studied (Naguleswaran 2002). In these two works, the Euler-Bernoulli beam is

discretized into n-portions with (n+1) particles, multiple masses. The generalized mode shape functions were built with the modified mode shape functions with dimensionless axial coordinate. The eigenfrequencies of the given system were obtained by solving the frequency equation of a second order determinant equated to zero.

1.3. Technical Needs

In the proposed study, an analytical solution considering various types of boundary conditions and additional masses will be used to describe the vibrating behavior of traffic signal structures. The basic theorem for analytical solution was studied from a book, vibration of continuous system (Rao 2007). To apply multiple point masses to a continuous system, the mathematical approach used in the earlier study was adopted and modified. For this approach, an Euler-Bernoulli beam carrying point masses with rotational inertia, were analyzed with discrete beam elements (Maiz et al. 2007). The mode shape functions for each element were provided, and then the frequency equation from the zero determinant of the matrix incorporating boundary, continuity and compatibility conditions is obtained in a closed-form expression. As mentioned, this study takes the analytical solution of the discretized model into account and the analytical solution is determined using a modified computational method.

1.4. Research Objectives

The proposed research focuses on analytical solutions for the vibration

characteristics of traffic signal structures through modal analysis of a continuous system. The objectives of this research are to investigate the vibrating mechanisms of a cantilevered traffic signal structure, to develop an analytical model of the structure, and to validate the analytical model with a numerical model and experimental measurement.

This thesis describes the development of analytical model including its solution, and verification of the validity of the analytical model. The case and parametric studies are simultaneously carried out to capture real geometric and boundary conditions. The use of a numerical solution along with experimental measurements, bolsters the validity of the analytical solution.

1.5. Thesis Structure

This thesis consists of five sections. The investigation of dynamic characteristics data from the previously conducted studies is in the following section. Next, to aid in the understanding of the dynamic behavior of traffic signal structure, the derivation of the analytical model is described. Then, numerical model of the given cantilevered traffic signal structure is provided. Following the results from the experimental field test are provided. Consequently, the last section verifies the validity of the analytical model with the supplied results from previous sections, results of numerical model and experimental results.

2. MODAL ANALYSIS OF CONVENTIONAL CONTINUOUS SYSTEM

2.1. Transverse Vibration in Conventional Continuous System Model

The traffic signal structure is initially assumed as a linearly elastic, continuous structure. This structure is also considered a low frequency structure due to its geometry and flexibility, and observed vibrations. Because this structure is an assemblage of two members which have different degrees of freedom, the complication makes an solution less attainable; however one may easily find an exact analytical solution in low-frequencies due to the initial assumptions even though the complex couple behavior in higher frequencies cannot be considered. As a result, in this thesis, the dynamic characteristics and responses of each member are determined, and then the response of total structure is analyzed through post-processing.

In conventional continuous system model, which is a basic and simple mathematical expressions for structural system vibrations, considerations of additional attachments might lead the inaccuracy of modal responses due to basic difficulties. Thus, in this section, the development of conventional continuous system model for members of traffic signal structure will be taken into account.

2.2. Equation of Motion for Flexural Member

The equation of motion for the transverse free vibration of a beam can be derived from the free body diagram taking into account the equilibrium of an

infinitesimal element in bending. As shown in Figure 2.1, the moment equilibrium of an element around the left edge yields

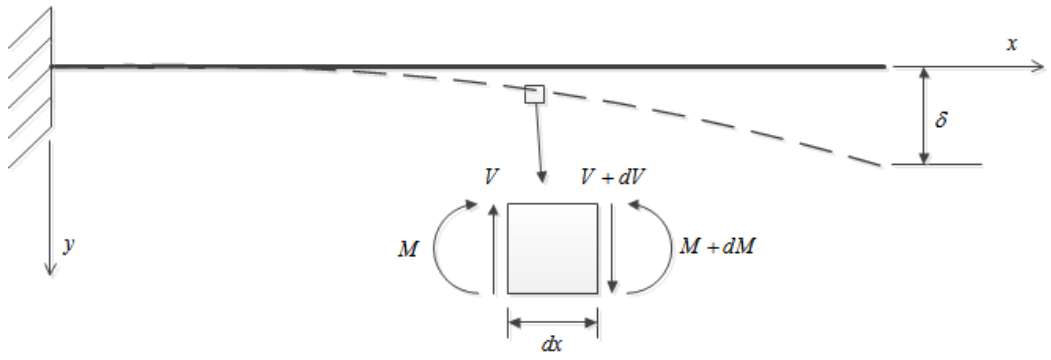

Figure 2.1 Flexural Cantilevered Beam in Bending

$$\sum M_0 = 0; \qquad (V + dV) \cdot dx + M - (M + dM) = 0$$

$$V \cdot dx - \frac{\partial M}{\partial x} \cdot dx = 0$$

$$V = \frac{\partial M}{\partial x} \tag{2.1}$$

The equilibrium of shear force in the infinitesimal element is expressed with Newton's second law for motion as

$$\sum F_y = m \cdot a = m \cdot \frac{\partial^2 y}{\partial t^2} \qquad \rightarrow \qquad \rho_a \cdot A_a \cdot dx \cdot \frac{\partial^2 y}{\partial t^2} = \frac{\partial V}{\partial x} \cdot dx$$

$$\frac{\partial V}{\partial x} = \rho_a \cdot A_a \cdot \frac{\partial^2 y}{\partial t^2}$$

$$\frac{\partial}{\partial x} \cdot \left(\frac{\partial M}{\partial x} \right) = \rho_a \cdot A_a \cdot \frac{\partial^2 y}{\partial t^2}$$

$$\frac{\partial^2 M}{\partial x^2} = \rho \cdot A_a \cdot \frac{\partial^2 y}{\partial t^2}$$

$$\frac{\partial^2}{\partial x^2}\left(-EI_a \frac{\partial^2 y}{\partial x^2}\right) = \rho \cdot A_a \cdot \frac{\partial^2 y}{\partial t^2} \quad . \tag{2.2}$$

where, A_a = cross-sectional area for a mast-arm

I_a = moment of inertia for a mast-arm

E = Young's Modulus

The equation of motion for transverse vibration was provided in Equation (2.2) from the equilibrium approach with the second law of Newton. The equation of motion can be simply rewritten as

$$-E \cdot I_a \frac{\partial^4 y}{\partial x^4} = \rho \cdot A_a \cdot \frac{\partial^2 y}{\partial t^2} \quad . \tag{2.3}$$

The solution of the equation of motion is expressed using the separation of variables, involving the multiplication of a space dependent function $f(x)$ and a time dependent function $g(t)$. The spatial function is the mode shape function or the eigenfunction for eigenfrequency. The solution for each mode can be assumed as

$$y_i(x,t) = f_i(x) \cdot g_i(t) \tag{2.4}$$

Then, equation (2.3) is expressed with substituting equation (2.4) such as

$$E \cdot I_a \cdot \frac{\partial^4}{\partial x^4}\left[f_i(x) \cdot g_i(t)\right] = -\rho \cdot A_a \cdot \frac{\partial^2}{\partial t^2}\left[f_i(x) \cdot g_i(t)\right] \tag{2.5}$$

$$\frac{E \cdot I_a}{\rho \cdot A_a} \cdot \frac{\partial^4}{\partial x^4}\left[f_i(x) \cdot g_i(t)\right] = -\frac{\partial^2}{\partial t^2}\left[f_i(x) \cdot g_i(t)\right] \tag{2.6}$$

$$c = \sqrt{\frac{E \cdot I_a}{\rho_a \cdot A_a}}$$

where c is a wave velocity for transverse vibration. Through the separation of variables, the partial differential Equation (2.3) is distinguished into two ordinary differential equation with independent variables, x and t, respectively.

$$\frac{d^4 f_i(x)}{dx^4} - \beta_i^4 \cdot f_i(x) = 0 \tag{2.7}$$

$$\text{where, } \beta_i = \sqrt{\frac{\omega_i}{c}}$$

$$\frac{d^2 g_i(t)}{dt^2} + \omega_i^2 \cdot g_i(t) = 0 \tag{2.8}$$

where a coefficient β_i is an eigenfrequency coefficient. For free vibration of the system, the ordinary differential equation of the spatial variable has a general solution rewritten by Euler equations as

$$f_i(x) = c_1 \cdot \cos\beta_i \cdot x + c_2 \cdot \sin\beta_i \cdot x + c_3 \cdot \cosh\beta_i \cdot x + c_4 \cdot \sinh\beta_i \cdot x \tag{2.9}$$

In addition, the solution of the ordinary differential equation for time variable in Equation (2.8) is determined as

$$g_i(x) = A_i \cdot \cos\omega_i \cdot t + B_i \cdot \sin\omega_i \cdot t \tag{2.10}$$

The general solutions of spatial and time function have respectively several constants in the equations, which will be obtained taking into account boundary and initial conditions of the given system.

2.3 Boundary Conditions, Eigenfrequency and Eigenfunction

The boundary conditions of the given system significantly affect the dynamic characteristics of the given structure. This section shows the application of boundary conditions of a cantilever beam configuration. As shown in Equation (2.9), a mode shape function for transverse vibration has four constants, which can be determined with four boundary conditions. For a cantilever beam, fixed free boundary conditions are normally applied to determine the solution. The boundary conditions are zero-displacement and zero deflection angle at $x = 0$ (fixed end) and zero-shear force and zero-bending moment at $x = L_a$ (free end). These can be written as

$$f_i(x)\big|_{x=0} = 0 \tag{2.11}$$

$$\left.\frac{df_i(x)}{dx}\right|_{x=0} = 0 \tag{2.12}$$

$$\left.\frac{d^3 f_i(x)}{dx^3}\right|_{x=L_a} = 0 \tag{2.13}$$

$$\left.\frac{d^2 f_i(x)}{dx^2}\right|_{x=L_a} = 0 \tag{2.14}$$

.

Substituting equation (2.9) into equations (2.11) to (2.14) gives the relationships of unknown constants as

$$c_1 = -c_3 \tag{2.15}$$

$$c_2 = -c_4 \tag{2.16}$$

$$-c_1 \cdot \cos\beta_i \cdot L_a - c_2 \cdot \sin\beta_i \cdot L_a + c_3 \cdot \cosh\beta_i \cdot L_a + c_4 \cdot \sinh\beta_i \cdot L_a = 0 \qquad (2.17)$$

$$c_1 \cdot \sin\beta_i \cdot L_a - c_2 \cdot \cos\beta_i \cdot L_a + c_3 \cdot \sinh\beta_i \cdot L_a + c_4 \cdot \cosh\beta_i \cdot L_a = 0 \qquad (2.18)$$

These equations represent the boundary conditions for fixed-free ends of the cantilever beam; they can be represented in a 4 by 4 matrix such as

$$\begin{bmatrix} 1 & 0 & 1 & 0 \\ 0 & 1 & 0 & 1 \\ -\cos\beta_i \cdot L_a & -\sin\beta_i \cdot L_a & \cosh\beta_i \cdot L_a & \sinh\beta_i \cdot L_a \\ \sin\beta_i \cdot L_a & -\cos\beta_i \cdot L_a & \sinh\beta_i \cdot L_a & \cosh\beta_i \cdot L_a \end{bmatrix} \cdot \begin{bmatrix} c_1 \\ c_2 \\ c_3 \\ c_4 \end{bmatrix} = \begin{bmatrix} 0 \\ 0 \\ 0 \\ 0 \end{bmatrix} \qquad (2.19)$$

This four-by-four matrix for the boundary conditions must be a singular matrix to satisfy Equation (2.19), resulting in the eigenfrequency equation as

$$1 + \cos\beta_i \cdot L_a \cdot \cosh\beta_i \cdot L_a = 0 \qquad (2.20)$$

Consequently, eigenfrequencies of the given cantilever beam are obtained by solving for the roots of Equation (2.20). Equation (2.20) gives eigenfrequency coefficients as solutions and the eigenfrequency coefficients yields the eigenfrequencies of the given system such as

$$\beta_i = \sqrt{\frac{\omega_i}{c}}$$

$$\omega_i = \beta_i^2 \cdot \sqrt{\frac{EI_a}{\rho_a A_a}} \qquad (2.21)$$

Thus, substituting eigenfrequencies, obtained from Equation (2.21), into Equation (2.9) yields the modal eigenfunctions, also called mode shape functions. Taking into account

the relationships in Equation (2.15) through (2.18), constants in the mode shape function can be expressed in terms of single constant such that,

$$c_1 \cdot (\sin \beta_i \cdot L_a - \sinh \beta_i \cdot L_a) - c_2 \cdot (\cos \beta_i \cdot L_a + \cosh \beta_i \cdot L_a) = 0$$

$$c_2 = \frac{(\sin \beta_i \cdot L_a - \sinh \beta_i \cdot L_a)}{(\cos \beta_i \cdot L_a + \cosh \beta_i \cdot L_a)} \cdot c_1 \quad . \tag{2.22}$$

Finally, substituting Equation (2.22) into the eigenfunction gives the eigenfunctions or mode shape functions of a flexural beam as follows

$$f_i(x) = c_{1i} \cdot \left\{ (\cos \beta_i \cdot x - \cosh \beta_i \cdot x) + \frac{(\sin \beta_i \cdot x - \sinh \beta_i \cdot x)}{(\cos \beta_i \cdot x + \cosh \beta_i \cdot x)} \cdot (\sin \beta_i \cdot x - \sinh \beta_i \cdot x) \right\} \quad . \tag{2.23}$$

2.4 Orthogonality Conditions of Eigenfunctions

The eigenfunctions have been determined in previous section, but there is an undetermined constant even though four boundary conditions were provided. Thus, one additional condition is requested to obtain the constant. In modal analysis, the total responses are expressed as the summation of modal responses such as

$$y(x,t) = \sum_{i=1}^{n} f_i(x) \cdot g_i(t) \tag{2.24}$$

Substituting Equation (2.24) into Equation (2.2) yields

$$\sum_{i=1}^{n} \frac{d^2}{dx^2} \cdot \left(-EI_a \cdot \frac{d^2 f_i(x)}{dx^2} \right) \cdot g_i(x) = \sum_{i=1}^{n} \rho_a \cdot A_a \cdot \frac{\partial^2 g_i(t)}{\partial t^2} \cdot f_i(x) \tag{2.25}$$

If Equation (2.25) is expressed only with i-th mode shape function $f_i(x)$, it gives

$$\sum_{i=1}^{n} \left\{ \frac{d^2}{dx^2} \cdot \left(EI_a \cdot \frac{d^2 f_i(x)}{dx^2} \right) \cdot g_i(t) - \rho_a \cdot A_a \cdot f_i(x) \cdot \omega_i^2 \cdot g_i(t) \right\} = 0$$

$$\frac{d^2}{dx^2} \cdot \left(EI_a \cdot \frac{d^2 f_i(x)}{dx^2} \right) = \rho_a \cdot A_a \cdot \omega_i^2 \cdot f_i(x) . \tag{2.26}$$

In a similar manner, Equation (2.26) can be expressed for the j-th mode shape function as

$$\frac{d^2}{dx^2} \cdot \left(EI_a \cdot \frac{d^2 f_j(x)}{dx^2} \right) = \rho_a \cdot A_a \cdot \omega_j^2 \cdot f_j(x) \tag{2.27}$$

Multiplying both sides of Equation (2.26) with $f_j(x)$ and integrating over the length of the beam yields

$$\int_0^{L_a} f_j(x)\cdot\frac{d^2}{dx^2}\cdot\left(EI_a\cdot\frac{d^2 f_i(x)}{dx^2}\right)\cdot dx=\int_0^{L_a} f_j(x)\cdot\rho_a\cdot A_a\cdot\omega_i^2\cdot f_i(x)\cdot dx \qquad (2.28)$$

The left term of the Equation (2.27) can be integrated by part such as

$$\int_0^{L_a} f_j(x)\cdot\frac{d^2}{dx^2}\cdot\left(EI_a\cdot\frac{d^2 f_i(x)}{dx^2}\right)\cdot dx=\int_0^{L_a} EI_a\cdot\frac{d^2 f_j(x)}{dx^2}\cdot\frac{d^2 f_i(x)}{dx^2}\cdot dx \qquad (2.29)$$

Thus, the Equation (2.27) consequently becomes

$$\int_0^{L_a} EI_a\cdot\frac{d^2 f_j(x)}{dx^2}\cdot\frac{d^2 f_i(x)}{dx^2}\cdot dx=\omega_i^2\cdot\int_0^{L_a}\rho_a\cdot A_a\cdot f_i(x)\cdot f_j(x)\cdot dx \qquad (2.30)$$

In a similar manner, multiplying both sides of Equation (2.26) with $f_j(x)$ and integrating over the length of the beam brings

$$\int_0^{L_a} EI_a\cdot\frac{d^2 f_i(x)}{dx^2}\cdot\frac{d^2 f_j(x)}{dx^2}\cdot dx=\omega_j^2\cdot\int_0^{L_a}\rho_a\cdot A_a\cdot f_j(x)\cdot f_i(x)\cdot dx \qquad (2.31)$$

Subtracting Equation (2.29) from (2.30) gives

$$(\omega_i^2-\omega_j^2)\cdot\int_0^{L_a}\rho_a\cdot A_a\cdot f_j(x)\cdot f_i(x)\cdot dx=0 \qquad (2.32)$$

$$\int_0^{L_a}\rho_a\cdot A_a\cdot f_j(x)\cdot f_i(x)\cdot dx=0 \qquad i,j=1,2,3..... \quad \omega_i^2\neq\omega_j^2 \qquad (2.33)$$

$$\int_0^{L_a} EI_a\cdot\frac{d^2 f_i(x)}{dx^2}\cdot\frac{d^2 f_j(x)}{dx^2}\cdot dx=0 \qquad i,j=1,2,3..... \quad \omega_i^2\neq\omega_j^2 \qquad (2.34)$$

Equations (2.33) and (2.34) express the orthogonality relations for normal functions, normalizing the i-th mode such so that

$$\int_0^{L_a} \rho_a \cdot A_a \cdot f_i(x)^2 \cdot dx = 1 \qquad i = 1,2,... \tag{2.35}$$

.

Equations (2.32) and (2.34) can be expressed using the Kronecker delta as,

$$\int_0^{L_a} \rho_a \cdot A_a \cdot f_j(x) \cdot f_i(x) \cdot dx = \delta_{ij} \tag{2.36}$$

$$\delta_{ij} = \begin{cases} 0, & i \neq j \\ 1, & i = j \end{cases}$$

.

Therefore, as shown in Equation (2.23), the mode function has already determined and it can be applied to Equation(2.36). Through consideration of i-th mode function with orthogonality condition expressed in Equations (2.34) or (2.35), a constant to ensure an orthogonal mode shape function is

$$c_{1i}{}^2 \cdot \int_0^{L_a} \rho_a \cdot A_a \cdot \left\{ (\cos\beta_i \cdot x - \cosh\beta_i \cdot x) + \frac{(\sin\beta_i \cdot x - \sinh\beta_i \cdot x)}{(\cos\beta_i \cdot x + \cosh\beta_i \cdot x)} \cdot (\sin\beta_i \cdot x - \sinh\beta_i \cdot x) \right\}^2 \cdot dx = 1$$

$$c_{1i} = \left\{ \frac{1}{\int_0^{L_a} \rho_a A_a \cdot \left\{ (\cos\beta_i \cdot x - \cosh\beta_i \cdot x) + \frac{(\sin\beta_i \cdot x - \sinh\beta_i \cdot x)}{(\cos\beta_i \cdot x + \cosh\beta_i \cdot x)} \cdot (\sin\beta_i \cdot x - \sinh\beta_i \cdot x) \right\}^2 dx} \right\}^{\frac{1}{2}} \tag{2.37}$$

.

As shown, the constant of the mode function undetermined through boundary conditions application is obtained with the orthogonality condition of normal mode functions.

2.5 Initial Conditions and the Time Dependent Function

In the equation of motion, the ordinary differential equation with the independent variable of time which is from separation of variables is already derived in previous section provided in Equation (2.8) and (2.10).

For, the time dependent function, there must be two initial conditions that can yield the constants in the time function. The two initial conditions are provided as

$$y(x,t=0)=\sum_{i=1}^{n} f_i(x)\cdot g_i(0)=f_0(x) \tag{2.38}$$

and

$$\dot{y}(x,t=0)=\sum_{i=1}^{n} f_i(x)\cdot \dot{g}_i(0)=\dot{f}_0(x) \tag{2.39}$$

These represent the initial displacement (Equation (2.38)) and the initial velocity (Equation (2.39)) which can be supplied from the conditions of experimental tests like a pluck of snap-back test. To apply the given initial conditions to time dependent function for each mode, they should be transformed to eigenfrequency dependent initial conditions. For the initial conditions in Equation (2.39) and (2.40), the eigenvalue dependent initial displacement and velocity are considered such that

$$\sum_{i=1}^{\infty}\int_0^{L_a} \rho_a\cdot A_a\cdot f_i(x)\cdot f_i(x)\,dx\cdot g_i(0)=\int_0^{L_a} \rho_a\cdot A_a\cdot f_i(x)\cdot f_0(x)\,dx \tag{2.40}$$

$$\sum_{i=1}^{\infty}\int_0^{L_a} \rho_a\cdot A_a\cdot f_i(x)\cdot f_i(x)\,dx\cdot \dot{g}_i(0)=\int_0^{L_a} \rho_a\cdot A_a\cdot f_i(x)\cdot \dot{f}_0(x)\,dx \tag{2.41}$$

For orthogonality as shown in Equation (2.35), mode functions are normalized so that

$$\int_0^{L_a} \rho_a \cdot A_a \cdot f_i(x) \cdot f_i(x)\, dx = 1 \tag{2.42}$$

Therefore, the eigenvalue dependent initial conditions can be determined as

$$g_i(0) = \int_0^{L_a} \rho_a \cdot A_a \cdot f_i(x) \cdot f_0(x)\, dx \qquad i = 1,2,3,..... \tag{2.43}$$

$$\dot{g}_i(0) = \int_0^{L_a} \rho_a \cdot A_a \cdot f_i(x) \cdot \dot{f}_0(x)\, dx \qquad i = 1,2,3,..... \tag{2.44}$$

The given initial displacement, $f_0(x)$, is considered the static deflection of the beam when performing snap-back test and $\dot{f}_0(x)$ is its initial velocity. Consequently, the time dependent function is given as

$$g_i(t) = g_i(0) \cdot \cos \omega_i \cdot t + \frac{\dot{g}_i(0)}{\omega_i} \sin \omega_i \cdot t \tag{2.45}$$

2.6 Conclusion

The conventional continuous system model shown in this section provides a basic comprehension of the vibration of a traffic signal structure, although the conventional model contains critical limitations for modal analysis. The derivations of the analytical model for vibrations of a traffic signal structure are eventually used to determine the dynamic characteristics of the structure and to obtain the time domain responses of the structure. Moreover, the considerations of various boundary conditions should be significantly considered in this analytical solution. Thus, the latter section will separately cover these considerations.

3. MODAL ANALYSIS OF DISCRETIZED CONTINUOUS SYSTEM

3.1. Transverse Vibration in Discretized Continuous System Model

The conventional continuous system model, which is a basic mathematical model for vibrating system, has several limitations mentioned earlier. Due to simplified modeling, to consider a real motion of the structure, the effects caused by many additional parameters are difficult to take into account in post-processing. The boundary conditions are the only condition to apply the parameters, but it cannot provide agreeable mode shapes when parameters are applied on arbitrary points of the system. Thus, to overcome this problem of the conventional model, a discretized continuous system model is expanded by many researchers from the basic and conventional continuous system theories, as discussed in Section 1. In this thesis, this discretized continuous system model will be developed and discussed.

3.2. Equation of Motion for Analytical Solution

3.2.1. Constant Cross-sectioned Members

For the discretized model of a continuous system, the fundamental approach to derive the equation of motion is similar to that of the conventional continuous system model. The equation of motion for flexural beam is expressed in partial differential equation which is derived from free body diagram of an infinitesimal element of Euler-

Bernoulli beam in bending under consideration of the Newton's second law, shown in Equation (2.3).

The solution of this partial differential equation, as mentioned in the previous section, is initially assumed as the multiplication of space and time dependent functions taking into account the separation of variables, as shown in Equation (2.4). For the free vibration problem, the general eigenfunction has been determined earlier in Equation (2.9), where the eigenfrequency coefficient β_i is introduced. In addition, time dependent function $g_i(t)$ also has been obtained, which is same with the function in conventional model shown in Equation (2.10). During modal analysis, the total response of the system is expressed as the summation of the all modal responses as was shown in Equation (2.24).

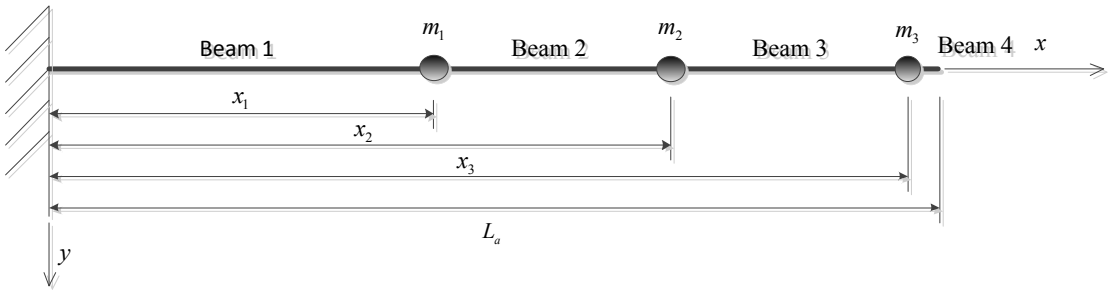

Figure 3.1: Discretized Continuous System for Constant Section Beam

The discretized continuous system model is used to apply multiple masses on the Euler-Bernoulli beam. Here, a constant cross-sectioned beam is discretized into several beam elements, as shown in Figure 3.1, and each beam element is considered as

a continuous system. To determine the response of the overall system, compatibility and continuity conditions are considered at each node connecting beam elements. Because each beam element is assumed to be a continuous system, the eigenfunctions for each beam element can be rewritten piece-wise, as follows

$$f_{1i}(x) = c_{1i} \cdot \cos \beta_i \cdot x + c_{2i} \cdot \sin \beta_i \cdot x + c_{3i} \cdot \cosh \beta_i \cdot x + c_{4i} \cdot \sinh \beta_i \cdot x \qquad (0 \le x \le x_1) \quad (3.1)$$

$$f_{2i}(x) = c_{5i} \cdot \cos \beta_i \cdot x + c_{6i} \cdot \sin \beta_i \cdot x + c_{7i} \cdot \cosh \beta_i \cdot x + c_{8i} \cdot \sinh \beta_i \cdot x \qquad (x_1 \le x \le x_2) \quad (3.2)$$

$$f_{3i}(x) = c_{9i} \cdot \cos \beta_i \cdot x + c_{10i} \cdot \sin \beta_i \cdot x + c_{11i} \cdot \cosh \beta_i \cdot x + c_{12i} \cdot \sinh \beta_i \cdot x \qquad (x_2 \le x \le x_3) \quad (3.3)$$

$$f_{4i}(x) = c_{13i} \cdot \cos \beta_i \cdot x + c_{14i} \cdot \sin \beta_i \cdot x + c_{15i} \cdot \cosh \beta_i \cdot x + c_{16i} \cdot \sinh \beta_i \cdot x \qquad (x_3 \le x \le L_a) \quad (3.4)$$

As seen in Equations (3.1) through (3.4), each of eigenfunctions has respectively four constants, so a total of sixteen boundary, continuity and compatibility conditions are required.

3.2.2. Tapered Cross-sectioned Member

Traffic signal structures normally have tapered section members, meaning variable geometric properties are required to consider. Using this discretized continuous system model, this tapered section model can be approximately expressed. The equation of motion for the tapered section member is basically same with the former case, shown in Equation (2.3). However, the geometric parameters like a cross-section area and a moment of inertia have variable values.

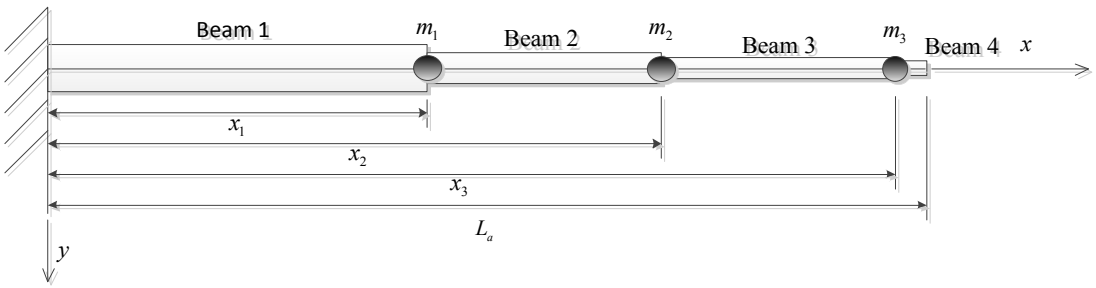

Figure 3.2: Discretized Continuous System for Tapered Section Beam

In this thesis, the tapered section beam is simply applied with four beam elements. As shown in Figure 3.2, a tapered flexural beam is depicted with simplified four element beam. As considered in the previous section, each element is an independent continuous system. Thus, the eigenfunctions for these four element are obtained as follows

$$f_{1i}(x) = c_{1i} \cdot \cos \gamma_1 \beta_i x + c_{2i} \cdot \sin \gamma_1 \beta_i x + c_{3i} \cdot \cosh \gamma_1 \beta_i x + c_{4i} \cdot \sinh \gamma_1 \beta_i x \qquad (0 \le x \le x_1) \quad (3.5)$$

$$f_{2i}(x) = c_{5i} \cdot \cos \gamma_2 \beta_i x + c_{6i} \cdot \sin \gamma_2 \beta_i x + c_{7i} \cdot \cosh \gamma_2 \beta_i x + c_{8i} \cdot \sinh \gamma_2 \beta_i x \qquad (x_1 \le x \le x_2) \quad (3.6)$$

$$f_{3i}(x) = c_{9i} \cdot \cos \gamma_3 \beta_i x + c_{10i} \cdot \sin \gamma_3 \beta_i x + c_{11i} \cdot \cosh \gamma_3 \beta_i x + c_{12i} \cdot \sinh \gamma_3 \beta_i x \quad (x_2 \le x \le x_3) \quad (3.7)$$

$$f_{4i}(x) = c_{13i} \cdot \cos \gamma_4 \beta_i x + c_{14i} \cdot \sin \gamma_4 \beta_i x + c_{15i} \cdot \cosh \gamma_4 \beta_i x + c_{16i} \cdot \sinh \gamma_4 \beta_i x \quad (x_3 \le x \le L_a) \quad (3.8)$$

$$\text{where} \qquad \gamma_n^{\,4} = \frac{\rho \cdot A_n}{E \cdot I_n} \qquad (3.9)$$

and

$$\beta_i^4 = \omega_i^2 \qquad (3.10)$$

A_n :Cross-sectional area of n-th element

I_n : Moment of inertia of n-th element

These eigenfunctions in Equation (3.5) through (3.8) can be applied to same boundary, continuity and compatibility conditions in a manner of the constant section member case. However, one should significantly consider the constant γ_n when differentiating the eigenfunctions to apply the boundary, continuity and compatibility conditions. As will see in the following section, the same boundary, continuity and compatibility conditions are provided for the constant and tapered cross-sectioned members, but the different mode shape functions are used dependent upon the cross-section type.

3.3. Boundary, Continuity and Compatibility Conditions

As mentioned, there are sixteen constants revealed in four eigenfunctions in Equation (3.1) to (3.4) (constant member) and in Equation (3.5) through (3.8) (tapered member). Thus, to determine the sixteen constants for each type of members, sixteen conditions should be supplied. As seen in Figure 3.1 and Figure 3.2, a continuous flexural beam is discretized into four beam elements. The first and last elements of the constant cross-sectioned beam, for instance, provides boundary conditions which are fixed free boundary conditions expressed as

$$f_{1i}(x)\big|_{x=0} = 0 \tag{3.11}$$

$$\left.\frac{df_{1i}(x)}{dx}\right|_{x=0} = 0 \tag{3.12}$$

$$\left.\frac{d^3 f_{4i}(x)}{dx^3}\right|_{x=L_a} = 0 \tag{3.13}$$

$$\left.\frac{d^2 f_{4i}(x)}{dx^2}\right|_{x=L_a} = 0 \tag{3.14}$$

Substituting piecewise eigenfunctions from equation (3.1) and (3.4), respectively for the first and last beam elements, into boundary condition in equation (3.11) to (3.14) yields

$$c_1 + c_3 = 0 \tag{3.15}$$

$$c_2 + c_4 = 0 \tag{3.16}$$

$$c_{13} \cdot \sin\beta_i \cdot L_a - c_{14} \cdot \cos\beta_i \cdot L_a + c_{15} \cdot \sinh\beta_i \cdot L_a + c_{16} \cdot \cosh\beta_i \cdot L_a = 0 \tag{3.17}$$

$$-c_{13}\cdot\cos\beta_i\cdot L_a - c_{14}\cdot\sin\beta_i\cdot L_a + c_{15}\cdot\cosh\beta_i\cdot L_a + c_{16}\cdot\sinh\beta_i\cdot L_a = 0 \qquad (3.18)$$

These equations have same shapes with conventional model shown in Equation (3.15) to (3.18). For the remaining conditions, one must investigate continuity and compatibility conditions at each connection point between beam elements. The continuity conditions state that the displacements and angles of deflection should be equal at connections two beam elements. Further, the compatibility conditions ensure the same bending moments and shear forces at the connections. These continuity and compatibility conditions can be expressed as

$$f_{1i}(x)\big|_{x=x_1} = f_{2i}(x)\big|_{x=x_1} \qquad (3.19)$$

$$\left.\frac{df_{1i}(x)}{dx}\right|_{x=x_1} = \left.\frac{df_{2i}(x)}{dx}\right|_{x=x_1} \qquad (3.20)$$

$$E\cdot I_a\cdot\left.\frac{d^2 f_{1i}(x)}{dx^2}\right|_{x=x_1} = E\cdot I_a\cdot\left.\frac{d^2 f_{2i}(x)}{dx^2}\right|_{x=x_1} \qquad (3.21)$$

$$E\cdot I_a\cdot\left.\frac{d^3 f_{1i}(x)}{dx^3}\right|_{x=x_1} + m_1\cdot\omega_i^{\,2}\cdot f_{1i}(x) = E\cdot I_a\cdot\left.\frac{d^3 f_{2i}(x)}{dx^3}\right|_{x=x_1}. \qquad (3.22)$$

Equations (3.19) through (3.22) show the continuity and compatibility at $x = x_1$, and attach the first mass m_1 between the first and second beam elements. Substituting the eigenfunctions Equation (3.1) through (3.4) of the first and second beam elements into these equations for continuity and compatibility conditions yields as

$$\begin{aligned} &c_1\cdot\cos\beta_i\cdot x_1 + c_2\cdot\sin\beta_i\cdot x_1 + c_3\cdot\cosh\beta_i\cdot x_1 + c_4\cdot\sinh\beta_i\cdot x_1 \\ &\quad -c_5\cdot\cos\beta_i\cdot x_1 - c_6\cdot\sin\beta_i\cdot x_1 - c_7\cdot\cosh\beta_i\cdot x_1 - c_8\cdot\sinh\beta_i\cdot x_1 = 0 \end{aligned} \qquad (3.23)$$

$$\begin{aligned}&-c_1\cdot\sin\beta_i\cdot x_1+c_2\cdot\cos\beta_i\cdot x_1+c_3\cdot\sinh\beta_i\cdot x_1+c_4\cdot\cosh\beta_i\cdot x_1\\&\quad+c_5\cdot\sin\beta_i\cdot x_1-c_6\cdot\cos\beta_i\cdot x_1-c_7\cdot\sinh\beta_i\cdot x_1-c_8\cdot\cosh\beta_i\cdot x_1=0\end{aligned}\tag{3.24}$$

$$\begin{aligned}&-c_1\cdot\cos\beta_i\cdot x_1-c_2\cdot\sin\beta_i\cdot x_1+c_3\cdot\cosh\beta_i\cdot x_1+c_4\cdot\sinh\beta_i\cdot x_1\\&\quad+c_5\cdot\cos\beta_i\cdot x_1+c_6\cdot\sin\beta_i\cdot x_1-c_7\cdot\cosh\beta_i\cdot x_1-c_8\cdot\sinh\beta_i\cdot x_1=0\end{aligned}\tag{3.25}$$

$$\begin{aligned}&c_1\cdot(\sin\beta_i\cdot x_1+\frac{m_i}{EI_a}\cdot\omega_i^2\cdot\cos\beta_i\cdot x_1)-c_2\cdot(\cos\beta_i\cdot x_1-\frac{m_i}{EI_a}\cdot\omega_i^2\cdot\sin\beta_i\cdot x_1)\\&+c_3\cdot(\sinh\beta_i\cdot x_1+\frac{m_i}{EI_a}\cdot\omega_i^2\cdot\cosh\beta_i\cdot x_1)+c_4\cdot(\cosh\beta_i\cdot x_1+\frac{m_i}{EI_a}\cdot\omega_i^2\cdot\sinh\beta_i\cdot x_1)\\&\quad-c_5\cdot\sin\beta_i\cdot x_1+c_6\cdot\cos\beta_i\cdot x_1-c_7\cdot\sinh\beta_i\cdot x_1-c_8\cdot\cosh\beta_i\cdot x_1=0\end{aligned}\tag{3.26}$$

Equation (3.26) which represents the compatibility condition of shear force can be simple rewritten using Equation (2.21), the relationship between eigenfrequency and eigenfrequency coefficient, as follows

$$\begin{aligned}&c_1\cdot(\sin\beta_i\cdot x_1+M_1\cdot\beta_i^4\cdot\cos\beta_i\cdot x_1)-c_2\cdot(\cos\beta_i\cdot x_1-M_1\cdot\beta_i^4\cdot\sin\beta_i\cdot x_1)\\&+c_3\cdot(\sinh\beta_i\cdot x_1+M_1\cdot\beta_i^4\cdot\cosh\beta_i\cdot x_1)+c_4\cdot(\cosh\beta_i\cdot x_1+M_1\cdot\beta_i^4\cdot\sinh\beta_i\cdot x_1)\\&\quad-c_5\cdot\sin\beta_i\cdot x_1+c_6\cdot\cos\beta_i\cdot x_1-c_7\cdot\sinh\beta_i\cdot x_1-c_8\cdot\cosh\beta_i\cdot x_1=0\end{aligned}\tag{3.27}$$

$$where,\ M_1=\frac{m_1}{\rho_a A_a}$$

If the continuity and compatibility conditions are considered at the second and the third points of masses in a similar manner, a total of twelve conditions are supplied. When including the four boundary conditions, sixteen conditions are provided. For computation, the continuity and compatibility conditions must be expressed in more generalized form such that

$$f_{ni}(x)\big|_{x=x_n}=f_{(n+1)i}(x)\big|_{x=x_n}\tag{3.28}$$

$$\left.\frac{df_{ni}(x)}{dx}\right|_{x=x_n} = \left.\frac{df_{(n+1)i}(x)}{dx}\right|_{x=x_n} \tag{3.29}$$

$$E \cdot I_n \cdot \left.\frac{d^2 f_{ni}(x)}{dx^2}\right|_{x=x_n} = E \cdot I_n \cdot \left.\frac{d^2 f_{(n+1)i}(x)}{dx^2}\right|_{x=x_n} \tag{3.30}$$

$$E \cdot I_n \cdot \left.\frac{d^3 f_{ni}(x)}{dx^3}\right|_{x=x_n} + M_n \cdot \beta_i^4 \cdot f_{ni}(x) = E \cdot I_n \cdot \left.\frac{d^3 f_{(n+1)i}(x)}{dx^3}\right|_{x=x_n} \tag{3.31}$$

where, $M_n = \dfrac{m_n}{\rho_a A_a}$ $\qquad n = 1,\ 2,\ 3,.....$

I_n : Moment of inertia of each element

These generalized Equations (3.28) through (3.31) for continuity and compatibility conditions can be applied not only to the constant section member, but also to the tapered member.

As a result, there are sixteen equations resulting from four beam elements, with sixteen unknowns. Using the four known boundary conditions and twelve continuity and compatibility conditions at the three connecting may be found eigenfrequency coefficients, then eigenfrequencies. The sixteen equations are very complicated, but they can be written in matrix form collected by the unknown constants c_1 to c_{16}. The 16 by 16 square matrix for boundary, continuity, and compatibility conditions are shown in equation (B.1) through (B.12) of Appendix 0. This reforming process is required for the calculations of the eigenfrequency coefficients.

3.4. Eigenfrequencies of Discretized Continuous System

The eigenfrequency coefficients can be determined through consideration of the singularity of the 16 by 16 matrix for the non-trivial solution. Once the eigenfrequency coefficients are obtained, and then they can be transformed to eigenfrequencies. To solve the problem, MATLAB has been used in this study. The large matrix is expressed by many symbolic letters in the MATLAB. Thus, it is expected that the determinant of the large matrix would be expressed as a complicated equation with extreme numbers of symbolic terms, meaning the solution process would be highly expensive in terms of computation time. However, in MATLAB, the computation time for the determinant of a large matrix with only numbers is considerably short. With this MATLAB feature, eigenfrequency computation is implemented using a concept of the bisection method for numerical calculations. The bisection method is a simple numerical method to find roots of an equation based on the property of interval. In this method, it runs a repetitively bisecting process to find an interval within a calculation tolerance that contains root of an equation. In this thesis, the basic concept of the bisection method is followed, then modified to increase the accuracy of the computation and to decrease the computation time. A detailed description of the modified bisection method is provided in Appendix A. The symbols in the large matrix have all known values except for the eigenfrequency coefficients β_i. Substituting the known values into the symbols, the determinant of the large symbolic matrix can be taken into account as an equation with one independent variable, and then the roots of the equation are obtained as eigenfrequency coefficients

with the modified bisection method. This modified bisection method can guarantee faster computation time and certain accuracy of the solution. As mentioned earlier, the eigenfrequency coefficients β_i are related to eigenfrequencies by Equation (2.21) for constant section member and Equation (3.10) for tapered section member and eigenfrequencies can be computed.

3.5. Constants of Eigenfunctions

As can be seen in the equation (3.1) to (3.4), there are four constants for each of the eigenfunctions. For the case of Euler-Bernoulli beam with three multiple masses, a continuous beam is discretized into four beam elements and they contain a total of sixteen constants. The sixteen constants must be determined in order to express each mode shape. Therefore, sixteen conditions are required. Taking into account the boundary conditions at the fixed end, one can recognize the relationships between constants in the first eigenfunction. Rewriting equations (3.15) and (3.16) brings the relationships such as

$$c_1 = -c_3 \tag{3.32}$$

$$c_2 = -c_4 . \tag{3.33}$$

Thus, if one defines $c_1 = A$ and $c_2 = B$, the first eigenfunction (mode function) can be rewritten as

$$f_{1i}(x) = A \cdot (\cos \beta_i \cdot x - \cosh \beta_i \cdot x) + B \cdot (\sin \beta_i \cdot x - \sinh \beta_i \cdot x) . \tag{3.34}$$

Considering the continuity and compatibility conditions in equation (3.28) to (3.31) at $x = x_1$ of mass m_1 with the rewritten eigenfunction of the first beam element in equation (3.34), and the eigenfunction of the second beam element in equation (3.2) yields

$$\begin{aligned} &A\cdot(\cos\beta_i\cdot x_1-\cosh\beta_i\cdot x_1)+B\cdot(\sin\beta_i\cdot x_1-\sinh\beta_i\cdot x_1)\\ &\qquad -c_5\cdot\cos\beta_i\cdot x_1-c_6\cdot\sin\beta_i\cdot x_1-c_7\cdot\cosh\beta_i\cdot x_1-c_8\cdot\sinh\beta_i\cdot x_1=0 \end{aligned} \tag{3.35}$$

$$\begin{aligned} &A\cdot(-\sin\beta_i\cdot x_1-\sinh\beta_i\cdot x_1)+B\cdot(\cos\beta_i\cdot x_1-\cosh\beta_i\cdot x_1)\\ &\qquad +c_5\cdot\sin\beta_i\cdot x_1-c_6\cdot\cos\beta_i\cdot x_1-c_7\cdot\sinh\beta_i\cdot x_1-c_8\cdot\cosh\beta_i\cdot x_1=0 \end{aligned} \tag{3.36}$$

$$\begin{aligned} &A\cdot(-\cos\beta_i\cdot x_1-\cosh\beta_i\cdot x_1)+B\cdot(-\sin\beta_i\cdot x_1-\sinh\beta_i\cdot x_1)\\ &\qquad +c_5\cdot\cos\beta_i\cdot x_1+c_6\cdot\sin\beta_i\cdot x_1-c_7\cdot\cosh\beta_i\cdot x_1-c_8\cdot\sinh\beta_i\cdot x_1=0 \end{aligned} \tag{3.37}$$

$$\begin{aligned} &A\cdot\{(\sin\beta_i\cdot x_1-\sinh\beta_i\cdot x_1)+M_1\cdot\beta_i\cdot(\cos\beta_i\cdot x_1-\cosh\beta_i\cdot x_1)\}\\ &\quad +B\cdot\{(-\cos\beta_i\cdot x_1-\cosh\beta_i\cdot x_1)+M_1\cdot\beta_i\cdot(\sin\beta_i\cdot x_1-\sinh\beta_i\cdot x_1)\}\\ &\qquad -c_5\cdot\sin\beta_i\cdot x_1+c_6\cdot\cos\beta_i\cdot x_1-c_7\cdot\sinh\beta_i\cdot x_1-c_8\cdot\cosh\beta_i\cdot x_1=0 \end{aligned} \tag{3.38}$$

The summation of equations (3.35) and (3.38) gives a new relation of constants as

$$-A\cdot\cosh\beta_i\cdot x_1-B\cdot\sinh\beta_i\cdot x_1-c_7\cdot\cosh\beta_i\cdot x_1-c_8\cdot\sinh\beta_i\cdot x_1=0 \tag{3.39}$$

Subtracting equation (3.37) from equation (3.35) yields

$$A\cdot\cos\beta_i\cdot x_1+B\cdot\sin\beta_i\cdot x_1-c_5\cdot\cos\beta_i\cdot x_1-c_6\cdot\sin\beta_i\cdot x_1=0 \tag{3.40}$$

In a similar manner, the summation of equation (3.36) and (3.38) gives the relation of constants as

$$A\cdot\left\{-\sinh\beta_i\cdot x_1+\frac{1}{2}M_1\cdot\beta_i\cdot(\cos\beta_i\cdot x_1-\cosh\beta_i\cdot x_1)\right\}$$
$$+B\cdot\left\{-\cosh\beta_i\cdot x_1+\frac{1}{2}M_1\cdot\beta_i\cdot(\sin\beta_i\cdot x_1-\sinh\beta_i\cdot x_1)\right\} \tag{3.41}$$
$$-c_7\cdot\sinh\beta_i\cdot x_1-c_8\cdot\cosh\beta_i\cdot x_1=0.$$

Subtracting equation (3.38) from (3.36) yields a relation as

$$A\cdot\left\{-\sin\beta_i\cdot x_1+\frac{1}{2}M_1\cdot\beta_i\cdot(-\cos\beta_i\cdot x_1+\cosh\beta_i\cdot x_1)\right\}$$
$$+B\cdot\left\{\cos\beta_i\cdot x_1+\frac{1}{2}M_1\cdot\beta_i\cdot(-\sin\beta_i\cdot x_1+\sinh\beta_i\cdot x_1)\right\}+c_5\cdot\sin\beta_i\cdot x_1-c_6\cdot\cos\beta_i\cdot x_1=0 \tag{3.42}$$
.

It can be seen that equations (3.41) and (3.39) are expressed by constants c_7 and c_8, and equations (3.42) and (3.40) contains constants c_5 and c_6. Thus, the constants in the second eigenfunction can be determined with constants A and B from the first eigenfunction using relations given by equations (3.39) to (3.42).

$$c_5=\left\{1+\frac{1}{2}\cdot M_1\cdot\beta_i\cdot(\cos\beta_i\cdot x_1\cdot\sin\beta_i\cdot x_1-\cosh\beta_i\cdot x_1\cdot\sin\beta_i\cdot x_1)\right\}\cdot A$$
$$+\frac{1}{2}\cdot M_1\cdot\beta_i\cdot\left\{1-\cos^2\beta_i\cdot x_1-\sinh\beta_i\cdot x_1\cdot\sin\beta_i\cdot x_1\right\}\cdot B \tag{3.43}$$

$$c_6=\frac{1}{2}\cdot M_1\cdot\beta_i\cdot\left\{-\cos^2\beta_i\cdot x_1+\cosh\beta_i\cdot x_1\cdot\cos\beta_i\cdot x_1\right\}\cdot A$$
$$+\left\{1+\frac{1}{2}\cdot M_1\cdot\beta_i\cdot(\sinh\beta_i\cdot x_1\cdot\cos\beta_i\cdot x_1-\cos\beta_i\cdot x_1\cdot\sin\beta_i\cdot x_1)\right\}\cdot B \tag{3.44}$$

$$c_7=\left\{-1-\frac{1}{2}\cdot M_1\cdot\beta_i\cdot(\cos\beta_i\cdot x_1\cdot\sinh\beta_i\cdot x_1-\cosh\beta_i\cdot x_1\cdot\sinh\beta_i\cdot x_1)\right\}\cdot A$$
$$+\frac{1}{2}\cdot M_1\cdot\beta_i\cdot\left\{-1+\cosh^2\beta_i\cdot x_1-\sinh\beta_i\cdot x_1\cdot\sin\beta_i\cdot x_1\right\}\cdot B \tag{3.45}$$

$$c_8 = \frac{1}{2} \cdot M_1 \cdot \beta_i \cdot \left\{ \cos \beta_i \cdot x_1 \cdot \cosh \beta_i \cdot x_1 - \cosh^2 \beta_i \cdot x_1 \right\} \cdot A - \left\{ 1 + \frac{1}{2} \cdot M_1 \cdot \beta_i \cdot (\cosh \beta_i \cdot x_1 \cdot \sinh \beta_i \cdot x_1 - \cosh \beta_i \cdot x_1 \cdot \sin \beta_i \cdot x_1) \right\} \cdot B \quad (3.46)$$

In a similar manner, the constants c_9 to c_{12} can be expressed with the constants c_5 to c_8, which means the constants c_9 to c_{12} can be expressed again with the constants A and B. In this manner, all sixteen constants in four eigenfunctions can be rewritten with the constants A and B. This abovementioned process to transform all sixteen constants only with A and B with has been verified with the mathematics software MAPLE, with supplied code in Appendix D. Consequently, the eigenfunction of the last beam element also contains only the constants A and B. Then the relationship of the constants A and B can be obtained by considering the boundary conditions at $x = L_a$ which is a free end.

$$c_{13} \cdot \sin \beta_i \cdot L_a - c_{14} \cdot \cos \beta_i \cdot L_a + c_{15} \cdot \sinh \beta_i \cdot L_a + c_{16} \cdot \cosh \beta_i \cdot L_a = 0 \quad (3.47)$$

As can be seen in Equation (3.47), the boundary conditions at $x = L_a$ are expressed with the constants c_{13} to c_{16}. The constants c_{13} to c_{16} are, as mentioned, can be transformed with the constants A and B. Thus, all constants from c_1 to c_{16} have been rewritten by constants A and B. The sixteen constants expressed with A and B are all provided in Appendix B. As can be seen in Appendix B, eight constants in eigenfunctions of the third and fourth beam elements are very complex. The relationship between constants A and B is therefore considerably difficult to show, so the process

to transform all constants to a constant A is verified with the mathematics software, MAPLE. Base on the verification, using MATLAB, the process to determine all of sixteen constants is performed. The relationship between constant A and B is expressed as

$$B = \mathrm{K}_i \cdot A \tag{3.48}$$

where K_i = coefficient of the relationship between constant A and B

Now, the eigenfunctions have been reformed only with the constant A. Substituting $A = 1$ into all of four eigenfunctions, the normalized mode shapes can be obtained. As verified in the prior procedure, the eigenfunctions (mode functions) are expressed only with constant A. However, the constant A cannot be obtained using the sixteen conditions. To define the constant A, at least one more additional condition should be supplied. As taken into account when covering the conventional continuous system model, the orthogonality condition of mode shape functions must be met. As already considered in the conventional model, the orthogonality condition of normal mode shape functions is shown in Equation (2.36) with δ_{ij} is Kronecker delta. Although there are four eigenfunctions for each of four discretized beam elements, each should satisfy the orthogonality condition. Therefore, for convenient calculation, first eigenfunction, which is the simple function provided in Equation (3.29), can be used.

$$f_{1i}(x) = C_{1i} \cdot \left\{ (\cos \beta_i \cdot x - \cosh \beta_i \cdot x) + \mathrm{K}_i \cdot (\sin \beta_i \cdot x - \sinh \beta_i \cdot x) \right\} \tag{3.49}$$

here, $C_{1i} = A$

Substituting Equation (3.49) into the orthogonality condition,

$$\int_0^{L_a} \rho_a \cdot A_a \cdot f_i(x) \cdot f_j(x)\, dx = \rho \cdot A \cdot \int_0^{L_a} f_i(x)^2\, dx$$

$$= \rho_a \cdot A_a \cdot C_{1i}{}^2 \cdot \int_0^{L_a} \left\{(\cos\beta_i \cdot x - \cosh\beta_i \cdot x) + \mathrm{K}_i \cdot (\sin\beta_i \cdot x - \sinh\beta_i \cdot x)\right\}^2 dx = 1$$

$$C_{1i} = \left\{ \frac{1}{\rho_a \cdot A_a \cdot \int_0^{L_a} \left\{(\cos\beta_i \cdot x - \cosh\beta_i \cdot x) + \mathrm{K}_i \cdot (\sin\beta_i \cdot x - \sinh\beta_i \cdot x)\right\}^2 dx} \right\}^{\frac{1}{2}} . \qquad (3.50)$$

The process to determine the sixteen constants of four eigenfunctions is applicable to the constant section and approximate tapered section models. When considering this process for the tapered section model, one must be aware the geometric properties, mentioned in (3.10), while in differentiating eigenfunctions.

3.6. Initial Conditions and Time Dependent Function

The analytical solution with a discretized continuous system model contains a spatial function and a time function. The spatial function has been discussed in this section to apply the additional parameters like multiple masses and rotational inertia. However, the initial conditions are already provided and it is not influenced by addition of geometric or material properties. Therefore, the same initial conditions and corresponding time dependent function provided in section 2.5 of Section 2 are taken into account for the post-processing.

3.7. Conclusion

The discretized model of a continuous system enables the addition of additional concentrated masses on traffic signal structure, contrary to conventional model. In addition, using this discretized model, the analytical model for the approximate tapered section member was developed. During modal analysis of these analytical models, obtaining exact modal responses is significant because the time domain responses will be used to determine the fundamental frequencies of the structure. The analytical model developed from this section will provide the eigenfrequencies of the members of traffic signal structure and it will be discussed in following sections.

4. VARIOUS BOUNDARY, CONTINUITY AND COMPATIBILITY CONDITIONS

4.1. Various Types of Boundary Conditions

For the modal analysis of traffic signal structures incorporating the distributed parameter method (continuous system), the boundary conditions of the system are significant. In the continuous system approach, modifications to the boundary conditions will take into account the geometric properties of the rest of the system. As a result, it is required to accurately describe the characteristics of the system and apply them to the boundaries. Furthermore, traffic signal structure systems have very simple geometric configuration, thus static analyses can be simply undertaken. However, for dynamic analyses, because the dynamic characteristics of the system are sensitive to boundary conditions, one must develop a model using multiple boundary conditions to capture the realistic behaviors of the given traffic signal structure.

4.1.1. Fixed-Free Boundary Conditions

The vibrations of a traffic signal structure can be distinguished into two motions, in- and out-of-plane. Fixed-free boundary conditions are the most basic assumption for the cantilevered flexural beam. These boundary conditions present zero-displacement and zero-angle of deflection, and zero-shear force and zero-bending moment, which can be mathematically expressed as

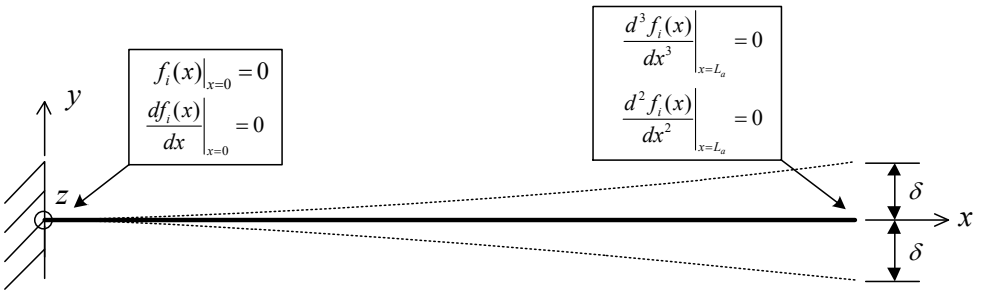

Figure 4.1: Transverse Vibration with Fixed-Free Boundary Conditions

These boundary conditions have been already discussed, as seen in Figure 4.1, in the previous section 2.3 of Section 2, expressed in Equation (3.11) through (3.14). Substituting the mode shape function given in Equation (2.9) into boundary conditions yields Equations (2.15) through (2.18) and the reformed matrix for the boundary condition is shown in Equation (2.19). As have seen in the section, the determinant of the matrix of the boundary conditions provides the eigenfrequency equation shown in Equation (2.20). Through computing this equation, eigenfrequencies of the structure with fixed-free ends are obtained.

4.1.2. Rotational Spring and Free Boundary Conditions

In investigating vibrations of traffic signal structure, it is initially assumed that the support types of the members, mast arm and pole, have fixed-free boundary conditions. However, a certain amount of stiffness does exist at the support and effects of the stiffness in not negligible to comprehend the dynamic characteristics of traffic signal structure. When considering in-plane motion, with fixed-free boundary conditions, the eigenfrequencies tends to be overestimated. It is due to infinite stiffness at the fixed end.

Therefore, rotational spring stiffness equivalent to bending stiffness of a pole is applied at left end of the flexural beam, taking into account the pole's effect. In a similar manner, for out-of-plane motion, an equivalent rotational spring stiffness equivalent to torsional stiffness of a pole is considered. Thus, the boundary conditions shown in Figure 4.2 are supplied in mathematical expression as follows

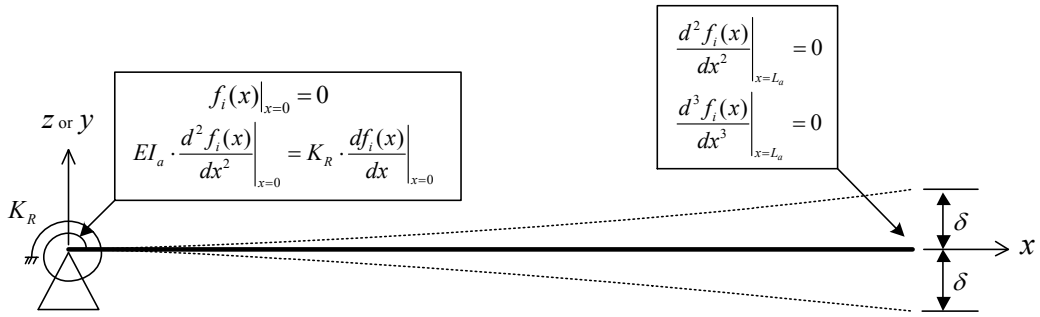

Figure 4.2: Transverse Vibration with Rotational Spring and Free Boundary Conditions

$$f_i(x)\big|_{x=0} = 0 \tag{4.1}$$

$$EI_a \cdot \frac{d^2 f_i(x)}{dx^2}\bigg|_{x=0} = K_R \cdot \frac{d\, f_i(x)}{dx}\bigg|_{x=0} \tag{4.2}$$

$$\frac{d^2 f_i(x)}{dx^2}\bigg|_{x=L_a} = 0 \tag{4.3}$$

$$\frac{d^3 f_i(x)}{dx^3}\bigg|_{x=L_a} = 0 \tag{4.4}$$

.

In Equation (4.13), a rotational spring stiffness K_R is introduced, which is equivalent to bending stiffness of a pole for the case of in-plane motion and to torsional stiffness of a pole for out-of-plane motion. The bending and torsional stiffness are expressed as follows

$$\text{In-plane: } K_R = \frac{E \cdot I_{zz\_pole}}{L_p} = \frac{E}{L_p}\left(\frac{\pi}{64} \cdot \left(d_{po}^4 - d_{pi}^4\right)\right) = \frac{E \cdot \pi}{32 L_p} \cdot \left(d_{po}^4 - d_{pi}^4\right) \tag{4.5}$$

$$\text{Out-of-plane: } K_R = \frac{G \cdot J_{pole}}{L_p} = \frac{G}{L_p}\left(\frac{\pi}{32} \cdot \left(d_{po}^4 - d_{pi}^4\right)\right) = \frac{G\pi}{32 L_p} \cdot \left(d_{po}^4 - d_{pi}^4\right) \tag{4.6}$$

.

where I_{zz_pole}: Moment of Inertia of a pole around z-axis

J_{pole} : Polar Moment of Inertia of a pole around y-axis

Thus, applying the mode function $f_i(x)$ to the given boundary conditions yields as

$$c_1 + c_3 = 0 \tag{4.7}$$

$$c_1 + \frac{K_R}{EI_a\beta_i} \cdot c_2 - c_3 + \frac{K_R}{EI_a\beta_i} \cdot c_4 = 0 \tag{4.8}$$

$$-c_1 \cdot \cos\beta_i \cdot L_a - c_2 \cdot \sin\beta_i \cdot L_a + c_3 \cdot \cosh\beta_i \cdot L_a + c_4 \cdot \sinh\beta_i \cdot L_a = 0 \quad (4.9)$$

$$c_1 \cdot \sin\beta_i \cdot L_a - c_2 \cdot \cos\beta_i \cdot L_a + c_3 \cdot \sinh\beta_i \cdot L_a + c_4 \cdot \cosh\beta_i \cdot L_a = 0\,. \quad (4.10)$$

Equations (4.7) to (4.10) can be rewritten in the matrix form as

$$\begin{bmatrix} 1 & 0 & 1 & 0 \\ 1 & \dfrac{K_R}{EI_a\beta_i} & -1 & \dfrac{K_R}{EI_a\beta_i} \\ -\cos\beta_i \cdot L_a & -\sin\beta_i \cdot L_a & \cosh\beta_i \cdot L_a & \sinh\beta_i \cdot L_a \\ \sin\beta_i \cdot L_a & -\cos\beta_i \cdot L_a & \sinh\beta_i \cdot L_a & \cosh\beta_i \cdot L_a \end{bmatrix} \cdot \begin{Bmatrix} c_1 \\ c_2 \\ c_3 \\ c_4 \end{Bmatrix} = \begin{bmatrix} 0 \\ 0 \\ 0 \\ 0 \end{bmatrix} \quad (4.11)$$

For the satisfactory of Equation (4.11), it is required to take into account the singularity of matrix. For conventional model of continuous beam system, Equation (4.11) provides the eigenfrequency equation as

$$1 + \cos\beta_i \cdot L_a \cdot \cosh\beta_i \cdot L_a - \frac{EI\beta_i}{K_R}(\sin\beta_i \cdot L_a \cdot \cosh\beta_i \cdot L_a - \sinh\beta_i \cdot L_a \cdot \cos\beta_i \cdot L_a) = 0 \quad (4.12)$$

.

From this eigenfrequency equation, the values of the eigenfrequency coefficients β_i can be determined, and then eigenfrequencies are consequently obtained from the coefficients.

4.1.3. Fixed Free Boundary Conditions with a Point Mass and Rotational Inertia at the Tip

The fixed-free boundary conditions for cantilever beam were taken into account in previous section. In this section, an additional mass is attached to the cantilever pole, which leads to modification of boundary conditions. Suppose that there is a point mass at the tip of a pole and inertia generated through rotation of the point mass. In this case, boundary conditions ate the fixed end do not have any change, but free end. These conditions can be mathematically expressed as

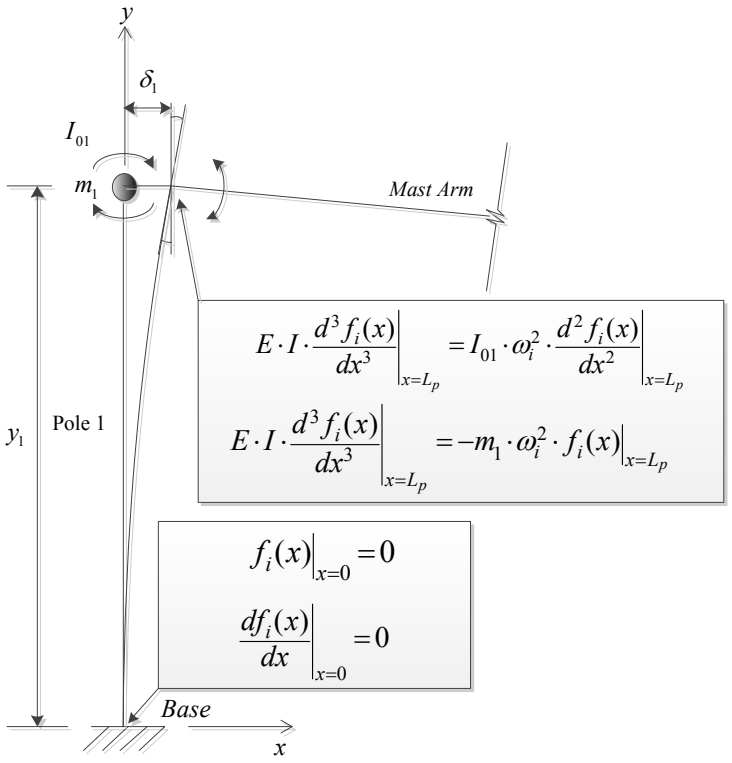

Figure 4.3: Fixed and Free Boundary Conditions with Mass and Rotational Inertia

$$f_i(y)\big|_{y=0} = 0 \tag{4.13}$$

$$\left.\frac{df_i(y)}{dy}\right|_{y=0} = 0 \tag{4.14}$$

$$E \cdot I \cdot \left.\frac{d^2 f_i(y)}{dy^2}\right|_{y=L_p} = I_{01} \cdot \omega_i^2 \cdot \left.\frac{d^2 f_i(y)}{dy^2}\right|_{y=L_p} \tag{4.15}$$

$$E \cdot I \cdot \left.\frac{d^3 f_i(y)}{dy^3}\right|_{y=L_p} = -m_1 \cdot \omega_i^2 \cdot f_i(y)\big|_{y=L_p} \tag{4.16}$$

.

where I_{01} is the mass moment of inertia for rotating motion of attachments and m_1 is the mass of the attachments, as depicted in Figure 4.3. The equations provided above can be re-expressed substituting the spatial function $f_i(x)$ such as

$$c_1 = -c_3 \tag{4.17}$$

$$c_2 = -c_4 \tag{4.18}$$

$$\begin{aligned}&\left(\cos\beta_i L_p - \eta_p \cdot \beta_i^3 \cdot \sin\beta_i L_p\right)\cdot c_1 + \left(\sin\beta_i L_p + \eta_p \cdot \beta_i^3 \cdot \cos\beta_i L_p\right)\cdot c_2 \\ &+\left(-\cosh\beta_i L_p + \eta_p \cdot \beta_i^3 \cdot \sinh\beta_i L_p\right)\cdot c_3 + \left(-\sinh\beta_i L_p + \eta_p \cdot \beta_i^3 \cdot \cosh\beta_i L_p\right)\cdot c_4 = 0\end{aligned} \tag{4.19}$$

$$\begin{aligned}&\left(\sin\beta_i L_p - \xi_p \cdot \beta_i \cdot \cos\beta_i L_p\right)\cdot c_1 + \left(-\cos\beta_i L_p + \xi_p \cdot \beta_i \cdot \sin\beta_i L_p\right)\cdot c_2 \\ &+\left(\sinh\beta_i L_p + \xi_p \cdot \beta_i \cdot \cosh\beta_i L_p\right)\cdot c_3 + \left(\cosh\beta_i L_p + \xi_p \cdot \beta_i \cdot \sinh\beta_i L_p\right)\cdot c_4 = 0\end{aligned} \tag{4.20}$$

.

where, $\eta_p = \dfrac{I_{01}}{\rho_p A_p}$ and $\xi_p = \dfrac{m_1}{\rho_p A_p}$

The Equations (4.23) to (4.26) can be reformed in matrix form such as

$$\begin{bmatrix} A_{11} & A_{12} & A_{13} & A_{14} \\ A_{21} & A_{22} & A_{23} & A_{24} \\ A_{31} & A_{32} & A_{33} & A_{34} \\ A_{41} & A_{42} & A_{43} & A_{44} \end{bmatrix} \cdot \begin{Bmatrix} c_1 \\ c_2 \\ c_3 \\ c_4 \end{Bmatrix} = \begin{bmatrix} 0 \\ 0 \\ 0 \\ 0 \end{bmatrix} \tag{4.21}$$

$$A_{11} = 1 \quad A_{12} = 0 \qquad A_{13} = 1 \quad A_{14} = 0$$

$$A_{21} = 0 \quad A_{22} = 1 \qquad A_{23} = 0 \quad A_{24} = 0$$

$$A_{31} = \cos\beta_i L_p - \eta_p \cdot \beta_i^3 \cdot \sin\beta_i L_p \qquad A_{32} = \sin\beta_i L_p + \eta_p \cdot \beta_i^3 \cdot \cos\beta_i L_p$$

$$A_{33} = -\cosh\beta_i L_p + \eta_p \cdot \beta_i^3 \cdot \sinh\beta_i L_p \qquad A_{34} = -\sinh\beta_i L_p + \eta_p \cdot \beta_i^3 \cdot \cosh\beta_i L_p$$

$$A_{41} = \sin\beta_i L_p - \xi_p \cdot \beta_i \cdot \cos\beta_i L_p \qquad A_{42} = -\cos\beta_i L_p + \xi_p \cdot \beta_i \cdot \sin\beta_i L_p$$

$$A_{43} = \sinh\beta_i L_p + \xi_p \cdot \beta_i \cdot \cosh\beta_i L_p \qquad A_{44} = \cosh\beta_i L_p + \xi_p \cdot \beta_i \cdot \sinh\beta_i L_p \quad .$$

As repeatedly mentioned earlier, matrix provided in equation (4.27) is used to solve the eigenfrequency coefficients, eventually eigenfrequency. Moreover, the matrix of boundary, continuity and compatibility condition in the discretized model may contain if boundary conditions of a real model has same properties.

4.1.4. Rotational Spring-Free Boundary Conditions with a Point Mass and Rotational Inertia at the Tip

In the previous section, it was concerned about the fixed support and free boundary conditions attached a point mass and rotational inertia of attachments. Now, under same conditions, the support type is changed to apply a rotational spring as seen in Figure 4.4.

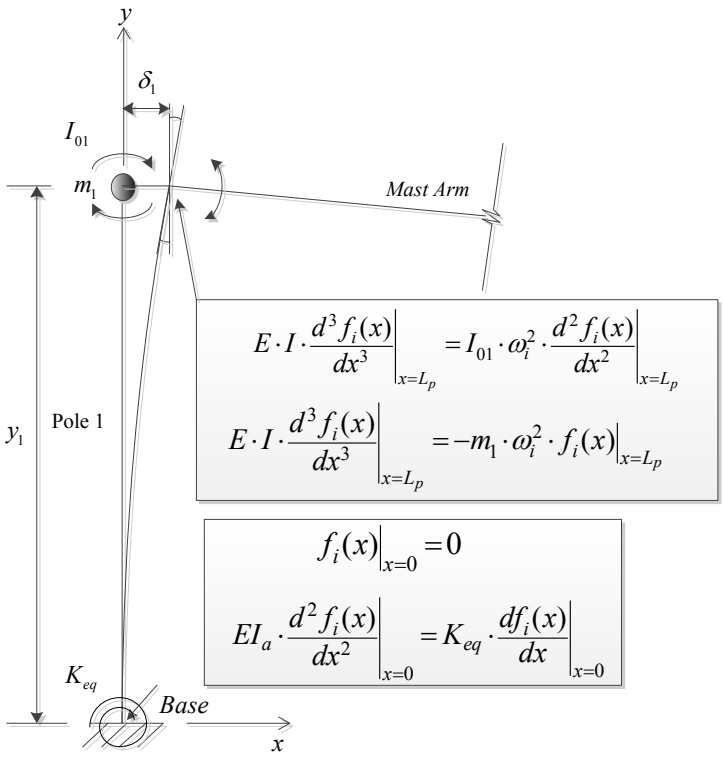

Figure 4.4: Rotational Spring-Free Boundary Condition with Mass and Inertia

$$f_i(x)\big|_{x=0} = 0 \tag{4.22}$$

$$EI_p \cdot \frac{d^2 f_i(x)}{dx^2}\bigg|_{x=0} = K_{eq} \cdot \frac{df_i(x)}{dx}\bigg|_{x=0} \tag{4.23}$$

$$E \cdot I \cdot \frac{d^3 f_i(x)}{dx^3}\bigg|_{x=L_p} = I_{01} \cdot \omega_i^2 \cdot \frac{d^2 f_i(x)}{dx^2}\bigg|_{x=L_p} \tag{4.24}$$

$$E \cdot I \cdot \frac{d^3 f_i(x)}{dx^3}\bigg|_{x=L_p} = -m_1 \cdot \omega_i^2 \cdot f_i(x)\big|_{x=L_p} \tag{4.25}$$

.

where K_{eq} is the equivalent rotational spring stiffness. The equations provided above can be re-expressed substituting the spatial function $f_i(x)$ such as

$$c_1 = -c_3 \tag{4.26}$$

$$c_1 + \frac{K_{eq}}{EI_p\beta_i} \cdot c_2 - c_3 + \frac{K_{eq}}{EI_p\beta_i} \cdot c_4 = 0 \tag{4.27}$$

$$\begin{aligned}&\left(\cos\beta_i L_p - \eta_p \cdot \beta_i^3 \cdot \sin\beta_i L_p\right) \cdot c_1 + \left(\sin\beta_i L_p + \eta_p \cdot \beta_i^3 \cdot \cos\beta_i L_p\right) \cdot c_2 \\ &+ \left(-\cosh\beta_i L_p + \eta_p \cdot \beta_i^3 \cdot \sinh\beta_i L_p\right) \cdot c_3 + \left(-\sinh\beta_i L_p + \eta_p \cdot \beta_i^3 \cdot \cosh\beta_i L_p\right) \cdot c_4 = 0\end{aligned} \tag{4.28}$$

$$\begin{aligned}&\left(\sin\beta_i L_p - \xi_p \cdot \beta_i \cdot \cos\beta_i L_p\right) \cdot c_1 + \left(-\cos\beta_i L_p + \xi_p \cdot \beta_i \cdot \sin\beta_i L_p\right) \cdot c_2 \\ &+ \left(\sinh\beta_i L_p + \xi_p \cdot \beta_i \cdot \cosh\beta_i L_p\right) \cdot c_3 + \left(\cosh\beta_i L_p + \xi_p \cdot \beta_i \cdot \sinh\beta_i L_p\right) \cdot c_4 = 0\end{aligned} \tag{4.29}$$

.

where, $\eta_p = \dfrac{I_{0\_arm}}{\rho_p A_p}$ *and* $\xi_p = \dfrac{m_a}{\rho_p A_p}$

The Equations (4.26) to (4.29) can be reformed in matrix form shown in (4.30).

$$\begin{bmatrix} A_{11} & A_{12} & A_{13} & A_{14} \\ A_{21} & A_{22} & A_{23} & A_{24} \\ A_{31} & A_{32} & A_{33} & A_{34} \\ A_{41} & A_{42} & A_{43} & A_{44} \end{bmatrix} \cdot \begin{Bmatrix} c_1 \\ c_2 \\ c_3 \\ c_4 \end{Bmatrix} = \begin{bmatrix} 0 \\ 0 \\ 0 \\ 0 \end{bmatrix} \tag{4.30}$$

$$A_{11} = 1 \quad A_{12} = 0 \qquad A_{13} = 1 \quad A_{14} = 0$$

$$A_{21} = 1 \quad A_{22} = \frac{K_{eq}}{EI_p\beta_i} \qquad A_{23} = -1 \quad A_{24} = \frac{K_{eq}}{EI_p\beta_i}$$

$$A_{31} = \cos\beta_i L_p - \eta_p \cdot \beta_i^3 \cdot \sin\beta_i L_p \qquad A_{32} = \sin\beta_i L_p + \eta_p \cdot \beta_i^3 \cdot \cos\beta_i L_p$$

$$A_{33} = -\cosh\beta_i L_p + \eta_p \cdot \beta_i^3 \cdot \sinh\beta_i L_p \qquad A_{34} = -\sinh\beta_i L_p + \eta_p \cdot \beta_i^3 \cdot \cosh\beta_i L_p$$

$$A_{41} = \sin\beta_i L_p - \xi_p \cdot \beta_i \cdot \cos\beta_i L_p \qquad A_{42} = -\cos\beta_i L_p + \xi_p \cdot \beta_i \cdot \sin\beta_i L_p$$

$$A_{43} = \sinh\beta_i L_p + \xi_p \cdot \beta_i \cdot \cosh\beta_i L_p \qquad A_{44} = \cosh\beta_i L_p + \xi_p \cdot \beta_i \cdot \sinh\beta_i L_p \quad .$$

A matrix provided in Equation (4.30) is used to solve the eigenfrequency coefficients, eventually eigenfrequency. This boundary conditions will be taken into account to reach to the real motion of the given traffic signal structure.

4.2. Various Types of Continuity and Compatibility Conditions

In the discretized continuous system model, it is critical to take into account continuity and compatibility conditions at connecting points of discrete beam elements. When attaching additional parameters like point masses or inertia between elements, the effects of the parameters can be mathematically expressed and eigenfrequencies and mode shapes can be solved. In this section, therefore several types of continuity and compatibility conditions which can be applied to a traffic signal structure are studied and derived to adopt the analytical model.

4.2.1. Multiple Concentrated Masses on Flexural Beam

There are typically several attachments on the mast arm of a traffic signal structures. In this section, the effect of the multiple point masses is considered to account for traffic signal clusters.

As seen in Figure 4.5, the continuity and compatibility conditions are attached point multiple masses. These generalized expressions for these conditions have already supplied earlier. For convenience, those are provided herein again as follows

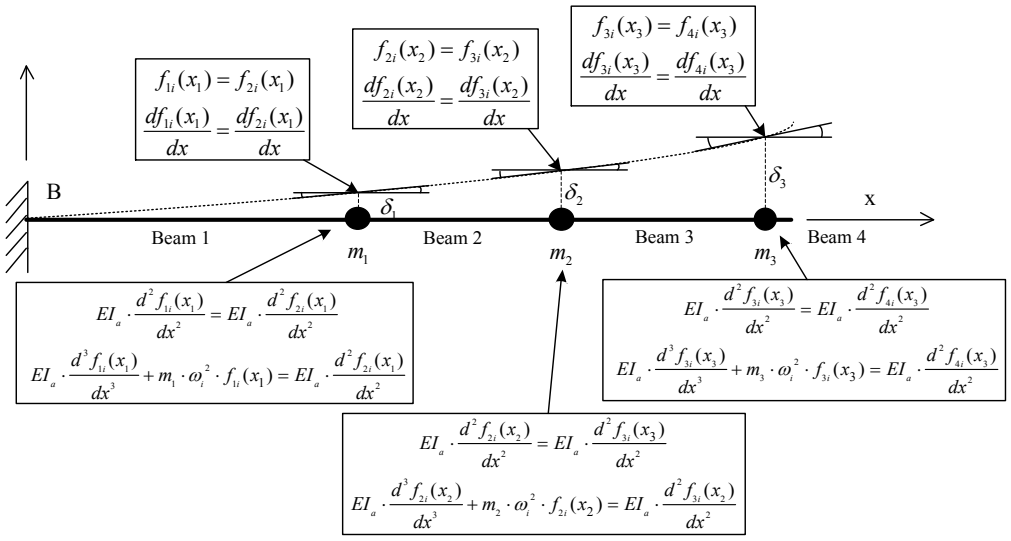

Figure 4.5: Continuity and Compatibility Conditions with Multiple Masses

$$f_{ni}(x)\Big|_{x=x_n} = f_{(n+1)i}(x)\Big|_{x=x_n} \tag{4.31}$$

$$\frac{df_{ni}(x)}{dx}\Big|_{x=x_n} = \frac{df_{(n+1)i}(x)}{dx}\Big|_{x=x_n} \tag{4.32}$$

$$\frac{d^2 f_{ni}(x)}{dx^2}\Big|_{x=x_n} = \frac{d^2 f_{(n+1)i}(x)}{dx^2}\Big|_{x=x_n} \tag{4.33}$$

$$\frac{d^3 f_{ni}(x)}{dx^3}\Big|_{x=x_n} + M_n \cdot \beta_i^4 \cdot f_{ni}(x) = \frac{d^3 f_{(n+1)i}(x)}{dx^3}\Big|_{x=x_n} \tag{4.34}$$

$$\text{where, } M_n = \frac{m_n}{\rho_a A_a} \qquad n = 1,\ 2,\ 3,.....$$

.

These generalized expressions for continuity and compatibility conditions are applied at each connecting point, therefore a total of twelve equations are provided if there are

three multiple point masses. Thus, if n multiple masses are provided, $4n$ equations are obtained. The twelve equations of continuity and compatibility conditions for the given system in Figure 4.6 can be check in section B.1 of Appendix B.

4.2.2. Concentrated Mass and Rotational Inertia on the Flexural Pole

The continuity and compatibility conditions of a mast arm with three signal clusters were taken into account in the previous section. However, for the case of a pole, the types of additional parameter are the combination of mass and rotational inertia from various attachments. Vibrations of a pole are influenced not only by the concentrated mass of a mast arm and connection plates, but also by their rotational inertia.

As can be seen in Figure 4.6, a pole is discretized into two flexural pole elements. In addition, a concentrated mass and a rotational inertia of a mast arm are applied to the connecting point of two elements. These conditions can be mathematically expressed as follows

$$f_{1i}(y_1) = f_{2i}(y_1) \tag{4.35}$$

$$\frac{df_{1i}(y_1)}{dy} = \frac{df_{2i}(y_1)}{dy} \tag{4.36}$$

$$EI_a \cdot \frac{d^2 f_{1i}(y_1)}{dy^2} + I_{o1} \cdot \omega_i^2 \cdot \frac{df_i(y_1)}{dy} = EI_a \cdot \frac{d^2 f_{2i}(y_1)}{dy^2} \tag{4.37}$$

$$EI_a \cdot \frac{d^3 f_{1i}(y_1)}{dy^3} + m_1 \cdot \omega_i^2 \cdot f_{1i}(y_1) = EI_a \cdot \frac{d^2 f_{2i}(y_1)}{dy^2} \tag{4.38}$$

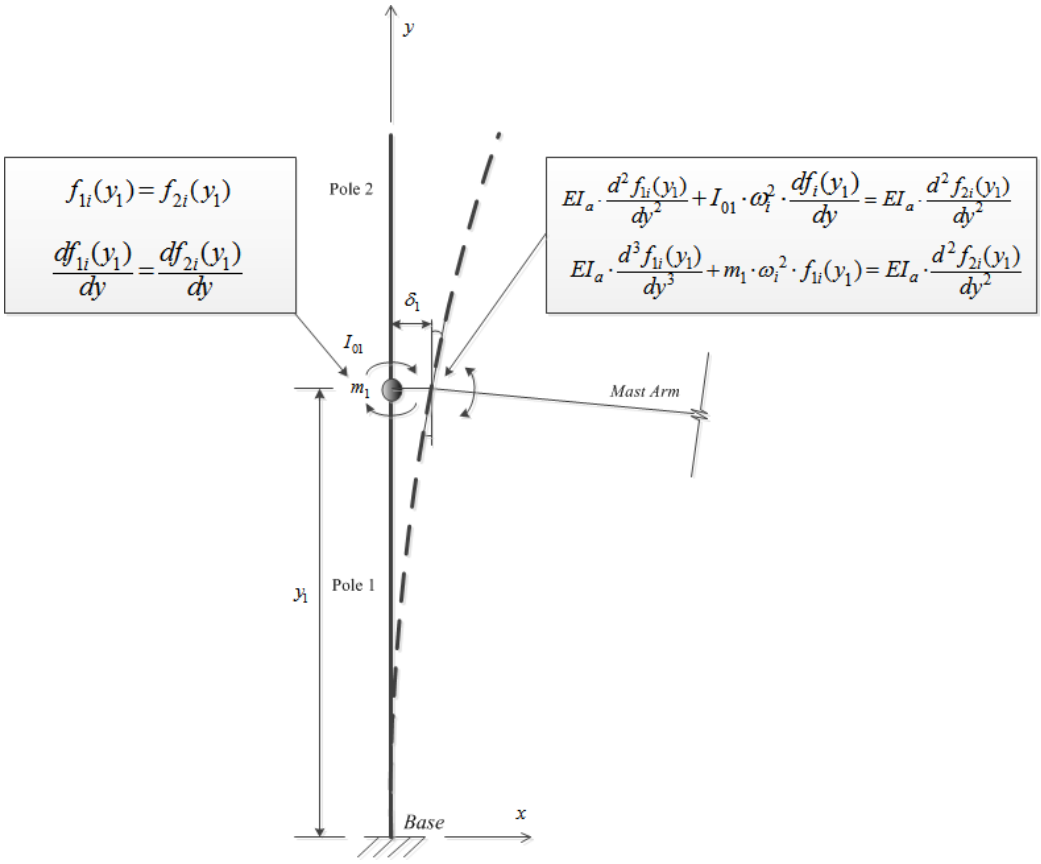

Figure 4.6: Continuity and Compatibility Conditions with Mass and Inertia

Equations (4.35) to (4.38) represent the continuity and compatibility conditions at the arm-to-pole connection. These are for the case where there is only one connection point in the pole. For the case which will be considered the given parameters at different multi-locations, and also for convenient application to computation works, the generalized form of the conditions is provided in this thesis, as follows

$$f_{ni}(y)\big|_{y=y_n} = f_{(n+1)i}(y)\big|_{y=y_n} \tag{4.39}$$

$$\left.\frac{df_{ni}(y)}{dy}\right|_{y=y_n} = \left.\frac{df_{(n+1)i}(y)}{dy}\right|_{y=y_n} \tag{4.40}$$

$$\left.\frac{d^2 f_{ni}(y)}{dy^2}\right|_{y=y_n} + I_{Mn}\cdot\beta_i^3\cdot\left.\frac{df_i(y)}{dy}\right|_{y=y_n} = \left.\frac{d^2 f_{(n+1)i}(y)}{dy^2}\right|_{y=y_n} \tag{4.41}$$

$$\left.\frac{d^3 f_{ni}(y)}{dy^3}\right|_{y=y_n} + M_n\cdot\beta_i\cdot f_{ni}(y) = \left.\frac{d^3 f_{(n+1)i}(y)}{dy^3}\right|_{y=y_n} \tag{4.42}$$

where,

$$M_n = \frac{m_n}{\rho_p A_p}$$

$$I_{Mn} = \frac{I_{on}}{\rho_p A_p}$$

$$n = 1,\ 2,\ 3,.....$$

4.3. Continuity and Compatibility Conditions for Superposition of Arm and Pole

The initial assumption is that the traffic signal structure system is linearly elastic and linearly continuous. For the initial assumption, one can take into account that members can be superposed at the arm-to-pole connection with consideration of connectivity conditions. The connectivity conditions at the arm-to-pole connection should be separately considered in two different motion, in-plane and out-of-plane motions.

4.3.1. Superposition of In-Plane Motion

For in-plane motion of traffic signal structure, both members, a mast-arm and a pole, have transverse vibrations. Thus, the transverse displacements of a pole at the tip, as described in Figure 4.7, can be superposed with axial displacements of a mast-arm and the transverse displacement of a mast-arm by deflection angle of a pole at the tip can be superposed to the transverse displacement for flexural motion of a mast-arm. It can be written

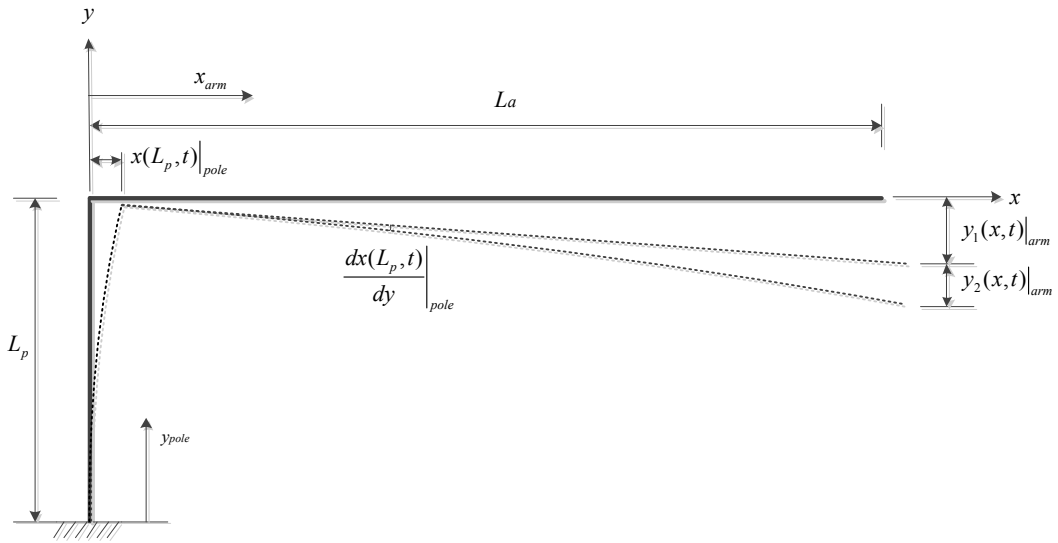

Figure 4.7: Superposition of Traffic Signal Structure Members for In-Plane Motion

$$x(t)\big|_{arm} = x + x(L_p,t)\big|_{pole} \tag{4.43}$$

$$y(x,t)\big|_{arm} = y_1(x,t)\big|_{arm} + y_2(x,t)\big|_{arm} \tag{4.44}$$

where, $$y_2(x,t)\big|_{arm} = x \cdot \frac{dx(L_p,t)}{dy}\bigg|_{pole}$$

Considering these relationships shown in equation (4.43) and (4.44), the total responses of a traffic signal structure can be determined, which is time domain responses.

4.3.2. Superposition of Out-of-Plane Motion

For the out-of-plane motion of traffic signal structure, mast-arm and pole have transverse vibrations. The response from the transverse vibration of mast arm, as seen in Figure 4.8, is $z_1(x,t)\big|_{arm}$ and the response of transverse vibration of pole at the tip is

$z_2(L_p,t)\big|_{pole}$. These responses are superposed for the final out-of-plane motion responses which can be written as follows

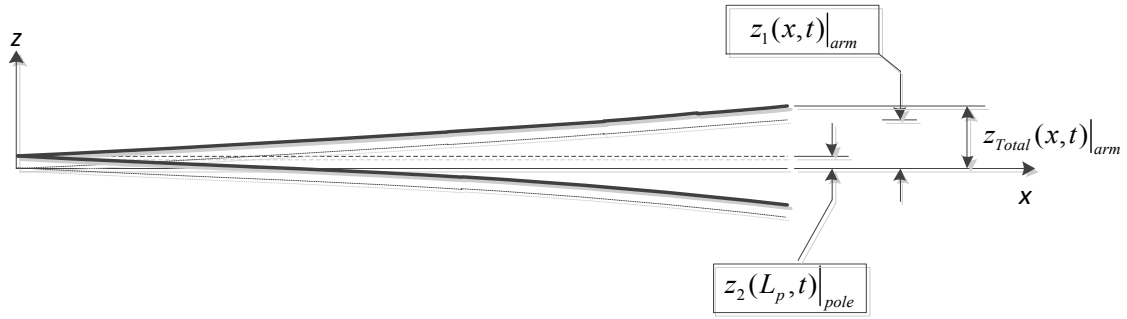

Figure 4.8: Superposition of Traffic Signal Structure Members for Out-of-Plane Motion

$$z_{Total}(x,t)\big|_{arm} = z_1(x,t)\big|_{arm} + z_2(L_p,t)\big|_{pole} \tag{4.45}$$

Consequently, the combined responses of a traffic signal structure for out-of-plane motion can be obtained with Equation (4.45). This provides the time domain responses of a traffic signal structure.

4.4.Conclusion

The modifications of boundary, continuity and compatibility conditions are considerably critical to obtain an analytical solution for dynamic characteristics of traffic signal structure. In this section, several types of boundary conditions, continuity and compatibility conditions have been discussed to describe real motion of traffic signal structures. The expressions are complex to comprehend at one glance, but t they reflect precise understanding of the vibration mechanisms. Because all boundary, continuity and compatibility conditions affect the behavior of the structure, the appropriate modifications of these conditions will be able to give the exact solutions of traffic signal structure vibration.

5. ANALYTICAL SOLUTIONS OF TRAFFIC SIGNAL STRUCTURE

5.1. Traffic Signal Structure with 44-ft. Mast Arm

In this thesis, a traffic signal structure with 44-ft. mast arm is used for validation of the analytical solution with the continuous system method. The dynamic characteristics of the structure are provided using the analytical model developed in previous sections. For the analytical solution, both the conventional and discretized continuous system models are solved and the corresponding results are presented in this chapter.

5.2. Geometric and Material Properties

For the input data to the analytical model, the geometric and material properties of the traffic signal structure with 44-ft. mast arm are provided according to the Texas Department of Transportation's (TxDOT) SMA-100(1)-99 specifications, as shown in Table 5.1. The numbers provided in the table are the dimensions from real measurements of the structure. Dimensions of the structure do not exactly match the installed traffic signal structure. Moreover, because the real linearly tapered member could not be applied to the analytical solution due to varying properties, the simplification of the dimensions are required for the analytical solutions. Therefore, the simple properties are used in the analytical model with conventional idea, which are provided in Table 5.2.

Table 5.1: Geometric Properties of 44-ft. Traffic Signal Structure

	Shaft Length [ft./in.]	D_B [in.][1]	D_T [in.][2]	t [in.][3]
Mast-Arm	43 / 516	10.98	5.01	0.239
Pole	30 / 360	14.64	10.35	0.25

Table 5.2: Geometric Properties of the Constant Traffic Signal Structure

Member	Shaft Length [ft./in.]	D_w [in.][4]	t [in/]
Mast-Arm	43 / 516	8.99	0.239
Pole	30 / 360	13.21	0.239

However, the discretized continuous system model can take into account the variable properties of the tapered section member although it is not fully tapered cross-section. The four-element discretized beam model, shown in Figure 5.1, provided in this study is shown in Table 5.3.

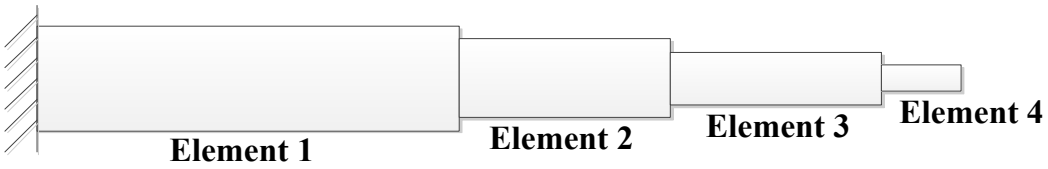

Figure 5.1: Discretized Continuous System of Traffic Signal Structure Members with Varying Cross-sections

[1] Diameter at the bottom plate of the member
[2] Diameter at the tip of the member
[3] Thickness of the member
[4] Diameter at 2/3 point

Table 5.3: Varying Cross-section Properties

	Element 1	Element 2	Element 3	Element 4
Length [ft.]	18	12	12	1
Diameter [in.]	9.73	7.65	5.98	5.08

As stated, the plates at the arm-to-pole connection have considerable mass which is not negligible in the eigenfrequency calculation of the given structure. Thus, the details of the connection for the assembly of two members, mast arm and pole, are shown in Table 5.4. The dimensions of the plates in Table 5.4 are measured dimensions, and do not match dimensions in the specification, TxDOT MA-C-09.

Table 5.4: Details of the Arm-to-Pole Connection

	Width [inch]	Depth [inch[	Thickness [inch]
Arm Base Plate	13	18	1.5 [5]
Pole Connection	13	18	1.5 [6]

The material used to fabricate members of the given traffic signal structure is a steel of which Young's modulus is 29,000,000 psi (200 GPa). The density of steel is 490 pcf (7.85 g/cm^3) and the Poisson's ratio is about 0.3. The given geometric and material properties above are used for the analytical solution as input information.

[5] The original dimension of the arm base plate from the specification of TxDOT is 3 in.
[6] The original dimension of the connection plate of pole from the specification of TxDOT is 1 3/4 in.

5.3. Analytical Solutions: Conventional Continuous System Model

The analytical solutions for the eigenfrequencies from the conventional continuous system model are shown in Table 5.5. As seen in the table, a wide arbitrary range of rotational spring stiffness is applied as boundary conditions. This application is to see the tendency of eigenfrequencies along with varying parameters on the boundary conditions of a cantilever beam. As depicted in Figure 5.2 and Figure 5.3, the eigenfrequencies shows a convergence to the eigenfrequency of the fixed support boundary conditions.

Table 5.5: Eigenfrequencies of Conventional Continuous System Model

UNIT: [Hz]	IN-PLANE				OUT-OF-PLANE			
	ARM		POLE		ARM		POLE	
K_R [7]	1st	2nd	1st	2nd	1st	2nd	1st	2nd
1.00E+06	0.327	5.788	0.520	16.893	0.327	5.788	0.500	15.476
1.00E+07	0.828	6.397	1.424	17.222	0.828	6.397	1.360	15.803
5.00E+07	1.144	7.338	2.466	18.431	1.144	7.338	2.327	17.020
1.00E+08	1.214	7.662	2.913	19.534	1.214	7.662	2.733	18.148
1.50E+08	1.236	7.774	3.139	20.344	1.236	7.774	2.935	18.992
2.50E+08	1.259	7.901	3.372	21.450	1.259	7.901	3.142	20.164
5.00E+08	1.277	8.007	3.593	22.858	1.277	8.007	3.336	21.694
7.50E+08	1.283	8.045	3.680	23.529	1.283	8.045	3.411	22.437
1.00E+09	1.289	8.080	3.725	23.920	1.289	8.080	3.451	22.875
1.00E+10	1.298	8.131	3.861	25.218	1.298	8.131	3.568	24.348

[7] Rotational Spring Stiffness

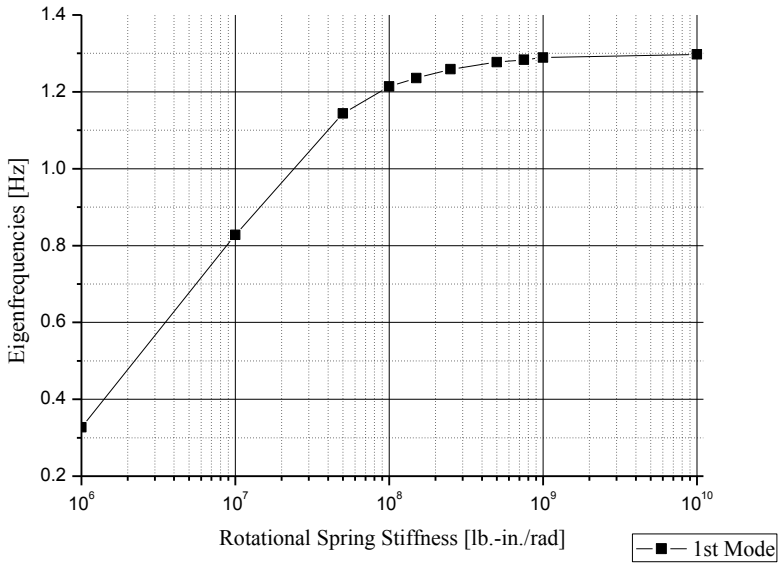

Figure 5.2: Eigenfrequency Variation of In-Plane Mast Arm

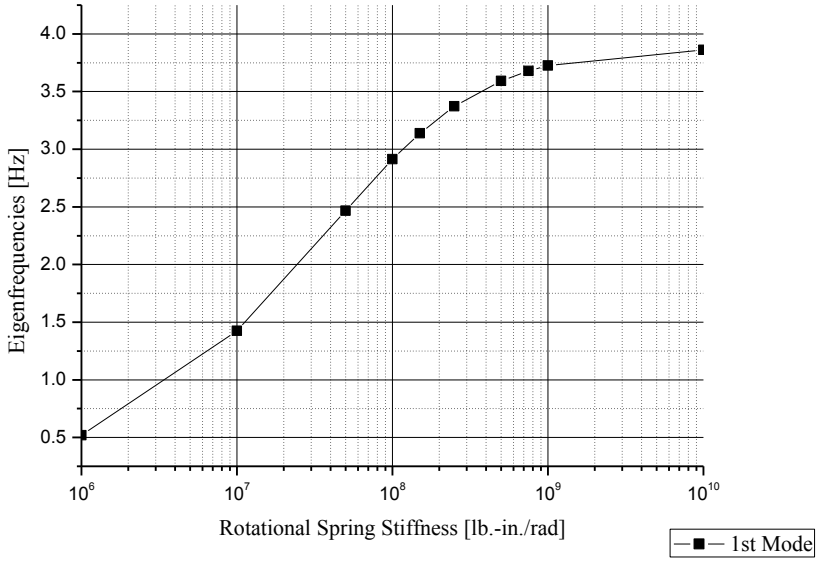

Figure 5.3: Eigenfrequency Variation of In-Plane Pole

5.4. Analytical Solutions: Discretized Continuous System Model (Constant Section)

From the analytical model with the discretized continuous system (constant section member), eigenfrequencies determined are shown in Table 5.6. The same range of rotational spring stiffness is considered on the boundary conditions of the members of the traffic signal structure with 44-ft. mast arm. The first two eigenfrequencies of each member for in- and out-of-plane motion are shown in Table 5.6.

The eigenfrequencies shown in Table 5.6 are plotted to see the variation tendency along with varying flexibility on the boundary conditions. As shown in Figure 5.4 and Figure 5.5 for in-plane motion, the convergence of the eigenfrequency with increasing rotational spring stiffness on boundary condition can be clearly verified. The converged value approaches the eigenfrequency of the system with fixed support boundary conditions. For the out-of-plane motion, as can be checked in Table 5.6, a similar converging tendency can be clearly verified.

Table 5.6: Eigenfrequencies of Discretized Continuous System Model

(Constant Section)

UNIT: [Hz]	IN-PLANE				OUT-OF-PLANE			
	ARM		POLE		ARM		POLE	
K_R [8]	1st	2nd	1st	2nd	1st	2nd	1st	2nd
1.00E+06	0.327	5.785	0.448	16.618	0.327	5.785	0.425	16.204
1.00E+07	0.827	6.394	1.335	17.089	0.827	6.394	1.267	16.628
5.00E+07	1.143	7.334	2.430	18.549	1.143	7.334	2.313	17.932
1.00E+08	1.213	7.658	2.880	19.589	1.213	7.658	2.746	18.851
1.50E+08	1.240	7.796	3.095	20.223	1.240	7.796	2.953	19.407
2.50E+08	1.262	7.919	3.306	20.955	1.262	7.919	3.158	20.045
5.00E+08	1.280	8.022	3.495	21.722	1.280	8.022	3.342	20.710
7.50E+08	1.286	8.058	3.565	22.039	1.286	8.058	3.410	20.984
1.00E+09	1.289	8.076	3.602	22.212	1.289	8.076	3.446	21.132
1.00E+10	1.297	8.127	3.707	22.734	1.297	8.127	3.549	21.581

[8] Rotational Spring Stiffness

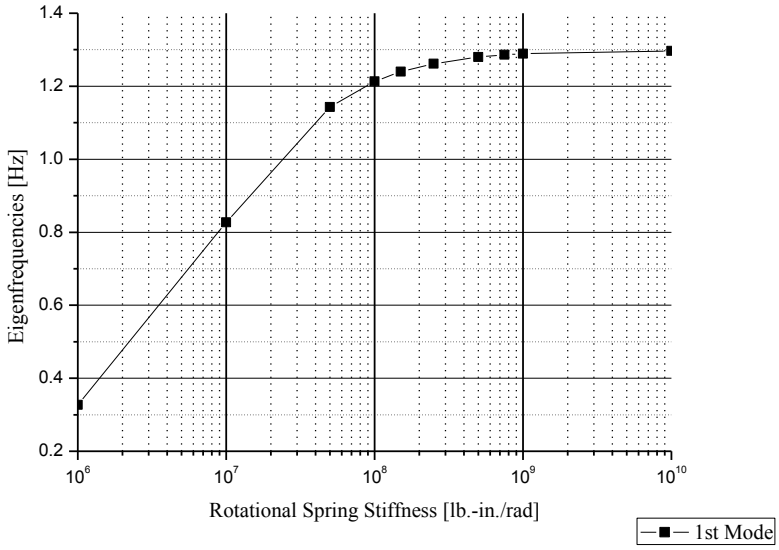

Figure 5.4: Eigenfrequency Variation of In-Plane Mast Arm

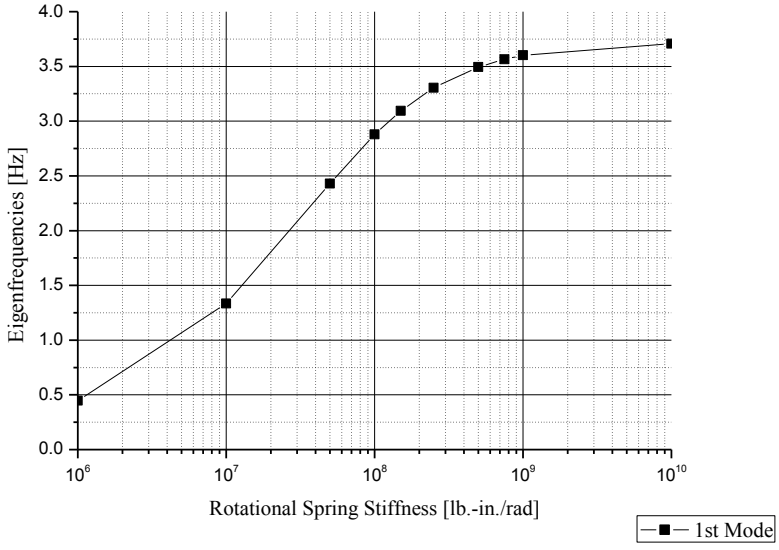

Figure 5.5: Eigenfrequency Variation of In-Plane Pole

5.5. Analytical Solutions: Discretized Continuous System Model (Varying Cross-section)

The eigenfrequencies of the varying cross-sectional member are determined using the analytical model with the discretized continuous system with dimensions as presented in Table 5.3. The analytical model of the varying cross-sectional member is very complicated to be expressed in a closed-form solution. However, as have seen in Section 2, the analytical model for the tapered member was developed with this discretized continuous system and it provides the eigenfrequencies in Table 5.7. An arbitrary range of the rotational spring stiffness is also applied to see the variation tendency of the eigenfrequencies. In Figure 5.6 through Figure 5.9, the eigenfrequency variations provided in Table 5.7 are plotted, showing the convergence of eigenfrequencies. Figure 5.6 and Figure 5.7 show the eigenfrequency variations of the in-plane mast arm and pole and Figure 5.8 and Figure 5.9 display for the out-of-plane mast arm and pole, respectively. These results will be compared and discussed in Section 3, Result Comparisons.

Table 5.7: Eigenfrequencies of Discretized Continuous System Model (Tapered Section)

UNIT: [Hz]	IN-PLANE				OUT-OF-PLANE			
	ARM		POLE		ARM		POLE	
K_R [9]	1st	2nd	1st	2nd	1st	2nd	1st	2nd
5.0.E+05	0.2734	5.3344	0.1902	4.8616	0.2734	5.3344	0.2342	13.7983
1.0.E+06	0.3817	5.3683	0.2679	4.8733	0.3817	5.3683	0.3302	13.8108
5.0.E+06	0.7760	5.6065	0.5795	4.9648	0.7760	5.6065	0.7226	13.9079
1.0.E+07	0.9940	5.8395	0.7883	5.0722	0.9940	5.8395	0.9958	14.0209
5.0.E+07	1.4161	6.6515	1.3849	5.7165	1.4161	6.6515	1.8782	14.6817
1.0.E+08	1.5149	6.9543	1.6034	6.1943	1.5149	6.9543	2.2753	15.1627
5.0.E+08	1.6096	7.3078	1.8688	7.2190	1.6096	7.3078	2.8717	16.1809
1.0.E+09	1.6227	7.3621	1.9108	7.4640	1.6227	7.3621	2.9837	16.4208
1.0.E+10	1.6346	7.4133	1.9506	7.7312	1.6346	7.4133	3.0962	16.6800

[9] Rotational Spring Stiffness

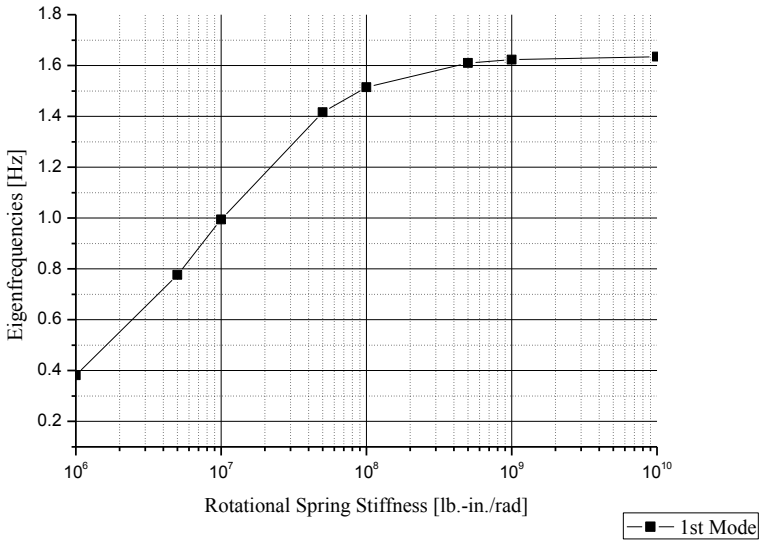

Figure 5.6: Eigenfrequency Variation of In-Plane Tapered Mast Arm

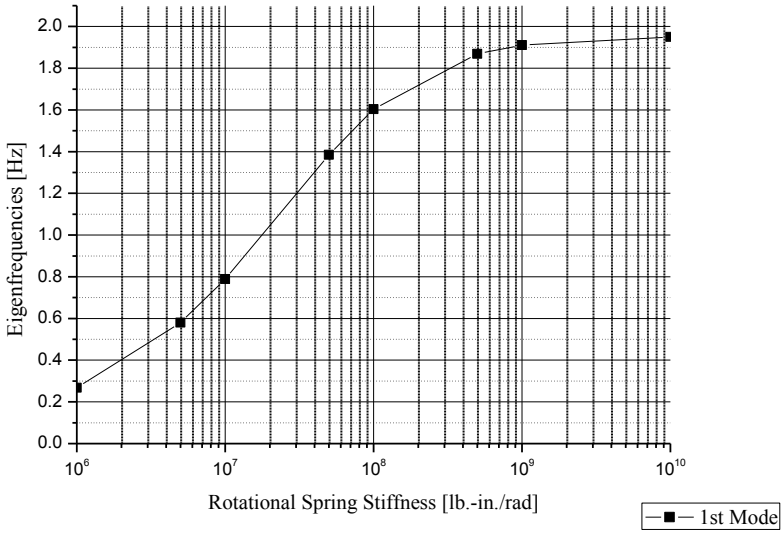

Figure 5.7: Eigenfrequency Variation of In-Plane Tapered Pole

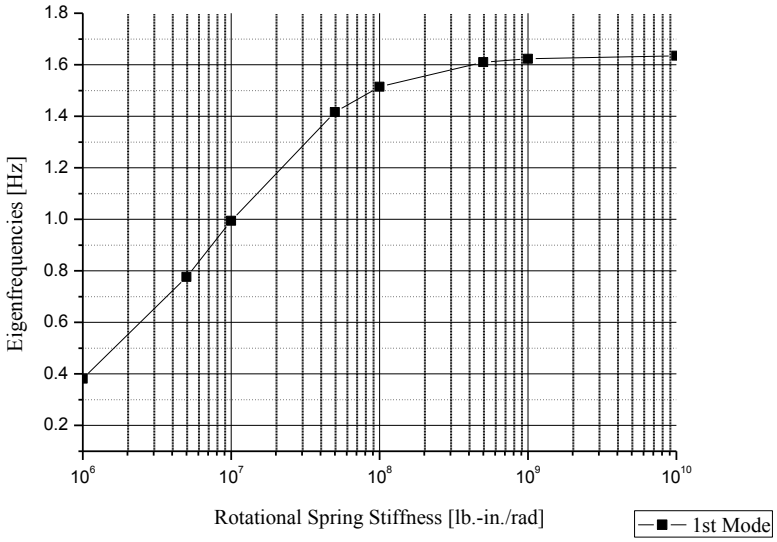

Figure 5.8: Eigenfrequency Variation of Out-of-Plane Tapered Mast Arm

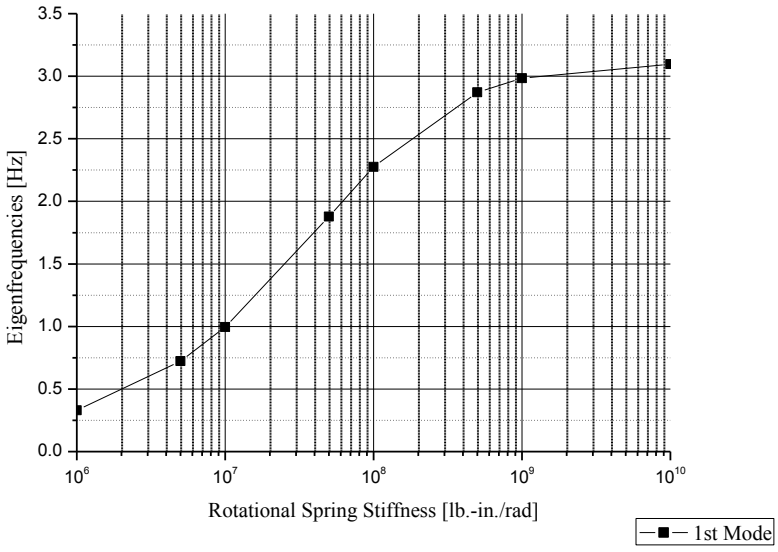

Figure 5.9: Eigenfrequency Variation of Out-of-Plane Tapered Pole

5.6. Conclusions

In this section, the eigenfrequencies of each member of the traffic signal structure with 44-ft. mast arm were determined using the analytical solution with continuous system theory. For the analytical solutions, two types of continuous system model were suggested, and the discretized model was again used with constant cross-sectional and varying cross-sectional members. The results for each member, for in- and out-of-plane motion, presented; the results showed the tendency of eigenfrequency related to flexibility at the boundary. As expected, eigenfrequencies converged to the eigenfrequencies of the fixed boundary conditions with increasing boundary stiffness. According to these results, the suggested analytical solution is partially verified that it could show the relationship of eigenfrequencies and structural flexibility.

6. EXPERIMENTAL STUDY OF TRAFFIC SIGNAL STRUCTURE

6.1. Traffic Signal Structure with 44-ft. Mast Arm

For the experimental study, a traffic signal structure with 44-ft. mast arm was installed in the field at the Riverside Campus of Texas A&M University. The traffic signal structure appeared to generally meet the Texas Department of Transportation's (TxDOT) SMA-100(1)-99 specifications. The TxDOT SMA-100(99) specification is provided in Appendix C. The geometric properties of the given structure are provided from this specification, which is shown Table 5.1. For the arm-to-pole connection, the details of the base plate of the mast arm and the connection plate on the pole are given in Table 5.4 from the TxDOT MA-C-09 specification[10].

6.2. Experimental Setup

The experimental setup consists of three sets of strain gauges placed near the arm-to-pole connection and another three sets placed near pole foundation connection to measure axial, in-plane bending and out-of-plane bending strains. The transducers were installed so each strain gage could serve as a side of a full bridge circuit allowing for temperature compensation and the exclusion of non-focal strain effects. Type AWC-8B-11-3LT gages, manufactured by Sokki Kenkyujo Co., Ltd (TML) were used.

The location of strain gauges near the arm-to-pole connection is 12.6 in. from

[10] TxDOT Standard assembly for traffic signal support structure – mast arm connections

the base plate attached to the mast arm along the centerline of the member. In Figure 6.1, the strain gauge locations along the mast arm and their arrangement around the diameter of the arm are depicted. Using a similar arrangement, strain gauges measuring strain effects near the pole-foundation connection, as depicted in Figure 6.2 are located 15.5 in. from the top surface of the base plate attached to the pole along the centerline of the member.

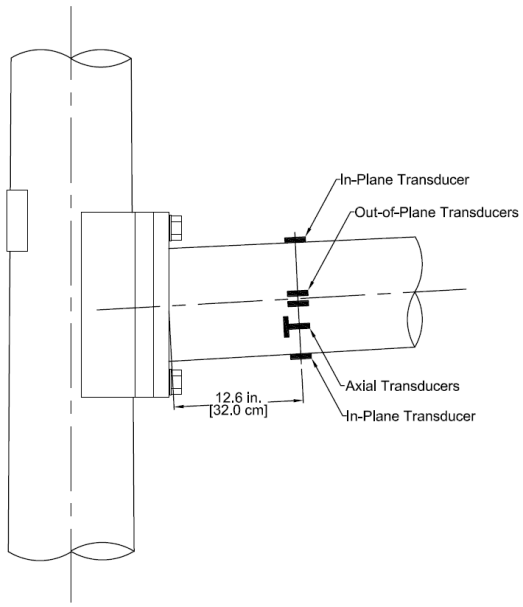

Figure 6.1: Strain Gage Location near Mast Arm-Pole Connection

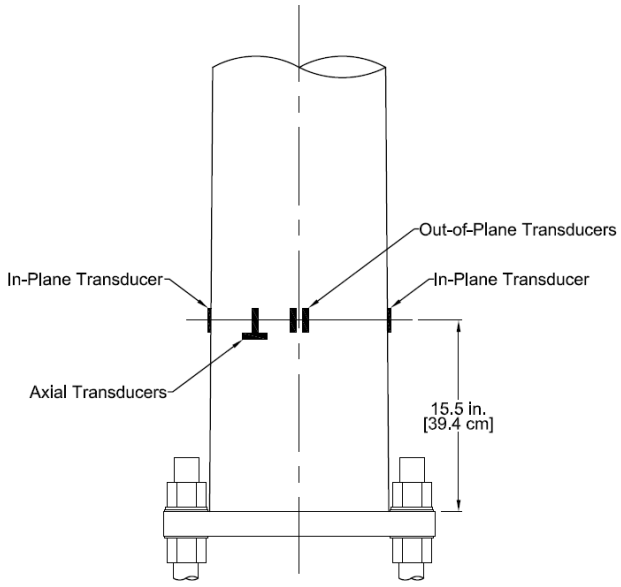

Figure 6.2: Strain Gage Location near Base of Pole.

6.3. Snap-back Test

In this experimental program, snap-back testing, shown in Figure 6.3, is adopted to obtain the eigenfrequencies of the 44-ft. traffic signal structure. For snap-back testing, a moderately large force was manually applied then quickly released. Thus, the freely vibrating responses are recorded. The data acquisition sampling rate was set to 100 Hz, as this gave the ability to accurately identify the first three natural frequencies of the structure. The first few eigenfrequencies are easily identified through post-processing. Snap-back tests were performed to determine the in- and out-of-plane dynamic properties of the traffic signal structure.

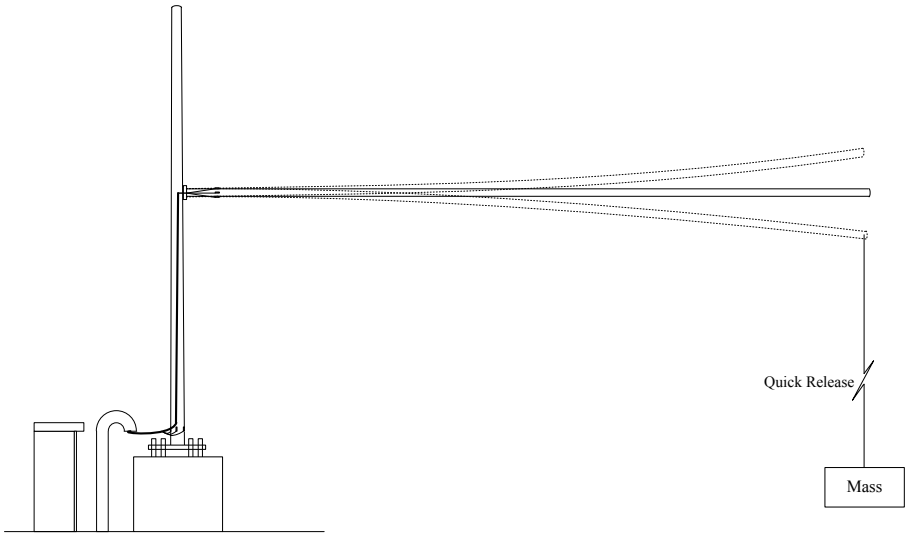

Figure 6.3: Snap-Back Experimental Test

Snap-back or free vibration testing commences when there is little to no noticeable vibrations in the traffic signal structure. This state is determined by a combination of visual inspection and viewing the real time stress in the traffic signal

structure in the locations where strain gages were installed. When the wind is below 5 mph, data acquisition is initiated. After recording data for 10-20 seconds, the force is manually applied by pulling a lightweight rope attached to the tip of the mast arm. The force is held constant for a moment, then immediately released. This test is done in the in-plane and out-of-plane directions separately. Typical recordings from free vibrations are shown in Figure 6.4. Natural frequencies are then identified through analysis in the frequency domain.

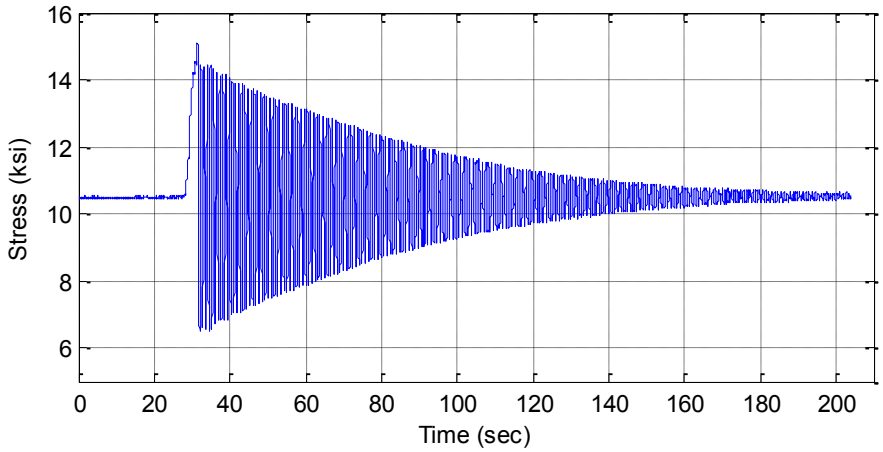

Figure 6.4: In-Plane Stresses near Arm-to-Pole Connection during Free Vibration Test

6.4. Experimental Results

The free vibration experimental measurements with snap-back testing provided the eigenfrequencies of the 44-ft. signal structure. As described earlier, the experimental results are for eigenfrequencies of the in- and out-of-plane vibrations. The results give clearly the first three eigenfrequencies of the structure and are displayed in Table 12. Table 6.1 presents the experimentally found natural frequencies of the traffic signal structure. The reported results are an average of three snap-back tests. These results will be discussed and used to verify the validity of the analytical model.

Table 6.1: Experimental Results of Free Vibration Test

	1st	**2nd**
In-Plane	1.270 Hz	3.442 Hz
Out-of-Plane	1.147 Hz	3.320 Hz

7. FINITE ELEMENT ANALYSYS OF TRAFFIC SIGNAL STRUCTURE

7.1. General Information of Finite Element Model

The finite element model of the traffic signal structure with 44-ft. mast arm is provided for validation of the analytical model based on continuous system theory. The input information has been already discussed in Section 5. The geometric and material properties given in the previous chapter are applied to setup the finite element model, with dimensions of field measurements. The detailed information is provided in Table 5.1. The analytical model discussed in previous chapters has used the simple geometric shown in Table 5.2 and Table 5.3. Therefore, the finite element model is constructed with the simple geometric properties previously provided. As mentioned, the connection plates have considerable amounts of mass so that the details of the connection parts were considered in analytical model, which are given in Table 5.4. These measured dimensions are used for this finite element model.

7.2. Finite Element Models and Numerical Solutions

In the finite element analysis, the vibration characteristics of the given traffic signal structure are simply investigated in modal analysis with commercial FEA software package, ABAQUS/CAE, version 6.8 (ABAQUS Inc.). A total of five finite element models were supplied to compare with the analytical solutions.

In Section 5, the analytical solutions for the members of the traffic signal

structure were provided. The results showed the eigenfrequencies of the mast arm and the pole respectively for in- and out-of-plane motion. Thus, finite element models were setup for each case as shown in Figure 7.1 and Figure 7.2 and the element section profile properties are given in Table 5.3.

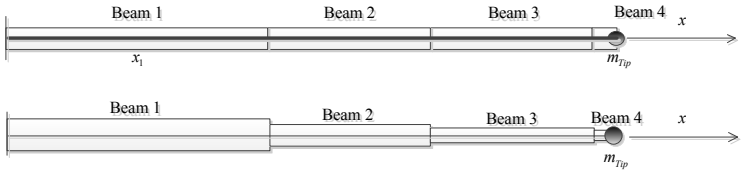

Figure 7.1: Finite Element Models of Constant and Tapered Section Mast Arms

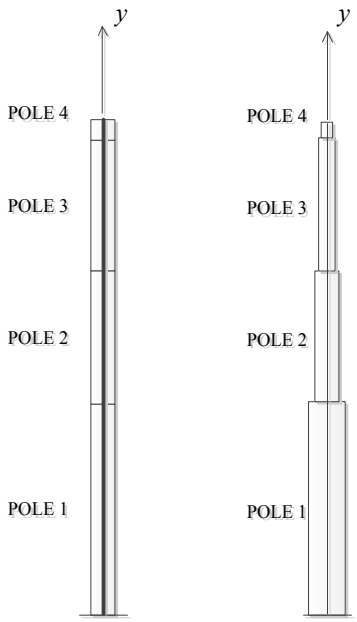

Figure 7.2: Finite Element Models of Constant and Tapered Section Pole

In this finite element analysis, several types of boundary conditions were taken into account to observe dynamic characteristics of the members of the traffic signal

structure. The boundary conditions on the mast arm reflect fixed and rotational spring ends of the cantilevered member, which the rotational spring stiffness is the torsional and bending (rotational) stiffness of the pole.

Table 7.1 shows the configurations of the varying cross-section members and Table 7.2 shows the eigenfrequencies of the constant and tapered section mast arm. In the table, the torsional spring represents the torsional stiffness of the tapered pole and rotational spring reflects the bending stiffness of the tapered pole. The difference between constant member and tapered member can be clearly checked, which can be interpreted that tapered section members have higher stiffness at the boundary.

Table 7.1: Element Section Profile Properties for Finite Element Model

		ARM				POLE			
CONSTANT	**Diameter [in.]**	8.99				13.21			
		Beam 1	Beam 2	Beam 3	Beam 4	POLE 1	POLE 2	POLE 3	POLE 4
TAPERED	**Length [ft.]**	18	12	12	1	6	6	6	12
	Diameter [in.]	9.73	7.65	5.98	5.08	14.10	13.03	11.96	10.89

Table 7.2: Eigenfrequencies of Mast Arm (FEM)

UNIT: [Hz]		CONSTATN CROSS-SECTION MEMBER				TAPERED CROSS-SECTION MEMBER			
		IP		OP		IP		OP	
		1st	2nd	1st	2nd	1st	2nd	1st	2nd
Fixed	W/O M_{Tip} [11]	1.291	8.066	1.291	8.066	1.659	7.527	1.659	7.527
	W/ M_{Tip}	1.279	7.992	1.279	7.992	1.634	7.396	1.634	7.396
Torsional Spring[12]	W/O M_{Tip}	N/A		1.007	6.810	N/A		1.247	6.316
	W/ M_{Tip}			0.998	6.751			1.232	6.208
Rotational Spring[13]	W/O M_{Tip}	1.056	6.970	N/A		1.316	6.458	N/A	
	W/ M_{Tip}	1.047	6.910			1.299	6.348		

[11] Tip mass which represents the tenon and tenon plate, as seen in SMA100(1)-99 specification
[12] Torsional spring stiffness equivalent to the tapered pole: 2.2195E+07 lb.-in./rad
[13] Rotational spring stiffness equivalent to the tapered pole: 2.8842E+07 lb.-in./rad

The finite element model of the pole provided the results, eigenfrequencies of the constant and the tapered cross-section mast arm respectively for in- and out-of-plane motions, as shown in Table 7.3.

Table 7.3: Eigenfrequencies of Pole (FEM)

UNIT : [Hz]		**CONSTANT CROSS-SECTION MEMBER**				**VARYING CROSS-SECTION MEMBER**			
		IP		**OP**		**IP**		**OP**	
B.C.		**1st**	**2nd**	**1st**	**2nd**	**1st**	**2nd**	**1st**	**2nd**
Fixed	**W/O** $M_a + I_a$	3.920	24.251	3.921	24.251	4.406	23.114	4.406	23.114
	I_a	2.140	11.476	3.921	24.251	2.151	11.516	4.406	23.114
	M_a	2.986	18.644	2.986	18.644	3.277	16.515	3.277	17.003
	$M_a + I_a$	1.963	8.386	2.986	18.644	1.996	8.100	3.2767	17.003
Fixed	**W/O** $M_{at} + I_{at}$	3.921	24.251	3.921	24.251	4.406	23.114	4.406	23.114
	I_{at}	2.140	11.475	3.921	24.251	2.211	11.515	4.406	23.114
	M_{at}	2.895	18.335	2.895	18.335	3.094	16.516	3.094	16.516
	$M_{at} + I_{at}$	1.921	7.991	2.895	18.335	1.958	7.666	3.094	16.516

M_a : Arm mass only = 1.16295E+005[lb.-in.^{2}]

I_a : Rotational Inertia of only Arm = 2.2401[lb.-s^2 / in.^{2}]

M_{at} : Arm mass + tenon set = 1.1633E+005 [lb.-in.^{2}]

I_{at} : Rotational Inertia of Arm + tenon set = 2.8356 [lb.-s^2 / in.^{2}]

Table 7.3 also shows the fact that eigenfrequencies of the tapered cross-section member are higher than constant section member. This fact is interpretable that the tapered section member has higher structural stiffness at boundary for flexural vibration. In this case, another noticeable fact is that rotational inertia around vertical axis

(Rotational y-axis, direction 5 in ABAQUS[14]) does not affect to the transverse vibration of the pole, observing same eigenfrequencies of the out-of-plane motion without and with a rotational inertia. To consider the whole structure, the finite element model of the traffic signal structure with 44-ft. mast arm is constructed as shown in Figure 7.3

The cantilever traffic signal structure shown in Figure 7.3 is modeled with beam elements. These beam elements are thin beams, so called Euler-Bernoulli beam, which does not take into account shear deformation. The analytical model with continuous system is also built based on the thin beam theory. This cantilevered traffic signal structure is a statically determinate structure. Because the shafts of the arm and pole have tapered cross-section property, each element should have different constant section profiles. The cross-sectional profile properties of all elements are shown in Table 7.4. The eigenfrequencies of the whole structure are provided in Table 7.5 and Table 7.6. This finite element model has a fixed boundary condition at the pole base and also considers the masses of the connection plates and tenon and tenon plate at the tip. The results will be discussed in the following section.

[14] In ABAQUS, global coordinate system consists of direction 1 for x-axis, 2 for y-axis, 3 for z-axis, 4 for rotation around x-axis, 5 for rotation around y-axis, and 6 for rotation around z-axis.

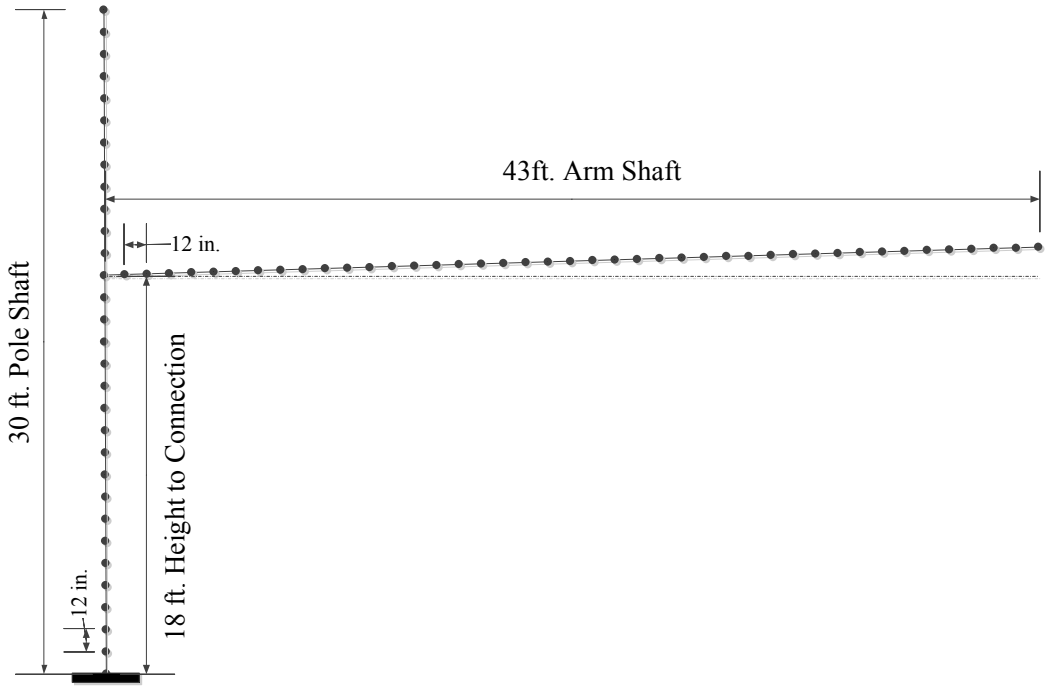

Figure 7.3: Finite Element Model of 44-ft. Signal Structure (TxDOT SMA-100)

Table 7.4: Cross-section Profile Properties of FEM Model

Arm			Pole		
x-coordinate [in.]	Diameter [in.]	Radius [in.]	y-coordinate [in.]	Diameter [in.]	Radius [in.]
43	5.1	2.55	30	10.3	5.15
42	5.24	2.62	29	10.44	5.22
41	5.37	2.69	28	10.58	5.29
40	5.51	2.76	27	10.72	5.36
39	5.65	2.82	26	10.86	5.43
38	5.79	2.89	25	11	5.5
37	5.92	2.96	24	11.14	5.57
36	6.06	3.03	23	11.28	5.64
35	6.2	3.1	22	11.42	5.71
34	6.33	3.17	21	11.56	5.78
33	6.47	3.24	20	11.7	5.85
32	6.61	3.3	19	11.84	5.92
31	6.75	3.37	18	11.98	5.99
30	6.88	3.44	17	12.12	6.06
29	7.02	3.51	16	12.26	6.13
28	7.16	3.58	15	12.4	6.2
27	7.3	3.65	14	12.54	6.27
26	7.43	3.72	13	12.68	6.34
25	7.57	3.78	12	12.82	6.41
24	7.71	3.85	11	12.96	6.48
23	7.84	3.92	10	13.1	6.55
22	7.98	3.99	9	13.24	6.62
21	8.12	4.06	8	13.38	6.69
20	8.26	4.13	7	13.52	6.76
19	8.39	4.2	6	13.66	6.83
18	8.53	4.27	5	13.8	6.9
17	8.67	4.33	4	13.94	6.97
16	8.8	4.4	3	14.08	7.04
15	8.94	4.47	2	14.22	7.11
14	9.08	4.54	1	14.36	7.18
13	9.22	4.61	0	14.64	7.25
12	9.35	4.68			
11	9.49	4.75			
10	9.63	4.81			
9	9.77	4.88			
8	9.9	4.95			
7	10.04	5.02			
6	10.18	5.09			
5	10.31	5.16			
4	10.45	5.23			
3	10.59	5.29			
2	10.73	5.36			
1	10.86	5.43			
0	10.98	5.5			

Table 7.5: In-Plane Eigenfrequencies and Participation Factors

[In-plane] FEA Model of 44-ft. TSS				
Mode	EF[15]	PF-x[16]	PF-y	PF-z
1	**1.2883 Hz**	-0.797097	1.57185	2.43E-16
2	**3.7150 Hz**	1.64526	0.0262386	-2.24E-14

✓ This finite element model considered the masses of connection plates and tenon detail.

Table 7.6: Out-of-Plane Eigenfrequencies and Participation Factors

[Out-of-plane] FEA Model of 44-ft. TSS				
Mode	EF	PF-x	PF-y	PF-z
1	**1.2265 Hz**	1.17E-16	-1.93E-16	1.85502
2	**3.6144 Hz**	2.94E-14	4.77E-16	1.59687

✓ This finite element model considered the masses of connection plates and tenon set.

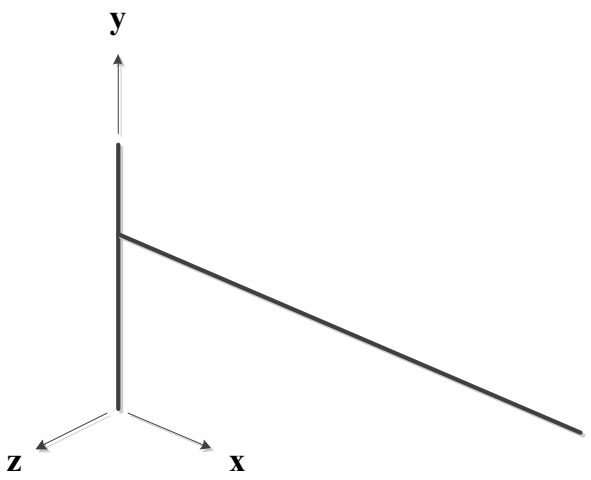

Figure 7.4: Global Coordinate of the Finite Element Model

[15] Eigenfrequencies: Unit [Hz]

[16] PF-x: Participation Factor of x-direction, PF-y: Participation Factor of y-direction, PF-z: Participation Factor of z-direction, see Figure 7.4

8. DISCUSSION

8.1. Conventional and Discretized Models

Conventional and discretized analytical models based on continuous system theory have been developed to analyze the dynamic characteristics of the traffic signal structure with 44-ft. mast arm. As mentioned earlier, the conventional analytical model is unable to determine the dynamic characteristics of a system with additional masses at arbitrary locations. Thus, as a solution to overcome the difficulty, the discretized model is implemented in this study. In actuality, with the conventional analytical model, it may be possible to get eigenfrequencies of the system with attachments; however, the corresponding mode shape may be inaccurate. Therefore, through comparison of the results of two analytical solutions, the lower usability of the conventional analytical model will be verified.

As can be seen in Figure 8.1 and Table 8.1, the eigenfrequency variations of the mast arm between conventional and discretized models were compared. The mast arm for this study does not attach any attachment like signal cluster or other devices. Thus, as seen, these two analytical models provide almost same solutions for the structure. However, for the models shown in Figure 8.2, Figure 8.3 shows considerable differences between two analytical solutions and the differences can be checked in Table 8.2. Thus, through these results, it is realized the conventional analytical model is usable to analyze the mast arm only, but has differences with other cases. Those differences are considered

due to several assumptions to simplify the structure in order to express as conventional model. It is expected that the assumptions are insufficient to perfectly express the realistic motion of the structure. Thus, conventional model is excluded in further result comparisons.

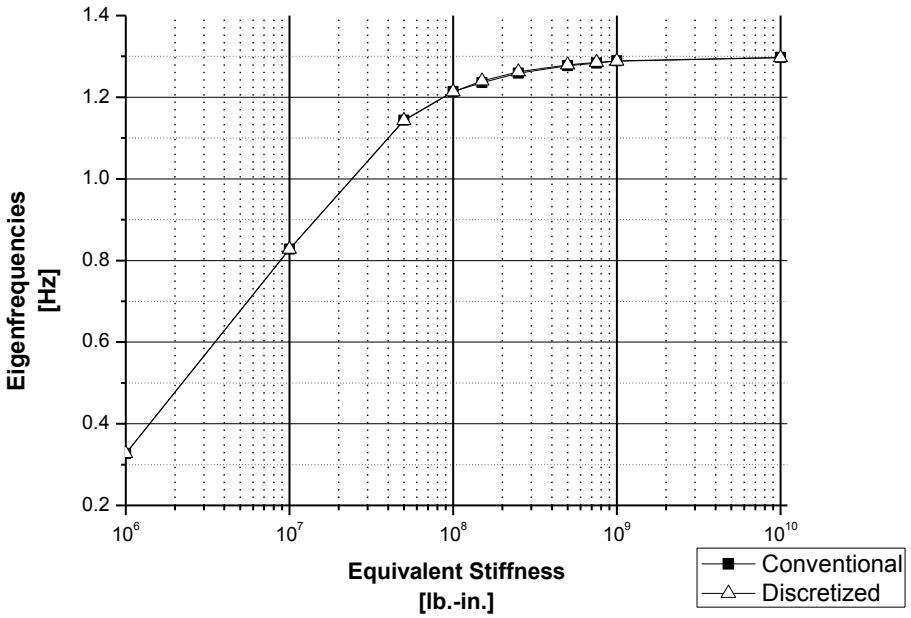

Figure 8.1: Comparison between Conventional and Discretized Models (Constant Mast Arm)

Table 8.1: Comparison of the First Eigenfrequencies for the Constant Mast Arm

	Conventional	Discretized	Error [%]
1.00E+06	0.327	0.327	0.0471
1.00E+07	0.828	0.827	0.0484
5.00E+07	1.144	1.143	0.0491
1.00E+08	1.214	1.213	0.0499
1.50E+08	1.236	1.24	0.3058
2.50E+08	1.259	1.262	0.236
5.00E+08	1.277	1.280	0.1803
7.50E+08	1.283	1.286	0.1611
1.00E+09	1.289	1.289	0.0499
1.00E+10	1.298	1.297	0.0499

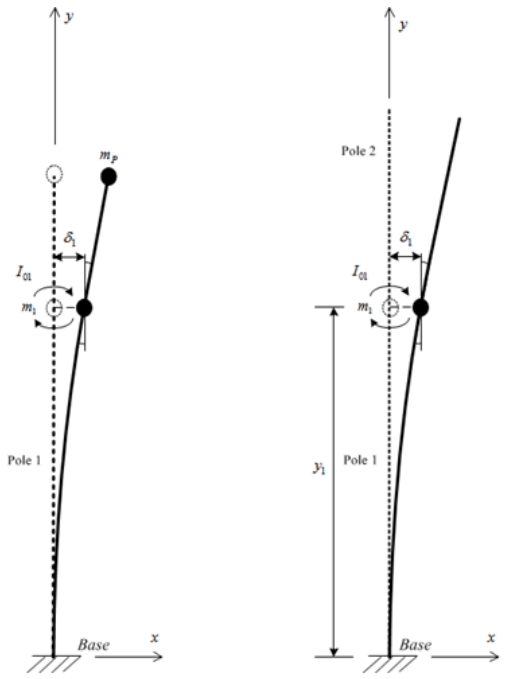

Figure 8.2: Approaches of Conventional and Discretized Models for the Pole

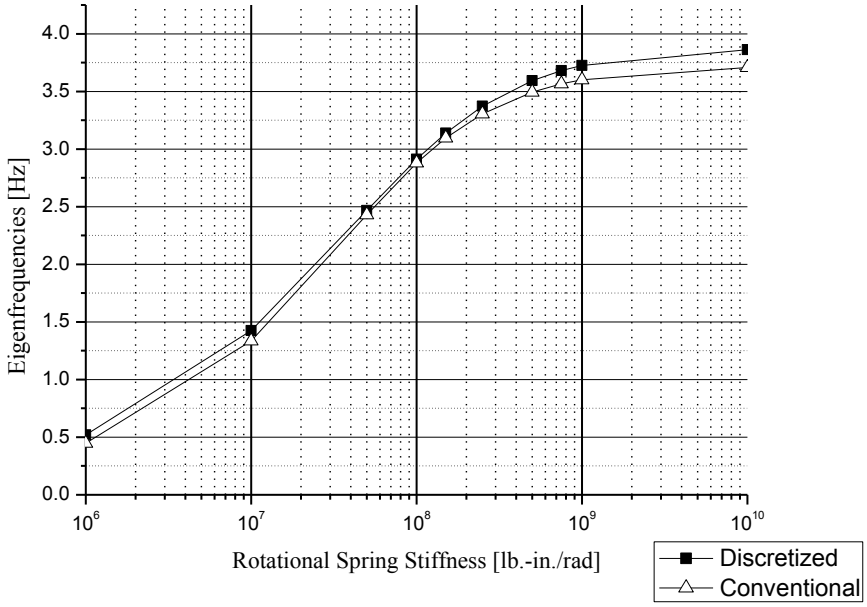

Figure 8.3: Comparison between Conventional and Discretized Models (Constant Pole)

Table 8.2: Comparison of the First Eigenfrequencies of the Constant Pole

	Conventional	Discretized	Error [%]
1.00E+06	0.520	0.448	13.846
1.00E+07	1.424	1.335	6.250
5.00E+07	2.466	2.430	1.460
1.00E+08	2.913	2.880	1.133
1.50E+08	3.139	3.095	1.402
2.50E+08	3.372	3.306	1.957
5.00E+08	3.593	3.495	2.728
7.50E+08	3.680	3.565	3.125
1.00E+09	3.725	3.602	3.302
1.00E+10	3.861	3.707	3.989

8.2. Verifications

For validation of the analytical models, accuracy verification is performed in this section. This verification is carried out by comparing with results from the finite element models. The finite element models were provided in subsection 7.2 of Section 7. Table 8.3 shows the comparisons between the analytical and numerical solutions. The results are for the models depicted in Figure 7.1, for constant and varying cross-sectional mast arms. The considered boundary conditions are fixed-free ends, which eigenfrequencies for in- and out-of-plane motions are same. As can be seen in the tables, the differences between the analytical and numerical solutions are less than 0.5%. In this table, the differences of the eigenfrequencies between constant and tapered section models are considerably large about 22% and 7.5% respectively for the first and second modes.

In Table 8.4, the comparisons of the eigenfrequencies for the poles, shown in Figure 7.2, in-plane motion are provided. The differences between the numerical and analytical models are less than about 0.4% for the first mode, meaning that the analytical model accurately describes the dynamic characteristics of the structure. This table also shows the large differences of the eigenfrequencies between constant and tapered section members.

Table 8.5 shows the result comparisons for the out-of-plane motion of the pole. The differences are less than 0.4%. In the table, as can be seen, the two of rotational inertia, I_a or I_{at}, are not applicable to the out-of-plane motion of the pole, because they

do not affect the transverse vibration of the pole. The reason for that phenomenon is that the degrees of freedom for in-plane are all constrained, so any coupling effects cannot be analyzed.

In conclusion, the solutions from the analytical model were compared with the numerical solution of the finite element models. The comparisons are shown in Table 8.3 through Table 8.5, which all show considerably small differences between the analytical and the numerical solutions. The accuracy of the analytical solution hereby is verified and interpreted that the precise analysis for the dynamic characteristics of structures can be performed with this analytical model.

Table 8.3: Comparisons between FEM and Analytical Models of the Mast Arm (Fixed-Free Boundary Conditions)

		FEM		**ANALYTICAL**			
UNIT: [Hz]		**IP / OP**		**IP / OP**		**Error [%]**	
		1st	2nd	1st	2nd	1st	2nd
Constant	W/O M_{Tip} [17]	1.291	8.066	1.292	8.096	0.086	0.381
	W/ M_{Tip}	1.279	7.992	1.283	8.019	0.363	0.340
Tapered	W/O M_{Tip}	1.659	7.527	1.660	7.551	0.093	0.318
	W/ M_{Tip}	1.634	7.396	1.636	7.419	0.095	0.313
Difference between Constant and Varying Cross-section [%]		22.185	7.156	22.190	7.223		
		21.757	8.062	21.548	8.092		

[17] Tip mass which represents the tenon and tenon plate

Table 8.4: Comparisons between FEM and Analytical Models of the In-Plane Pole (Fixed-Free Boundary Conditions)

UNIT: [Hz]		ABAQUS		MATLAB			
		IP		IP		Error [%]	
		1st	2nd	1st	2nd	1st	2nd
Constant [Fixed]	W/O	3.921	24.251	3.930	24.629	0.240	1.559
	M_{at}	2.986	18.644	2.996	18.900	0.311	1.370
	I_{at}	2.140	11.476	2.141	11.629	0.047	1.335
	$M_{at}+I_{at}$	1.963	8.386	1.964	8.498	0.082	1.326
Tapered [Fixed] 4 Elements	W/O	4.406	23.114	4.417	23.425	0.252	1.344
	M_{at}	3.277	16.515	3.287	17.192	0.304	4.100
	I_{at}	2.151	11.516	2.152	11.661	0.039	1.258
	$M_{at}+I_{at}$	1.996	8.100	1.997	8.202	0.058	1.262
Difference between Constant and Varying Cross-section [%]		12.38	4.688	12.397	4.890		
		0.491	0.349	0.482	0.273		
		9.724	11.419	9.717	9.034		
		1.681	3.415	1.657	3.476		

M_{at} : Arm mass + tenon set = 1.1633 [lb.-in.^{2}]

I_{at} : Rotational Inertia of Arm + tenon set = 2.8356E+005 [lb.-s^2 / in.^{2}]

Table 8.5: Comparisons between FEM and Analytical Models of the Out-of-Plane Pole
(Fixed-Free Boundary Conditions)

UNIT: [Hz]		ABAQUS		MATLAB			
		OP		OP		Error [%]	
		1st	2nd	1st	2nd	1st	2nd
Constant [Fixed]	W/O	3.921	24.251	3.930	24.629	0.240	1.559
	M_{at}	2.986	18.644	2.996	18.900	0.311	1.370
	I_{at}	3.921	24.251	N/A	N/A	N/A	N/A
	$M_{at}+I_{at}$	2.986	18.644	N/A	N/A	N/A	N/A
Tapered [Fixed] 4 Elements	W/O	4.406	23.114	4.417	23.425	0.252	1.344
	M_{at}	3.277	17.003	3.287	17.192	0.304	1.113
	I_{at}	4.406	23.114	N/A	N/A	N/A	N/A
	$M_{at}+I_{at}$	3.277	17.003	N/A	N/A	N/A	N/A
Difference between Constant and Varying Cross-section [%]		11.019	4.919	11.029	5.141		
		11.019	4.919	N/A	N/A		
		8.863	9.651	8.856	9.931		
		8.863	9.651	N/A	N/A		

M_{at} : Arm mass + tenon set = 1.1633 [lb.-s^2 / in.^{2} lb.-in.^{2}]

I_{at} : Rotational Inertia of Arm + tenon set = 2.8356E+005 [lb.-in.^{2}]

8.3. Convergence Study

In the discretized continuous system model, varying cross-sectional members are applied to the analytical model. The tapered cross-section properties applied are not linearly varying properties, which are gradually decreased properties. Thus, through convergence study, the effects of the tapered section member will be discussed in this section.

As have seen in previous section, the results of the constant and the tapered cross-section members are already provided in Table 8.3 through Table 8.5. In the results comparisons, it is clearly expressed that the effect of tapered member, which have higher structural stiffness against transverse vibrations. However, the tapered members in those tables are, the mast arm and the pole, are just expressed with 4 constant cross-sectional elements, so it must have differences remain. For the precise analysis of the tapered section effect, a more discretized model is applied to the analytical solution, which section profile information is provided in Table 8.6 and Table 8.7. The numbers of the elements of each member are decided to make same element length, which is to represent gradually tapered members.

Table 8.6: Varying Cross-sectional Arm

	Element #	1	2	3	4	5	6	7	8
4 Elements	Element Length	18	12	12	1				
	Diameter	9.73	7.65	5.98	5.08				
8 Elements	Element Length	10	8	8	8	8	1		
	Diameter	10.29	9.18	8.06	6.95	5.84	5.70		
10 Elements	Element Length	6	6	6	6	6	6	6	1
	Diameter	10.61	9.86	9.11	8.37	7.62	6.88	6.13	5.38

Table 8.7: Varying Cross-sectional Pole

	Element #	1	2	3	4	5	6	7	8	9	10
4 Elements	Element Length	6	6	6	12						
	Diameter	14.1	13.03	11.96	10.89						
8 Elements	Element Length	5	5	4	4	4	4	4			
	Diameter	14.28	13.57	13.00	12.42	11.85	11.28	10.71			
10 Elements	Element Length	3	3	3	3	3	3	3	3	3	3
	Diameter	14.43	14.00	13.57	13.14	12.71	12.28	11.85	11.42	10.99	10.56

Table 8.8 shows the convergence of the eigenfrequencies of the mast arm along with changing to fine tapered member. In addition, the eigenfrequency convergence of the pole is shown in Table 8.9 . In these two tables, it is clearly shown the tendency of increasing eigenfrequency being fining tapered member, meaning the structural stiffness of the tapered member is considerably higher than constant section. The convergences

shown in Table 8.8 and Table 8.9 are depicted in Figure 8.4 and Figure 8.5.

Table 8.8: Eigenfrequency Convergence by Tapering Mast Arm

	In-Plane				Out-of-Plane			
	Constant	Element #			Constant	Element #		
		4	6	8		4	6	8
1st	1.047	1.299	1.323	1.337	0.999	1.233	1.251	1.266
2nd	6.928	6.362	6.515	6.485	6.770	6.221	6.357	6.323

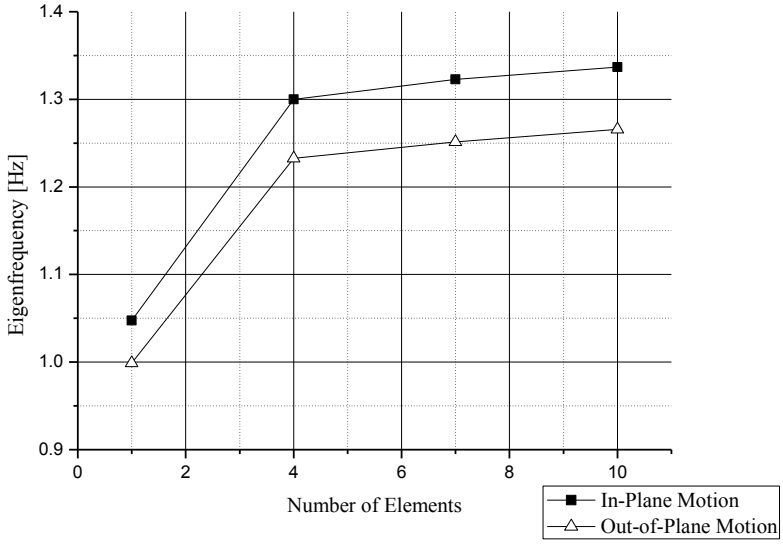

Figure 8.4: The First Eigenfrequency Convergence of Mast Arm

Table 8.9: Eigenfrequency Convergence by Tapering Pole

	In-Plane				Out-of-Plane			
	Constant	Element #			Constant	Element #		
		4	7	10		4	7	10
1st	2.825	3.075	3.143	3.153	2.787	3.061	3.094	3.104
2nd	18.132	17.51	16.41	17.652	16.964	16.609	16.619	16.560

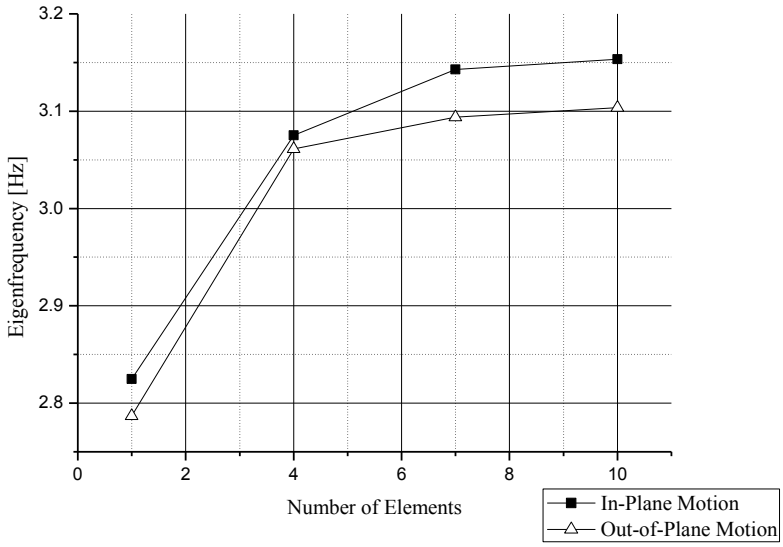

Figure 8.5: The First Eigenfrequency Convergence of Pole

8.4. Eigenfrequencies of the Total Traffic Signal Structure

In this analytical solution, the eigenfrequencies of the total structure is determined transforming the time domain responses of the traffic signal structure to the frequency domain responses by FFT. The time domain responses of the traffic signal structure, as mentioned, obtained by superposing the time domain responses of two members of the traffic signal structure at the arm-to-pole connection. The superposition of the members are performed in considerations of continuity conditions, provided in Equations (4.43) through (4.45), at the connection. The time domain responses were taken at the tip of the mast arm ($x = L_a$). As shown in Figure 8.6 and Figure 8.7, time domain responses of the traffic signal structure for in- and out-of-plane motion are provided. Figure 8.8 and Figure 8.9 show the frequency domain responses of the in- and out-of-plane motions transformed form Figure 8.6 and Figure 8.7, respectively. As can be seen in the spectral density plot, the first two eigenfrequencies are provided for each motion, which are 1.30 Hz and 3.263 Hz for in-plane motion and 1.233 Hz and 3.083 Hz for out-of-plane motion. These results are compared in Table 8.10 with experimental and numerical results, supplied in Table 6.1, Table 7.5, and Table 7.6. The results shows that the results of FEM has a close value of the first eigenfrequencies, which finite element model has 43 arm-element and 30 pole-element to express tapered sections. The analytical solution has 4 elements to express the tapered section members, but it shows the relatively large error from the experimental results.

Table 8.10: Result Comparisons

UNIT: [Hz]		Experimental Result	Numerical Solution [ABAQUS]		Analytical Solution [4Element Tapered]	
		Eigen frequency [Hz]	Eigen frequency [Hz]	Error [%]	Eigen frequency [Hz]	Error [%]
In-Plane	1st	1.270	1.288	1.449	1.300	2.362
	2nd	3.442	3.715	7.931	3.263	5.200
Out-of-Plane	1st	1.147	1.227	6.940	1.233	7.498
	2nd	3.320	3.614	8.867	3.083	7.139

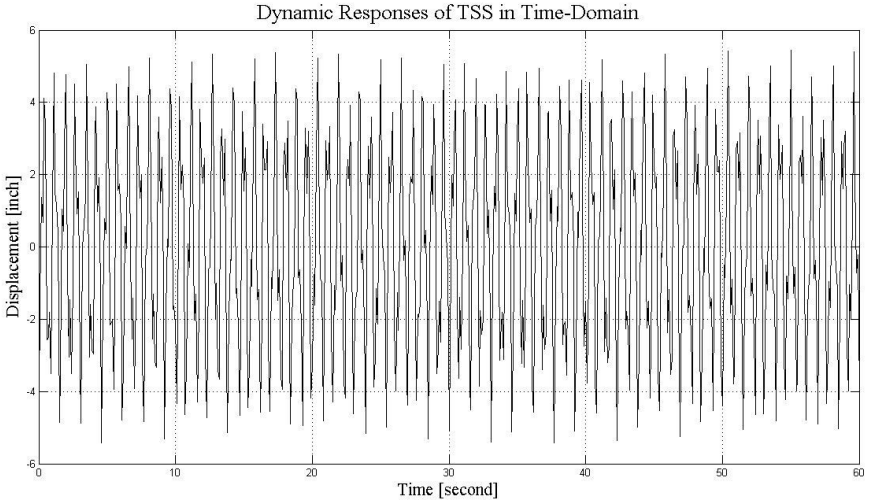

Figure 8.6: In-Plane Time-Domain Responses of Traffic Signal Structure ($x = L_a$)

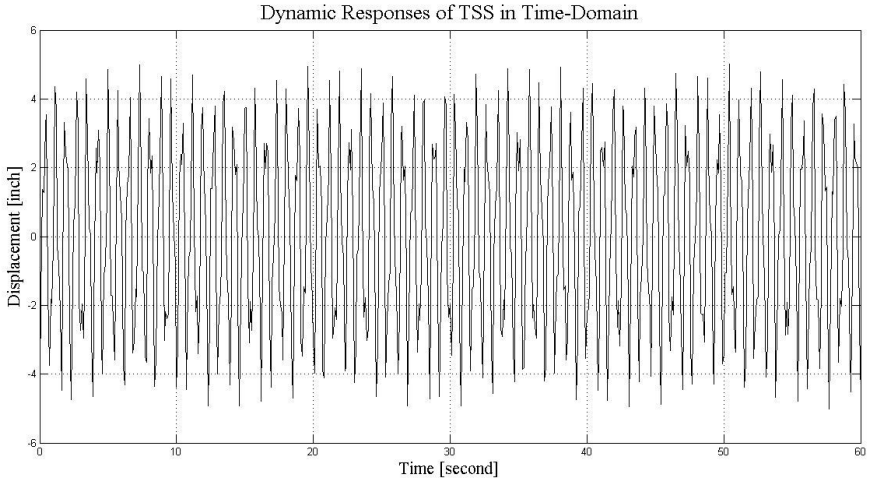

Figure 8.7: Out-of-Plane Time-Domain Responses of Traffic Signal Structure ($x = L_a$)

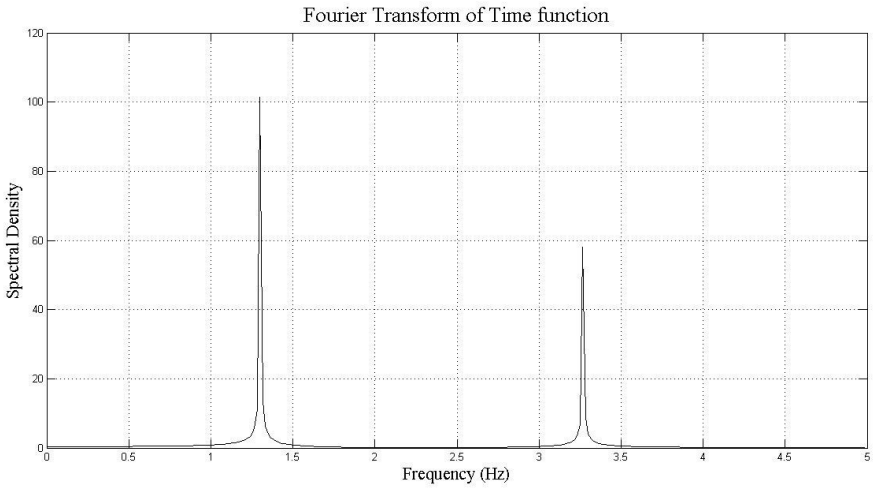

Figure 8.8: In-Plane Frequency Domain Responses ($x = L_a$)
(1st: 1.3 Hz and 2nd : 3.263 Hz)

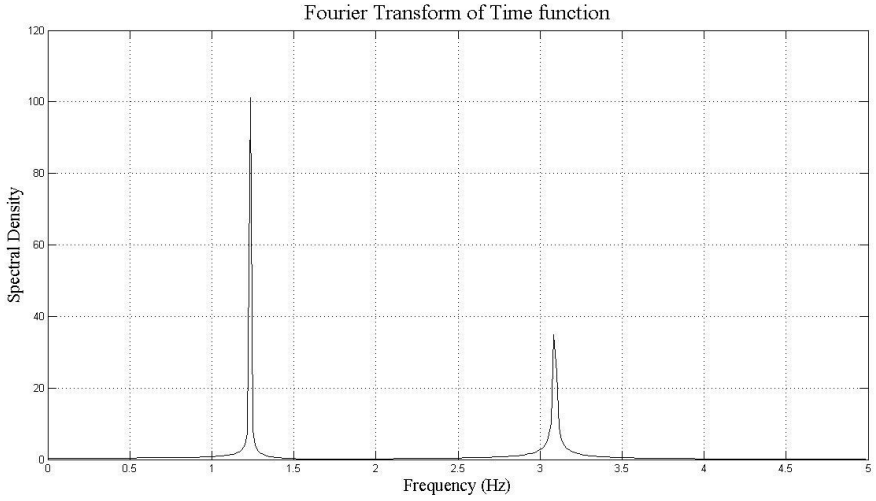

Figure 8.9: Out-of-Plane Frequency Domain Responses ($x = L_a$)
(1st: 1.233 Hz and 2nd : 3.083 Hz)

8.5. Conclusion

The analytical solutions suggested with continuous system theory have been verified in this section. These verifications are required to evaluate the validity of the applications of the analytical model to the traffic signal structure. For the verification, the results of the conventional continuous system model are compared with the discretized model suggested to overcome additional attachment problem. In Table 8.1 and Table 8.2, the results are compared and clearly showed that conventional continuous model should have considerable error when taking additional attachment into account. Therefore, the results of the conventional model were excluded in the result comparisons.

For the validation of the analytical model, the accuracy verification is carried out in this section. As shown in Table 8.3 through Table 8.5, the comparisons for the results of the single members showed considerably small errors between the results from the analytical model and from the finite element model. The errors are less than 0.5% for the first eigenfrequencies. The finite element models for these comparisons are built with totally same geometric and material properties. However, this piecewise tapered section member must have errors from the real fully tapered section member. That is, this analytical solution will have some errors comparing with the experimental results and the numerical solutions of the finite element model with fully tapered section. For this comprehension, the convergence study has been performed as shown in Figure 8.4 and Figure 8.5, and it shows that the eigenfrequencies are converging to the more discretized piecewise tapered section members. Moreover, with this piecewise tapered section

members, it has been tried to consider the dynamic behavior of the traffic signal structure with 44-ft. mast arm. Table 8.10 is to show the comparisons of all the results, analytical solution, experimental measurement, finite element analysis. As discussed, the finite element model has unit length elements, 43 elements (43-ft.) of mast arm and 30 elements (30-ft.) pole. The errors for the first eigenfrequency between FEM model and experimental results are relatively smaller than the analytical solution which has only 4 elements. However, it is expected that the analytical model can more precisely provide the dynamic characteristics of the traffic signal structure if models are more discretized so that can express better tapered cross-section member. The only limitation now is the computation speed using MATLAB. The better results with more discretized model can be expected with higher capacity computer.

Once this analytical model is verified with more discretized element system, this analytical model can be used for the considerations of parameters on the boundary conditions of systems. As have studied in this research, the analytical solutions can provide the eigenfrequency variation along with the parameter changes at boundaries. Thus, the analytical solution of the traffic signal structure can approximate the expecting value of the parameters like stiffness or inertia etc. This anticipation of the parameter can give the more precise observations when the complex supporting system exists. Therefore, this analytical solution can be utilized for the parameter observations of the system.

In conclusion, the analytical solution of the traffic signal structure using

discretized continuous system concept is developed in this research. To develop this analytical solution and to overcome the difficulties of the modeling, the several mathematical approaches of the continuous system have been taken into account from the conventional and basic idea to the discretized system concept. Moreover, to capture more realistic motion of the system, many types of boundary conditions have been considered and applied to setup the analytical model. The analytical model has been therefore verified the accuracy and usability for the traffic signal structure, although it still has small errors between analytical model and real model due to insufficient discretized elements. Finally, the analytical solutions will be more considerably accurate with supplying the more precise observation of the boundary parameters and the more discretized element of the system to consider the effects of the tapered cross-sectional member.

9. CONCLUSION

Traffic signal structures are very important basic infrastructure in modern society. There are many different types of traffic signal structures and a cantilevered type is one of the mostly using types of the traffic signal structure. However, as earlier mentioned, there have been many occurrences of failure or damage of cantilever traffic signal structures in this country, so many researches have been carried out to understand the dynamic behaviors of the traffic signal structure and to develop the vibrating mitigation strategies.

As a part of the efforts, the analytical solutions for dynamic characteristics of a traffic signal structure are provided in this thesis. To develop the analytical model, the distributed parameter method, simply called continuous system, is adopted and analyzed in modal analysis.

In the first approach, the conventional continuous system idea was applied to the traffic signal structure. However, it reveals that there are original difficulties to analyze structures which are combined different directional member like traffic signal structure. Moreover, while in investigating the structure with conventional continuous system concept, it is realized that additional attachment at arbitrary location on the member would cause the inaccurate analysis. Therefore, the discretized continuous system model was developed to overcome several difficulties from the conventional continuous system model. However, later it was realized that this discretized continuous system model can

take into account the tapered members with piecewise-tapered section properties.

Using the suggested analytical model through Sections 2 to 4, the eigenfrequency variations of each member of the traffic signal structure have been studied and shown in Section 5. In that section, the tendency of the eigenfrequency along with variations of the spring stiffness on the boundary conditions was observed.

However, the accuracy of the analytical solutions must be verified to be applied to the structure. Thus, for each single member, the analytical solutions were compared with numerical solution of the finite element model. As have seen, the analytical solutions show considerably small errors in the first eigenfrequencies from the finite element model. However, the results of the traffic signal structure application of this analytical solutions show large errors in the first and the second eigenfrequencies from the experimental measurements. The large errors are caused by the varying cross-sectional member in the analytical solution. However, because the computations of this analytical solution perform heavy symbolic matrix calculation to determine the zero-determinant and also to obtain the constants of the eigenfunctions, the capacity of computer is critical to the computation time of this analysis.

REFERENCES

Chun, K. R. (1972). "Free vibration of a beam with one end spring-hinged and the other free." *Journal of Applied Mechanics, Transactions ASME*, 39 Ser E(4), 1154-1155.

Dexter, R. J., Ricker, M. J. (2002). *Fatigue-resistant design of cantilevered signal, sign, and light supports*, National Academy Press, Washington, DC.

Ercoli, L., and Laura, P. A. A. (1987). "Analytical and experimental investigation on continuous beams carrying elastically mounted masses." *Journal of Sound and Vibration*, 114(3), 519-533.

Gürgöze, M. (1984). "A note on the vibrations of restrained beams and rods with point masses." *Journal of Sound and Vibration*, 96(4), 461-468.

Gürgöze, M. (1985). "On the vibrations of restrained beams and rods with heavy masses." *Journal of Sound and Vibration*, 100(4), 588-589.

Gürgöze, M. (1996). "On the eigenfrequencies of a cantilever beam with attached tip mass and a spring-mass system." *Journal of Sound and Vibration*, 190(2), 149-162.

Goel, R. P. (1973). "Vibrations of a beam carrying a concentrated mass." *Journal of Applied Mechanics, Transactions ASME*, 40 Ser E(3), 821-822.

Goel, R. P. (1976). "Free vibrations of a beam-mass system with elastically restrained ends." *Journal of Sound and Vibration*, 47(1), 9-14.

Jacquot, R. G., and Gibson, J. D. (1972). "The effects of discrete masses and elastic supports on continuous beam natural frequencies." *Journal of Sound and Vibration*, 23(2), 237-244.

Kaczinski, M. R., Dexter, R. J., and Van Dien, J. P. (1998). *Fatigue-resistant design of cantilevered signal, sign and light supports*, Transportation Research Board, Washington, DC.

Laura, P. A. A., Pombo, J. L., and Susemihl, E. A. (1974). "A note on the vibrations of a clamped-free beam with a mass at the free end." *Journal of Sound and Vibration*, 37(2), 161-168.

Laura, P. A. A., Verniere de Irassar, P., and Ficcadenti, G. M. (1983). "A note on transverse vibrations of continuous beams subject to an axial force and carrying concentrated masses." *Journal of Sound and Vibration*, 86(2), 279-284.

Letchford, C. W., Cruzado, H., and Zuo, D. (2008). "Risk Assessment Model for Wind-Induced Fatigue Failure of Cantilever Traffic Signal Structures." FHWA/TX-07-4586-4.

Low, K. H. (1991). "A comprehensive approach for the eigenproblem of beams with arbitrary boundary conditions." *Computers and Structures*, 39(6), 671-678.

Low, K. H. (1997). "An analytical-experimental comparative study of vibration analysis for loaded beams with variable boundary conditions." *Computers and Structures*, 65(1), 97-107.

Maiz, S., Bambill, D. V., Rossit, C. A., and Laura, P. A. A. (2007). "Transverse vibration of Bernoulli-Euler beams carrying point masses and taking into account their rotatory inertia: Exact solution." *Journal of Sound and Vibration*, 303(3-5), 895-908.

McDonald, J. R., Mehta, K., Oler, W., and Pulipaka, N. (1995). "Wind Load Effects on Signs, Luminaires and Traffic Signal Structures." *Texas Tech University*, Res Rept 1303-F, 196 p.

Rao, S. S. (2007). *Vibration of continuous systems*, Wiley Online Library, http://onlinelibrary.wiley.com/book/10.1002/9780470117866.

Wu, J. S., and Lin, T. L. (1990). "Free vibration analysis of a uniform cantilever beam with point masses by an analytical-and-numerical-combined method." *Journal of Sound and Vibration*, 136(2), 201-213.

Zuo, D., and Letchford, C. W. (2010). "Wind-induced vibration of a traffic-signal-support structure with cantilevered tapered circular mast arm." *Engineering Structures*, 32(10), 3171-3179.

APPENDIX A

- Modified Bisection Method

The bisection method is a root finding method by repeatedly bisecting an interval in which a root of the continuous equation must be. The concept of this simple and robust numerical calculation is adopted for the computation to find the roots to satisfy the singularity of the large matrix. In the modified concept of the bisection method, the interval in which roots are contained is multiply sectioned by the given number of segments. Then, it seeks the smaller interval which contains a root and the smaller interval is multiply sectioned again, as shown in Figure A.1. These repetitive processes are implemented over and over again until the interval is within the given tolerance.

This modified bisection method is properly designed from the concept of the bisection method to apply to the computations of eigenfrequency coefficients for this thesis. In the conventional idea to find the eigenfrequencies, it normally finds the eigenfrequency equation and solves the equation to obtain roots. However, the given symbolic matrix for boundary conditions are too large to find the eigenfrequency equation, thus it takes considerably long computation time. As a result, the modified bisection method suggested herein can guarantee the relatively quick computation and the proper accuracy of the roots. Moreover, the important advantage of this method is the solution for eigenfrequency coefficients from the large symbolic matrix can be found without processing eigenfrequency equation.

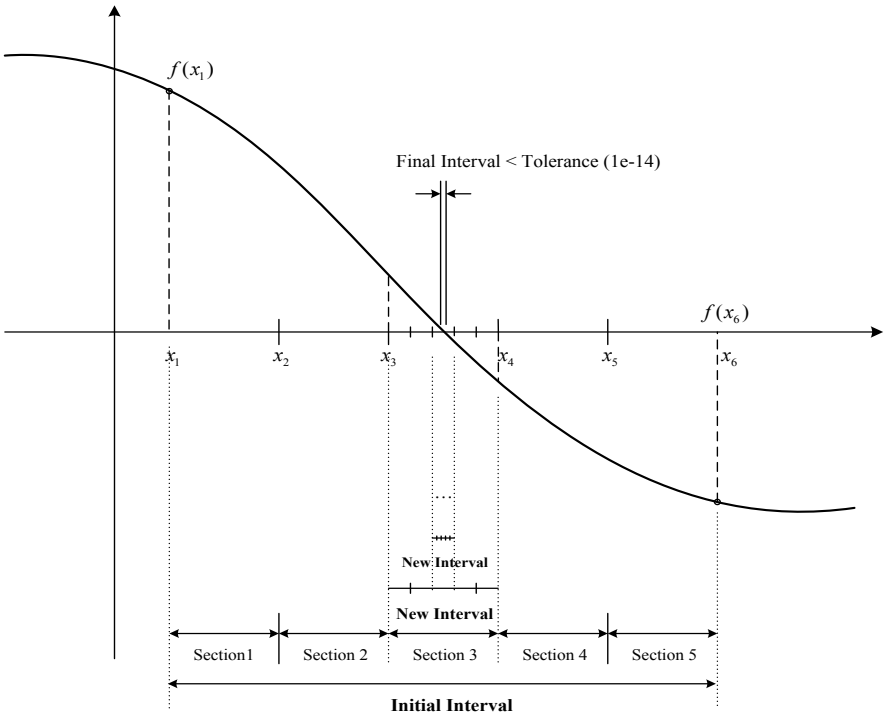

Figure A.1: Modified Bisection Method

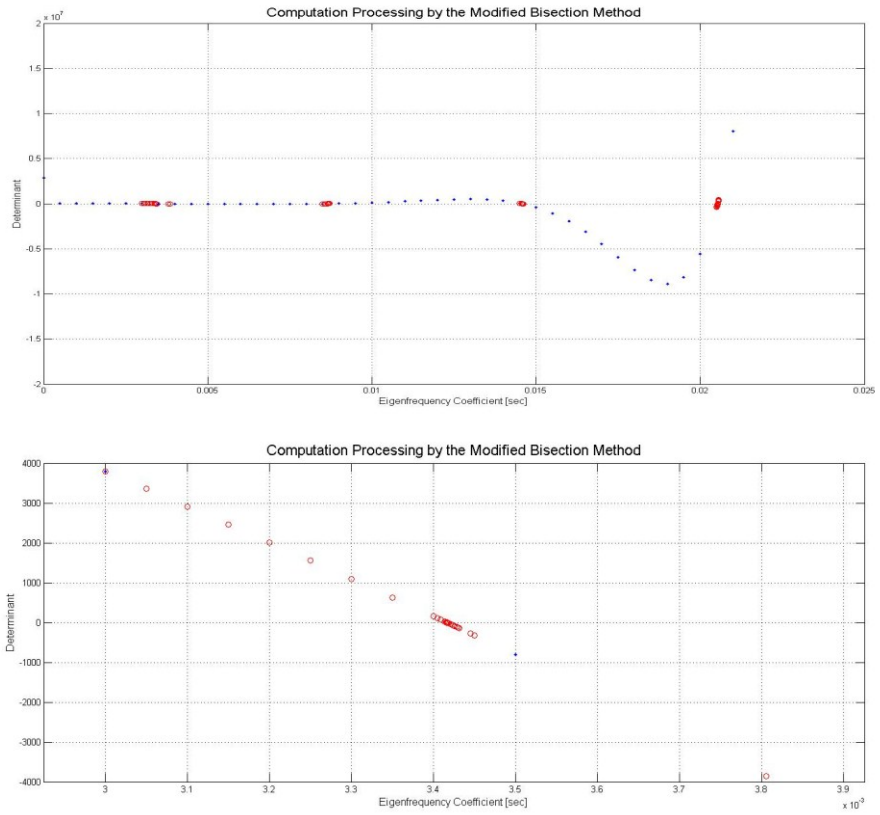

Figure A.2: Computation Processing of MATLAB with the Modified Bisection Method

APPENDIX B

Derivation of Continuity and Compatibility Conditions

a. First Point Mass at $x = x_1$

$$\begin{aligned} &c_1 \cdot \cos\beta_i \cdot x_1 + c_2 \cdot \sin\beta_i \cdot x_1 + c_3 \cdot \cosh\beta_i \cdot x_1 + c_4 \cdot \sinh\beta_i \cdot x_1 \\ &\quad - c_5 \cdot \cos\beta_i \cdot x_1 - c_6 \cdot \sin\beta_i \cdot x_1 - c_7 \cdot \cosh\beta_i \cdot x_1 - c_8 \cdot \sinh\beta_i \cdot x_1 = 0 \end{aligned} \tag{B.1}$$

$$\begin{aligned} &-c_1 \cdot \sin\beta_i \cdot x_1 + c_2 \cdot \cos\beta_i \cdot x_1 + c_3 \cdot \sinh\beta_i \cdot x_1 + c_4 \cdot \cosh\beta_i \cdot x_1 \\ &\quad + c_5 \cdot \sin\beta_i \cdot x_1 - c_6 \cdot \cos\beta_i \cdot x_1 - c_7 \cdot \sinh\beta_i \cdot x_1 - c_8 \cdot \cosh\beta_i \cdot x_1 = 0 \end{aligned} \tag{B.2}$$

$$\begin{aligned} &-c_1 \cdot \cos\beta_i \cdot x_1 - c_2 \cdot \sin\beta_i \cdot x_1 + c_3 \cdot \cosh\beta_i \cdot x_1 + c_4 \cdot \sinh\beta_i \cdot x_1 \\ &\quad + c_5 \cdot \cos\beta_i \cdot x_1 + c_6 \cdot \sin\beta_i \cdot x_1 - c_7 \cdot \cosh\beta_i \cdot x_1 - c_8 \cdot \sinh\beta_i \cdot x_1 = 0 \end{aligned} \tag{B.3}$$

$$\begin{aligned} &c_1 \cdot (\sin\beta_i \cdot x_1 + M_1 \cdot \beta_i^4 \cdot \cos\beta_i \cdot x_1) - c_2 \cdot (\cos\beta_i \cdot x_1 - M_1 \cdot \beta_i^4 \cdot \sin\beta_i \cdot x_1) \\ &+ c_3 \cdot (\sinh\beta_i \cdot x_1 + M_1 \cdot \beta_i^4 \cdot \cosh\beta_i \cdot x_1) + c_4 \cdot (\cosh\beta_i \cdot x_1 + M_1 \cdot \beta_i^4 \cdot \sinh\beta_i \cdot x_1) \\ &- c_5 \cdot \sin\beta_i \cdot x_1 + c_6 \cdot \cos\beta_i \cdot x_1 - c_7 \cdot \sinh\beta_i \cdot x_1 - c_8 \cdot \cosh\beta_i \cdot x_1 = 0 \end{aligned} \tag{B.4}$$

$$where,\ M_1 = \frac{m_1}{\rho_a A_a}$$

b. Second Point Mass at $x = x_2$

$$\begin{aligned} &c_5 \cdot \cos\beta_i \cdot x_2 + c_6 \cdot \sin\beta_i \cdot x_2 + c_7 \cdot \cosh\beta_i \cdot x_2 + c_8 \cdot \sinh\beta_i \cdot x_2 \\ &\quad - c_9 \cdot \cos\beta_i \cdot x_2 - c_{10} \cdot \sin\beta_i \cdot x_2 - c_{11} \cdot \cosh\beta_i \cdot x_2 - c_{12} \cdot \sinh\beta_i \cdot x_2 = 0 \end{aligned} \tag{B.5}$$

$$\begin{aligned} &-c_5 \cdot \sin\beta_i \cdot x_2 + c_6 \cdot \cos\beta_i \cdot x_2 + c_7 \cdot \sinh\beta_i \cdot x_2 + c_8 \cdot \cosh\beta_i \cdot x_2 \\ &\quad + c_9 \cdot \sin\beta_i \cdot x_2 - c_{10} \cdot \cos\beta_i \cdot x_2 - c_{11} \cdot \sinh\beta_i \cdot x_2 - c_{12} \cdot \cosh\beta_i \cdot x_2 = 0 \end{aligned} \tag{B.6}$$

$$\begin{aligned} &-c_5 \cdot \cos\beta_i \cdot x_2 - c_6 \cdot \sin\beta_i \cdot x_2 + c_7 \cdot \cosh\beta_i \cdot x_2 + c_8 \cdot \sinh\beta_i \cdot x_2 \\ &\quad + c_9 \cdot \cos\beta_i \cdot x_2 + c_{10} \cdot \sin\beta_i \cdot x_2 - c_{11} \cdot \cosh\beta_i \cdot x_2 - c_{12} \cdot \sinh\beta_i \cdot x_2 = 0 \end{aligned} \tag{B.7}$$

$$\begin{aligned} &c_5 \cdot (\sin\beta_i \cdot x_2 + M_2 \cdot \beta_i^4 \cdot \cos\beta_i \cdot x_2) - c_6 \cdot (\cos\beta_i \cdot x_2 - M_2 \cdot \beta_i^4 \cdot \sin\beta_i \cdot x_2) \\ &+ c_7 \cdot (\sinh\beta_i \cdot x_2 + M_2 \cdot \beta_i^4 \cdot \cosh\beta_i \cdot x_2) + c_8 \cdot (\cosh\beta_i \cdot x_2 + M_2 \cdot \beta_i^4 \cdot \sinh\beta_i \cdot x_2) \\ &- c_9 \cdot \sin\beta_i \cdot x_2 + c_{10} \cdot \cos\beta_i \cdot x_2 - c_{11} \cdot \sinh\beta_i \cdot x_2 - c_{12} \cdot \cosh\beta_i \cdot x_2 = 0 \end{aligned} \tag{B.8}$$

$$where,\ M_2 = \frac{m_2}{\rho_a A_a}$$

c. *Third Point Mass at* $x = x_3$

$$c_9 \cdot \cos\beta_i \cdot x_3 + c_{10} \cdot \sin\beta_i \cdot x_3 + c_{11} \cdot \cosh\beta_i \cdot x_3 + c_{12} \cdot \sinh\beta_i \cdot x_3 - c_{13} \cdot \cos\beta_i \cdot x_3 - c_{14} \cdot \sin\beta_i \cdot x_3 - c_{15} \cdot \cosh\beta_i \cdot x_3 - c_{16} \cdot \sinh\beta_i \cdot x_3 = 0 \quad \text{(B.9)}$$

$$-c_9 \cdot \sin\beta_i \cdot x_3 + c_{10} \cdot \cos\beta_i \cdot x_3 + c_{11} \cdot \sinh\beta_i \cdot x_3 + c_{12} \cdot \cosh\beta_i \cdot x_3 + c_{13} \cdot \sin\beta_i \cdot x_3 - c_{14} \cdot \cos\beta_i \cdot x_3 - c_{15} \cdot \sinh\beta_i \cdot x_3 - c_{16} \cdot \cosh\beta_i \cdot x_3 = 0 \quad \text{(B.10)}$$

$$-c_9 \cdot \cos\beta_i \cdot x_3 - c_{10} \cdot \sin\beta_i \cdot x_3 + c_{11} \cdot \cosh\beta_i \cdot x_3 + c_{12} \cdot \sinh\beta_i \cdot x_3 + c_{13} \cdot \cos\beta_i \cdot x_3 + c_{14} \cdot \sin\beta_i \cdot x_3 - c_{15} \cdot \cosh\beta_i \cdot x_3 - c_{16} \cdot \sinh\beta_i \cdot x_3 = 0 \quad \text{(B.11)}$$

$$c_9 \cdot (\sin\beta_i \cdot x_3 + M_3 \cdot \beta_i^4 \cdot \cos\beta_i \cdot x_3) - c_{10} \cdot (\cos\beta_i \cdot x_3 - M_3 \cdot \beta_i^4 \cdot \sin\beta_i \cdot x_3) + c_{11} \cdot (\sinh\beta_i \cdot x_3 + M_3 \cdot \beta_i^4 \cdot \cosh\beta_i \cdot x_3) + c_{12} \cdot (\cosh\beta_i \cdot x_3 + M_3 \cdot \beta_i^4 \cdot \sinh\beta_i \cdot x_3) - c_{13} \cdot \sin\beta_i \cdot x_3 + c_{14} \cdot \cos\beta_i \cdot x_3 - c_{15} \cdot \sinh\beta_i \cdot x_3 - c_{16} \cdot \cosh\beta_i \cdot x_3 = 0 \quad \text{(B.12)}$$

$$\textit{where, } M_3 = \frac{m_3}{\rho_a A_a}$$

APPENDIX C

- Matrix for Boundary, Continuity and Compatibility Conditions

The sixteen equations for boundary, continuity and compatibility conditions are expressed by Equation (3.11) through (3.14) and (3.28) to (3.31) These equations are reformed as a sixteen-by-sixteen matrix for the calculations for eigenfrequency coefficients which provides eigenfrequencies of the system. The large matrix is exhibited as follows

$$\begin{bmatrix} \begin{bmatrix} 2\times 4\ Matrix \\ \text{for} \\ \text{Boundary Conditions} \\ \text{at Left-End} \end{bmatrix} & \begin{matrix} 0 & 0 & 0 & 0 & 0 & 0 & 0 & 0 & 0 & 0 & 0 & 0 \\ 0 & 0 & 0 & 0 & 0 & 0 & 0 & 0 & 0 & 0 & 0 & 0 \end{matrix} \\ \begin{bmatrix} 4\times 8\ Matrix \\ \text{for} \\ \text{Continuity \& Compatibility Conditions} \\ \text{at NODE 1} \end{bmatrix} & \begin{matrix} 0 & 0 & 0 & 0 & 0 & 0 & 0 & 0 \\ 0 & 0 & 0 & 0 & 0 & 0 & 0 & 0 \\ 0 & 0 & 0 & 0 & 0 & 0 & 0 & 0 \\ 0 & 0 & 0 & 0 & 0 & 0 & 0 & 0 \end{matrix} \\ \begin{matrix} 0 & 0 & 0 & 0 \\ 0 & 0 & 0 & 0 \\ 0 & 0 & 0 & 0 \\ 0 & 0 & 0 & 0 \end{matrix} & \begin{bmatrix} 4\times 8\ Matrix \\ \text{for} \\ \text{Continuity \& Compatibility Conditions} \\ \text{at NODE 2} \end{bmatrix} & \begin{matrix} 0 & 0 & 0 & 0 \\ 0 & 0 & 0 & 0 \\ 0 & 0 & 0 & 0 \\ 0 & 0 & 0 & 0 \end{matrix} \\ \begin{matrix} 0 & 0 & 0 & 0 & 0 & 0 & 0 & 0 \\ 0 & 0 & 0 & 0 & 0 & 0 & 0 & 0 \\ 0 & 0 & 0 & 0 & 0 & 0 & 0 & 0 \\ 0 & 0 & 0 & 0 & 0 & 0 & 0 & 0 \end{matrix} & \begin{bmatrix} 4\times 8\ Matrix \\ \text{for} \\ \text{Continuity \& Compatibility Conditions} \\ \text{at NODE 3} \end{bmatrix} \\ \begin{matrix} 0 & 0 & 0 & 0 & 0 & 0 & 0 & 0 & 0 & 0 & 0 & 0 \\ 0 & 0 & 0 & 0 & 0 & 0 & 0 & 0 & 0 & 0 & 0 & 0 \end{matrix} & \begin{bmatrix} 2\times 4\ Matrix \\ \text{for} \\ \text{Boundary Conditions} \\ \text{at Right-End} \end{bmatrix} \end{bmatrix} \cdot \begin{Bmatrix} C_1 \\ C_2 \\ C_3 \\ C_4 \\ C_5 \\ C_6 \\ C_7 \\ C_8 \\ C_9 \\ C_{10} \\ C_{11} \\ C_{12} \\ C_{13} \\ C_{14} \\ C_{15} \\ C_{16} \end{Bmatrix} = \begin{bmatrix} 0 \\ 0 \\ 0 \\ 0 \\ 0 \\ 0 \\ 0 \\ 0 \\ 0 \\ 0 \\ 0 \\ 0 \\ 0 \\ 0 \\ 0 \\ 0 \end{bmatrix} \tag{C.1}$$

$$\mathrm{C_{ik}} = \cos \beta_i \cdot x_k \qquad \mathrm{S_{ik}} = \sin \beta_i \cdot x_k$$

$$\mathrm{Ch_{ik}} = \cosh \beta_i \cdot x_k \qquad \mathrm{Sh_{ik}} = \sinh \beta_i \cdot x_k$$

$$\mathrm{MB}_{ji} = M_j \cdot \beta_i^4$$

$$\begin{bmatrix} 2\times 4\ Matrix \\ \text{for} \\ \text{Boundary Conditions} \\ \text{at Left-End} \end{bmatrix} = \begin{bmatrix} 1 & 0 & 1 & 0 \\ 0 & 1 & 0 & 1 \end{bmatrix} \tag{C.2}$$

$$\begin{bmatrix} 4\times 8\ Matrix \\ \text{for} \\ \text{Continuity \& Compatibility Conditions} \\ \text{at NODE 1} \end{bmatrix} =$$

$$\begin{bmatrix} C_{i1} & S_{i1} & Ch_{i1} & Sh_{i1} & -C_{i1} & -S_{i1} & -Ch_{i1} & -Sh_{i1} \\ -S_{i1} & C_{i1} & Sh_{i1} & Ch_{i1} & S_{i1} & -C_{i1} & -Sh_{i1} & -Ch_{i1} \\ -C_{i1} & -S_{i1} & Ch_{i1} & Sh_{i1} & C_{i1} & S_{i1} & -Ch_{i1} & -Sh_{i1} \\ (S_{i1}+MB_{1i}\cdot C_{i1}) & -(C_{i1}-MB_{1i}\cdot S_{i1}) & (Ch_{i1}+MB_{1i}\cdot Sh_{i1}) & (Ch_{i1}+MB_{1i}\cdot Sh_{i1}) & -S_{i1} & C_{i1} & -Sh_{i1} & -Ch_{i1} \end{bmatrix} \tag{C.3}$$

$$\begin{bmatrix} 4\times 8\ Matrix \\ \text{for} \\ \text{Continuity \& Compatibility Conditions} \\ \text{at NODE 2} \end{bmatrix} =$$

$$\begin{bmatrix} C_{i2} & S_{i2} & Ch_{i2} & Sh_{i2} & -C_{i2} & -S_{i2} & -Ch_{i2} & -Sh_{i2} \\ -S_{i2} & C_{i2} & Sh_{i2} & Ch_{i2} & S_{i2} & -C_{i2} & -Sh_{i2} & -Ch_{i2} \\ -C_{i2} & -S_{i2} & Ch_{i2} & Sh_{i2} & C_{i2} & S_{i2} & -Ch_{i2} & -Sh_{i2} \\ (S_{i2}+MB_{2i}\cdot C_{i2}) & -(C_{i2}-MB_{2i}\cdot S_{i2}) & (Ch_{i2}+MB_{2i}\cdot Sh_{i2}) & (Ch_{i2}+MB_{2i}\cdot Sh_{i2}) & -S_{i2} & C_{i2} & -Sh_{i2} & -Ch_{i2} \end{bmatrix} \tag{C.4}$$

$$\begin{bmatrix} 4\times 8\ Matrix \\ \text{for} \\ \text{Continuity \& Compatibility Conditions} \\ \text{at NODE 3} \end{bmatrix} =$$

$$\begin{bmatrix} C_{i3} & S_{i3} & Ch_{i3} & Sh_{i3} & -C_{i3} & -S_{i3} & -Ch_{i3} & -Sh_{i3} \\ -S_{i3} & C_{i3} & Sh_{i3} & Ch_{i3} & S_{i3} & -C_{i3} & -Sh_{i3} & -Ch_{i3} \\ -C_{i3} & -S_{i3} & Ch_{i3} & Sh_{i3} & C_{i3} & S_{i3} & -Ch_{i3} & -Sh_{i3} \\ (S_{i3}+MB_{3i}\cdot C_{i3}) & -(C_{i3}-MB_{3i}\cdot S_{i3}) & (Ch_{i3}+MB_{3i}\cdot Sh_{i3}) & (Ch_{i3}+MB_{3i}\cdot Sh_{i3}) & -S_{i3} & C_{i3} & -Sh_{i3} & -Ch_{i3} \end{bmatrix} \tag{C.5}$$

$$\begin{bmatrix} 2\times 4\ Matrix \\ \text{for} \\ \text{Boundary Conditions} \\ \text{at Left-End} \end{bmatrix} = \begin{bmatrix} S_{ia} & -C_{ia} & Sh_{ia} & Ch_{ia} \\ -C_{ia} & -S_{ia} & Ch_{ia} & Sh_{ia} \end{bmatrix} \tag{C.6}$$

APPENDIX D

- Verification of Boundary, Continuity and Compatibility Conditions in MAPLE

$$V_1 := x \rightarrow c_1 \cdot cos(beta \cdot x) + c_2 \cdot sin(beta \cdot x) + c_3 \cdot cosh(beta \cdot x) + c_4 \cdot sinh(beta \cdot x);$$

$$x \rightarrow c_1 \cos(\beta x) + c_2 \sin(\beta x) + c_3 \cosh(\beta x) + c_4 \sinh(\beta x)$$

$$dV_1 := x \rightarrow diff(V_1(x), x) : dV_1(x) :$$

$$ddV_1 := x \rightarrow diff(dV_1(x), x) : ddV_1(x) :$$

$$dddV_1 := x \rightarrow diff(ddV_1(x), x) : dddV_1(x) :$$

$$V_2 := x \rightarrow c_5 \cdot cos(beta \cdot x) + c_6 \cdot sin(beta \cdot x) + c_7 \cdot cosh(beta \cdot x) + c_8 \cdot sinh(beta \cdot x);$$

$$x \rightarrow c_5 \cos(\beta x) + c_6 \sin(\beta x) + c_7 \cosh(\beta x) + c_8 \sinh(\beta x)$$

$$dV_2 := x \rightarrow diff(V_2(x), x) : dV_2(x) :$$

$$ddV_2 := x \rightarrow diff(dV_2(x), x) : ddV_2(x) :$$

$$dddV_2 := x \rightarrow diff(ddV_2(x), x) : dddV_2(x) :$$

$$V_3 := x \rightarrow c_9 \cdot cos(beta \cdot x) + c_{10} \cdot sin(beta \cdot x) + c_{11} \cdot cosh(beta \cdot x) + c_{12} \cdot sinh(beta \cdot x);$$

$$x \rightarrow c_9 \cos(\beta x) + c_{10} \sin(\beta x) + c_{11} \cosh(\beta x) + c_{12} \sinh(\beta x)$$

$$dV_3 := x \rightarrow diff(V_3(x), x) : dV_3(x) :$$

$$ddV_3 := x \rightarrow diff(dV_3(x), x) : ddV_3(x) :$$

$$dddV_3 := x \rightarrow diff(ddV_3(x), x) : dddV_3(x) :$$

$$V_4 := x \rightarrow c_{13} \cdot cos(beta \cdot x) + c_{14} \cdot sin(beta \cdot x) + c_{15} \cdot cosh(beta \cdot x) + c_{16} \cdot sinh(beta \cdot x);$$

$$x \rightarrow c_{13} \cos(\beta x) + c_{14} \sin(\beta x) + c_{15} \cosh(\beta x) + c_{16} \sinh(\beta x)$$

$$dV_4 := x \rightarrow diff(V_4(x), x) : dV_4(x) :$$

$$ddV_4 := x \rightarrow diff(dV_4(x), x) : ddV_4(x) :$$

$$dddV_4 := x \rightarrow diff(ddV_4(x), x) : dddV_4(x) :$$

****

BOUNDARY CONDITIONS I & II

****

$$BC1 := simplify(subs(x = 0, V_1(x))) :$$

$$BC2 := simplify\left(\frac{subs(x = 0, dV_1(x))}{beta \cdot La}\right) :$$

$$c_3 := -c_1 : c_1 := A :$$

$$c_4 := -c_2 : c_2 := B :$$

****

CONTINUITY and COMPATIBILITY CONDITIONS I

****

$$CC11 := collect\left(subs\left(x = L_1,\ V_1(x) \right) - subs\left(x = L_1,\ V_2(x) \right),\ \left[A,\ B,\ c_5,\ c_6,\ c_7,\ c_8 \right] \right) :$$

$$CC12 := collect\left(simplify\left(\frac{subs\left(x = L_1,\ dV_1(x) \right)}{beta} - \frac{subs\left(x = L_1,\ dV_2(x) \right)}{beta} \right),\ \left[A,\ B,\ c_5,\ c_6,\ c_7,\ c_8 \right] \right) :$$

$$CC13 := collect\left(simplify\left(\frac{subs\left(x = L_1,\ ddV_1(x) \right)}{(beta)^2} - \frac{subs\left(x = L_1,\ ddV_2(x) \right)}{(beta)^2} \right),\ \left[A,\ B,\ c_5,\ c_6,\ c_7,\ c_8 \right] \right) :$$

$$CC14 := collect\left(simplify\left(\frac{subs\left(x = L_1,\ dddV_1(x) \right)}{(beta)^3} \right) + simplify\left(\frac{M_1 \cdot \beta^4 \cdot subs\left(x = L_1,\ V_1(x) \right)}{(beta)^3} \right) - simplify\left(\frac{subs\left(x = L_1,\ dddV_2(x) \right)}{(beta)^3} \right),\ \left[A,\ B,\ c_5,\ c_6,\ c_7,\ c_8 \right] \right) :$$

****

$$step111 := \frac{simplify(CC11 + CC13)}{2} :$$

$$step112 := \frac{simplify(CC11 - CC13)}{2} :$$

$$step113 := \frac{collect\left(simplify(CC12 + CC14),\ \left[A,\ B,\ c_5,\ c_6,\ c_7,\ c_8 \right] \right)}{2} :$$

$$step114 := \frac{collect\left(simplify(CC12 - CC14),\ \left[A,\ B,\ c_5,\ c_6,\ c_7,\ c_8 \right] \right)}{2} :$$

****

$$step121 := collect\left(simplify\left(\frac{step111}{cosh\left(\beta\ L_1 \right)} - \frac{step113}{sinh\left(\beta\ L_1 \right)} \right),\ \left[A,\ B,\ c_5,\ c_6,\ c_7,\ c_8 \right] \right) :$$

$$step122 := collect\left(simplify\left(\frac{step111}{sinh(\beta\ L_1)} - \frac{step113}{cosh(\beta\ L_1)} \right), [A, B, c_5, c_6, c_7, c_8] \right) :$$

$$step123 := collect\left(simplify\left(\frac{step112}{cos(\beta\ L_1)} + \frac{step114}{sin(\beta\ L_1)} \right), [A, B, c_5, c_6, c_7, c_8] \right) :$$

$$step124 := collect\left(simplify\left(\frac{step112}{sin(\beta\ L_1)} - \frac{step114}{cos(\beta\ L_1)} \right), [A, B, c_5, c_6, c_7, c_8] \right) :$$

****

$$cc_8 := collect(simplify(solve(step121, c_8))), [A, B]) :$$

$$cc_7 := collect(simplify(solve(step122, c_7))), [A, B]) :$$

$$cc_6 := collect(simplify(solve(step123, c_6))), [A, B]) :$$

$$cc_5 := collect(simplify(solve(step124, c_5))), [A, B]) :$$

****

CONTINUITY and COMPATIBILITY CONDITIONS II

****

$$CC21 := collect(subs(x = L_2, V_2(x)) - subs(x = L_2, V_3(x)), [c_5, c_6, c_7, c_8, c_9, c_{10}, c_{11}, c_{12}]) :$$

$$CC22 := collect\left(simplify\left(\frac{subs(x = L_2, dV_2(x))}{beta} - \frac{subs(x = L_2, dV_3(x))}{beta} \right), [c_5, c_6, c_7, c_8, c_9, c_{10}, c_{11}, c_{12}] \right) :$$

$$CC23 := collect\left(simplify\left(\frac{subs\left(x = L_2,\ ddV_2(x) \right)}{(beta)^2} - \frac{subs\left(x = L_2,\ ddV_3(x) \right)}{(beta)^2} \right),\ [c_5, c_6, c_7, c_8, c_9, c_{10}, c_{11}, c_{12}] \right) :$$

$$CC24 := collect\left(simplify\left(\frac{subs\left(x = L_2,\ dddV_2(x) \right)}{(beta)^3} \right) + simplify\left(\frac{M_2 \cdot \beta^4 \cdot subs\left(x = L_2,\ V_2(x) \right)}{(beta)^3} \right) - simplify\left(\frac{subs\left(x = L_2,\ dddV_3(x) \right)}{(beta)^3} \right),\ [c_5, c_6, c_7, c_8, c_9, c_{10}, c_{11}, c_{12}] \right) :$$

****

$$step211 := \frac{simplify(CC21 + CC23)}{2} :$$

$$step212 := \frac{simplify(CC21 - CC23)}{2} :$$

$$step213 := \frac{collect\left(simplify(CC22 + CC24),\ [c_5, c_6, c_7, c_8, c_9, c_{10}, c_{11}, c_{12}] \right)}{2} :$$

$$step214 := \frac{collect\left(simplify(CC22 - CC24),\ [c_5, c_6, c_7, c_8, c_9, c_{10}, c_{11}, c_{12}] \right)}{2} :$$

****

$$step221 := collect\left(simplify\left(\frac{step211}{cosh\left(\beta\ L_2 \right)} - \frac{step213}{sinh\left(\beta\ L_2 \right)} \right),\ [c_5, c_6, c_7, c_8, c_9, c_{10}, c_{11}, c_{12}] \right) :$$

$$step222 := collect\left(simplify\left(\frac{step211}{sinh\left(\beta\ L_2 \right)} - \frac{step213}{cosh\left(\beta\ L_2 \right)} \right),\ [c_5, c_6, c_7, c_8, c_9, c_{10}, c_{11}, c_{12}] \right) :$$

$$step223 := collect\left(simplify\left(\frac{step212}{cos\left(\beta\ L_2 \right)} + \frac{step214}{sin\left(\beta\ L_2 \right)} \right),\ [c_5, c_6, c_7, c_8, c_9, c_{10}, c_{11}, c_{12}] \right) :$$

$$step224 := collect\left(simplify\left(\frac{step212}{sin(\beta\ L_2)} - \frac{step214}{cos(\beta\ L_2)} \right), [c_5, c_6, c_7, c_8, c_9, c_{10}, c_{11}, c_{12}] \right) :$$

****

$$bcc_{12} := simplify(solve(step221, c_{12})) :$$

$$bcc_{11} := simplify(solve(step222, c_{11})) :$$

$$bcc_{10} := simplify(solve(step223, c_{10})) :$$

$$bcc_9 := simplify(solve(step224, c_9)) :$$

****

$$cc_9 := collect(subs([c_5 = cc_5, c_6 = cc_6, c_7 = cc_7, c_8 = cc_8], bcc_9), [A, B]) :$$

$$cc_{10} := collect(subs([c_5 = cc_5, c_6 = cc_6, c_7 = cc_7, c_8 = cc_8], bcc_{10}), [A, B]) :$$

$$cc_{11} := collect(subs([c_5 = cc_5, c_6 = cc_6, c_7 = cc_7, c_8 = cc_8], bcc_{11}), [A, B]) :$$

$$cc_{12} := collect(subs([c_5 = cc_5, c_6 = cc_6, c_7 = cc_7, c_8 = cc_8], bcc_{12}), [A, B]) :$$

****

CONTINUITY and COMPATIBILITY CONDITIONS III

****

$$CC31 := collect(subs(x = L_3, V_3(x)) - subs(x = L_3, V_4(x)), [c_9, c_{10}, c_{11}, c_{12}, c_{13}, c_{14}, c_{15}, c_{16}]) :$$

$$CC32 := collect\left(simplify\left(\frac{subs\left(x = L_3,\ dV_3(x) \right)}{beta} - \frac{subs\left(x = L_3,\ dV_4(x) \right)}{beta} \right),\ [c_9,\ c_{10},\ c_{11},\ c_{12},\ c_{13},\ c_{14},\ c_{15},\ c_{16}] \right) :$$

$$CC33 := collect\left(simplify\left(\frac{subs\left(x = L_3,\ ddV_3(x) \right)}{(beta)^2} - \frac{subs\left(x = L_3,\ ddV_4(x) \right)}{(beta)^2} \right),\ [c_9,\ c_{10},\ c_{11},\ c_{12},\ c_{13},\ c_{14},\ c_{15},\ c_{16}] \right) :$$

$$CC34 := collect\left(simplify\left(\frac{subs\left(x = L_3,\ dddV_3(x) \right)}{(\beta)^3} \right) + simplify\left(\frac{M_3 \cdot \beta^4 \cdot subs\left(x = L_3,\ V_3(x) \right)}{(beta)^3} \right) - simplify\left(\frac{subs\left(x = L_3,\ dddV_4(x) \right)}{(beta)^3} \right),\ [c_9,\ c_{10},\ c_{11},\ c_{12},\ c_{13},\ c_{14},\ c_{15},\ c_{16}] \right) :$$

****

$$step311 := \frac{simplify(CC31 + CC33)}{2} :$$

$$step312 := \frac{simplify(CC31 - CC33)}{2} :$$

$$step313 := \frac{collect\left(simplify(CC32 + CC34),\ [c_9,\ c_{10},\ c_{11},\ c_{12},\ c_{13},\ c_{14},\ c_{15},\ c_{16}] \right)}{2} :$$

$$step314 := \frac{collect\left(simplify(CC32 - CC34),\ [c_9,\ c_{10},\ c_{11},\ c_{12},\ c_{13},\ c_{14},\ c_{15},\ c_{16}] \right)}{2} :$$

****

$$step321 := collect\left(simplify\left(\frac{step311}{cosh\left(\beta\ L_3 \right)} - \frac{step313}{sinh\left(\beta\ L_3 \right)} \right),\ [c_9,\ c_{10},\ c_{11},\ c_{12},\ c_{13},\ c_{14},\ c_{15},\ c_{16}] \right) :$$

$$step322 := collect\left(simplify\left(\frac{step311}{sinh\left(\beta\ L_3 \right)} - \frac{step313}{cosh\left(\beta\ L_3 \right)} \right),\ [c_9,\ c_{10},\ c_{11},\ c_{12},\ c_{13},\ c_{14},\ c_{15},\ c_{16}] \right) :$$

$$step323 := collect\left(simplify\left(\frac{step312}{cos(\beta\ L_3)} + \frac{step314}{sin(\beta\ L_3)} \right), [c_9, c_{10}, c_{11}, c_{12}, c_{13}, c_{14}, c_{15}, c_{16}] \right) :$$

$$step324 := collect\left(simplify\left(\frac{step312}{sin(\beta\ L_3)} - \frac{step314}{cos(\beta\ L_3)} \right), [c_9, c_{10}, c_{11}, c_{12}, c_{13}, c_{14}, c_{15}, c_{16}] \right) :$$

$$bcc_{16} := simplify(solve(step321, c_{16})) :$$

$$bcc_{15} := simplify(solve(step322, c_{15})) :$$

$$bcc_{14} := simplify(solve(step323, c_{14})) :$$

$$bcc_{13} := simplify(solve(step324, c_{13})) :$$

****

$$cc_{13} := collect(subs([c_9 = cc_9, c_{10} = cc_{10}, c_{11} = cc_{11}, c_{12} = cc_{12}], bcc_{13}), [A, B]) :$$

$$cc_{14} := collect(subs([c_9 = cc_9, c_{10} = cc_{10}, c_{11} = cc_{11}, c_{12} = cc_{12}], bcc_{14}), [A, B]) :$$

$$cc_{15} := collect(subs([c_9 = cc_9, c_{10} = cc_{10}, c_{11} = cc_{11}, c_{12} = cc_{12}], bcc_{15}), [A, B]) :$$

$$cc_{16} := collect(subs([c_9 = cc_9, c_{10} = cc_{10}, c_{11} = cc_{11}, c_{12} = cc_{12}], bcc_{16}), [A, B]) :$$

****

BOUNDARY CONDITIONS III & IV

****

$$BC3 := subs\left(x = La, simplify\left(\frac{ddV_4(x)}{(beta)^2} \right) = 0 \right) :$$

$$BC4 := subs\left(x = La, simplify\left(\frac{dddV_4(x)}{(beta)^3} \right) = 0 \right) :$$

$$BBC3 := collect\left(subs\left(\left[c_{13} = cc_{13}, c_{14} = cc_{14}, c_{15} = cc_{15}, c_{16} = cc_{16} \right], BC3 \right), \left[A, B \right] \right) :$$

APPENDIX E

- Constants of Eigenfunctions from MAPLE

a. Constants of the eigenfunction of the first beam element: $c_1 \sim c_4$

$c_1 = A$

$c_2 = B$

$c_3 = -A$

$c_4 = -B$

b. Constants of the eigenfunction of the second beam element: $c_5 \sim c_8$

$$c_5 = \left(1+\frac{1}{2}\cos(\beta L_1)\, M_1 \beta \sin(\beta L_1) - \frac{1}{2}\cosh(\beta L_1)\, M_1 \beta \sin(\beta L_1)\right) A + \left(\frac{1}{2} M_1 \beta - \frac{1}{2} M_1 \beta \cos(\beta L_1)^2 - \frac{1}{2}\sinh(\beta L_1)\, M_1 \beta \sin(\beta L_1)\right) B$$

$$c_6 = \left(-\frac{1}{2} M_1 \beta \cos(\beta L_1)^2 + \frac{1}{2}\cosh(\beta L_1)\, M_1 \beta \cos(\beta L_1)\right) A + \left(-\frac{1}{2}\cos(\beta L_1)\, M_1 \beta \sin(\beta L_1) + 1 + \frac{1}{2}\sinh(\beta L_1)\, M_1 \beta \cos(\beta L_1)\right) B$$

$$c_7 = \left(-1-\frac{1}{2}\sinh(\beta L_1)\, M_1 \beta \cos(\beta L_1) + \frac{1}{2}\cosh(\beta L_1)\, M_1 \beta \sinh(\beta L_1)\right) A + \left(-\frac{1}{2} M_1 \beta - \frac{1}{2}\sinh(\beta L_1)\, M_1 \beta \sin(\beta L_1) + \frac{1}{2} M_1 \beta \cosh(\beta L_1)^2\right) B$$

$$c_8 = \left(\frac{1}{2}\cosh(\beta L_1)\, M_1 \beta \cos(\beta L_1) - \frac{1}{2} M_1 \beta \cosh(\beta L_1)^2\right) A + \left(\frac{1}{2}\cosh(\beta L_1)\, M_1 \beta \sin(\beta L_1) - 1 - \frac{1}{2}\cosh(\beta L_1)\, M_1 \beta \sinh(\beta L_1)\right) B$$

c. Constants of the eigenfunction of the third beam element: $c_9 \sim c_{12}$

$c_9 =$

$$\left(\frac{1}{2}\sin(\beta L_2)\left(1+\frac{1}{2}\cos(\beta L_1)\,M_1\,\beta\sin(\beta L_1)-\frac{1}{2}\cosh(\beta L_1)\,M_1\,\beta\sin(\beta L_1)\right)M_2\,\beta\cos(\beta L_2)+\frac{1}{2}\left(-\frac{1}{2}M_1\,\beta\cos(\beta L_1)^2\right.\right.$$
$$\left.+\frac{1}{2}\cosh(\beta L_1)\,M_1\,\beta\cos(\beta L_1)\right)M_2\,\beta-\frac{1}{2}\left(-\frac{1}{2}M_1\,\beta\cos(\beta L_1)^2+\frac{1}{2}\cosh(\beta L_1)\,M_1\,\beta\cos(\beta L_1)\right)M_2\,\beta\cos(\beta L_2)^2+1$$
$$+\frac{1}{2}\cos(\beta L_1)\,M_1\,\beta\sin(\beta L_1)-\frac{1}{2}\cosh(\beta L_1)\,M_1\,\beta\sin(\beta L_1)+\frac{1}{2}\sin(\beta L_2)\left(-1-\frac{1}{2}\sinh(\beta L_1)\,M_1\,\beta\cos(\beta L_1)\right.$$
$$\left.+\frac{1}{2}\cosh(\beta L_1)\,M_1\,\beta\sinh(\beta L_1)\right)M_2\,\beta\cosh(\beta L_2)+\frac{1}{2}M_2\,\beta\sin(\beta L_2)\left(\frac{1}{2}\cosh(\beta L_1)\,M_1\,\beta\cos(\beta L_1)\right.$$
$$\left.-\frac{1}{2}M_1\,\beta\cosh(\beta L_1)^2\right)\sinh(\beta L_2)\Big)A+\left(\frac{1}{2}\left(-\frac{1}{2}\cos(\beta L_1)\,M_1\,\beta\sin(\beta L_1)+1+\frac{1}{2}\sinh(\beta L_1)\,M_1\,\beta\cos(\beta L_1)\right)M_2\,\beta+\frac{1}{2}M_1\,\beta\right.$$
$$-\frac{1}{2}M_1\,\beta\cos(\beta L_1)^2-\frac{1}{2}\sinh(\beta L_1)\,M_1\,\beta\sin(\beta L_1)+\frac{1}{2}\sin(\beta L_2)\left(\frac{1}{2}M_1\,\beta-\frac{1}{2}M_1\,\beta\cos(\beta L_1)^2\right.$$
$$\left.-\frac{1}{2}\sinh(\beta L_1)\,M_1\,\beta\sin(\beta L_1)\right)M_2\,\beta\cos(\beta L_2)+\frac{1}{2}\sin(\beta L_2)\left(-\frac{1}{2}M_1\,\beta-\frac{1}{2}\sinh(\beta L_1)\,M_1\,\beta\sin(\beta L_1)\right.$$
$$\left.+\frac{1}{2}M_1\,\beta\cosh(\beta L_1)^2\right)M_2\,\beta\cosh(\beta L_2)-\frac{1}{2}\left(-\frac{1}{2}\cos(\beta L_1)\,M_1\,\beta\sin(\beta L_1)+1+\frac{1}{2}\sinh(\beta L_1)\,M_1\,\beta\cos(\beta L_1)\right)M_2\,\beta\cos(\beta L_2)^2$$
$$\left.+\frac{1}{2}M_2\,\beta\sin(\beta L_2)\left(\frac{1}{2}\cosh(\beta L_1)\,M_1\,\beta\sin(\beta L_1)-1-\frac{1}{2}\cosh(\beta L_1)\,M_1\,\beta\sinh(\beta L_1)\right)\sinh(\beta L_2)\right)B$$

$c_{10} =$

$$\left(-\frac{1}{2}\cos(\beta L_2)\left(-\frac{1}{2}M_1\,\beta\cos(\beta L_1)^2+\frac{1}{2}\cosh(\beta L_1)\,M_1\,\beta\cos(\beta L_1)\right)M_2\,\beta\sin(\beta L_2)-\frac{1}{2}\left(1+\frac{1}{2}\cos(\beta L_1)\,M_1\,\beta\sin(\beta L_1)\right.\right.$$
$$\left.-\frac{1}{2}\cosh(\beta L_1)\,M_1\,\beta\sin(\beta L_1)\right)M_2\,\beta\cos(\beta L_2)^2-\frac{1}{2}\cos(\beta L_2)\left(-1-\frac{1}{2}\sinh(\beta L_1)\,M_1\,\beta\cos(\beta L_1)\right.$$
$$\left.+\frac{1}{2}\cosh(\beta L_1)\,M_1\,\beta\sinh(\beta L_1)\right)M_2\,\beta\cosh(\beta L_2)-\frac{1}{2}M_1\,\beta\cos(\beta L_1)^2+\frac{1}{2}\cosh(\beta L_1)\,M_1\,\beta\cos(\beta L_1)$$
$$-\frac{1}{2}M_2\,\beta\cos(\beta L_2)\left(\frac{1}{2}\cosh(\beta L_1)\,M_1\,\beta\cos(\beta L_1)-\frac{1}{2}M_1\,\beta\cosh(\beta L_1)^2\right)\sinh(\beta L_2)\Big)A+\left(-\frac{1}{2}\left(\frac{1}{2}M_1\,\beta-\frac{1}{2}M_1\,\beta\cos(\beta L_1)^2\right.\right.$$
$$\left.-\frac{1}{2}\sinh(\beta L_1)\,M_1\,\beta\sin(\beta L_1)\right)M_2\,\beta\cos(\beta L_2)^2-\frac{1}{2}\cos(\beta L_1)\,M_1\,\beta\sin(\beta L_1)+1+\frac{1}{2}\sinh(\beta L_1)\,M_1\,\beta\cos(\beta L_1)-\frac{1}{2}\cos(\beta L_2)\left(\right.$$
$$\left.-\frac{1}{2}\cos(\beta L_1)\,M_1\,\beta\sin(\beta L_1)+1+\frac{1}{2}\sinh(\beta L_1)\,M_1\,\beta\cos(\beta L_1)\right)M_2\,\beta\sin(\beta L_2)-\frac{1}{2}M_2\,\beta\cos(\beta L_2)\left(\frac{1}{2}\cosh(\beta L_1)\,M_1\,\beta\sin(\beta L_1)-1\right.$$
$$\left.-\frac{1}{2}\cosh(\beta L_1)\,M_1\,\beta\sinh(\beta L_1)\right)\sinh(\beta L_2)-\frac{1}{2}\cos(\beta L_2)\left(-\frac{1}{2}M_1\,\beta-\frac{1}{2}\sinh(\beta L_1)\,M_1\,\beta\sin(\beta L_1)\right.$$
$$\left.+\frac{1}{2}M_1\,\beta\cosh(\beta L_1)^2\right)M_2\,\beta\cosh(\beta L_2)\Big)B$$

$c_{11} =$

$$\left(-\frac{1}{2}\sinh(\beta L_2)\left(1+\frac{1}{2}\cos(\beta L_1)M_1\beta\sin(\beta L_1)-\frac{1}{2}\cosh(\beta L_1)M_1\beta\sin(\beta L_1)\right)M_2\beta\cos(\beta L_2)-\frac{1}{2}\sinh(\beta L_2)\left(-1\right.\right.$$
$$-\frac{1}{2}\sinh(\beta L_1)M_1\beta\cos(\beta L_1)+\frac{1}{2}\cosh(\beta L_1)M_1\beta\sinh(\beta L_1)\Big)M_2\beta\cosh(\beta L_2)-\frac{1}{2}\sinh(\beta L_2)\left(-\frac{1}{2}M_1\beta\cos(\beta L_1)^2\right.$$
$$\left.+\frac{1}{2}\cosh(\beta L_1)M_1\beta\cos(\beta L_1)\right)M_2\beta\sin(\beta L_2)-\frac{1}{2}M_2\beta\left(\frac{1}{2}\cosh(\beta L_1)M_1\beta\cos(\beta L_1)-\frac{1}{2}M_1\beta\cosh(\beta L_1)^2\right)\cosh(\beta L_2)^2-1$$
$$\left.-\frac{1}{2}\sinh(\beta L_1)M_1\beta\cos(\beta L_1)+\frac{1}{2}\cosh(\beta L_1)M_1\beta\sinh(\beta L_1)+\frac{1}{2}M_2\beta\left(\frac{1}{2}\cosh(\beta L_1)M_1\beta\cos(\beta L_1)-\frac{1}{2}M_1\beta\cosh(\beta L_1)^2\right)\right)A+\Big($$
$$-\frac{1}{2}\sinh(\beta L_2)\left(\frac{1}{2}M_1\beta-\frac{1}{2}M_1\beta\cos(\beta L_1)^2-\frac{1}{2}\sinh(\beta L_1)M_1\beta\sin(\beta L_1)\right)M_2\beta\cos(\beta L_2)-\frac{1}{2}\sinh(\beta L_2)\Big($$
$$-\frac{1}{2}\cos(\beta L_1)M_1\beta\sin(\beta L_1)+1+\frac{1}{2}\sinh(\beta L_1)M_1\beta\cos(\beta L_1)\Big)M_2\beta\sin(\beta L_2)-\frac{1}{2}M_1\beta-\frac{1}{2}\sinh(\beta L_1)M_1\beta\sin(\beta L_1)$$
$$+\frac{1}{2}M_1\beta\cosh(\beta L_1)^2-\frac{1}{2}\sinh(\beta L_2)\left(-\frac{1}{2}M_1\beta-\frac{1}{2}\sinh(\beta L_1)M_1\beta\sin(\beta L_1)+\frac{1}{2}M_1\beta\cosh(\beta L_1)^2\right)M_2\beta\cosh(\beta L_2)$$
$$+\frac{1}{2}M_2\beta\left(\frac{1}{2}\cosh(\beta L_1)M_1\beta\sin(\beta L_1)-1-\frac{1}{2}\cosh(\beta L_1)M_1\beta\sinh(\beta L_1)\right)-\frac{1}{2}M_2\beta\left(\frac{1}{2}\cosh(\beta L_1)M_1\beta\sin(\beta L_1)-1\right.$$
$$\left.\left.-\frac{1}{2}\cosh(\beta L_1)M_1\beta\sinh(\beta L_1)\right)\cosh(\beta L_2)^2\right)B$$

$c_{12} =$

$$\left(\frac{1}{2}\cosh(\beta L_2)\left(1+\frac{1}{2}\cos(\beta L_1)M_1\beta\sin(\beta L_1)-\frac{1}{2}\cosh(\beta L_1)M_1\beta\sin(\beta L_1)\right)M_2\beta\cos(\beta L_2)+\frac{1}{2}\left(-1-\frac{1}{2}\sinh(\beta L_1)M_1\beta\cos(\beta L_1)\right.\right.$$
$$+\frac{1}{2}\cosh(\beta L_1)M_1\beta\sinh(\beta L_1)\Big)M_2\beta\cosh(\beta L_2)^2+\frac{1}{2}\cosh(\beta L_1)M_1\beta\cos(\beta L_1)-\frac{1}{2}M_1\beta\cosh(\beta L_1)^2+\frac{1}{2}\cosh(\beta L_2)\Big($$
$$-\frac{1}{2}M_1\beta\cos(\beta L_1)^2+\frac{1}{2}\cosh(\beta L_1)M_1\beta\cos(\beta L_1)\Big)M_2\beta\sin(\beta L_2)+\frac{1}{2}M_2\beta\cosh(\beta L_2)\left(\frac{1}{2}\cosh(\beta L_1)M_1\beta\cos(\beta L_1)\right.$$
$$\left.\left.-\frac{1}{2}M_1\beta\cosh(\beta L_1)^2\right)\sinh(\beta L_2)\right)A+\left(\frac{1}{2}\cosh(\beta L_2)\left(\frac{1}{2}M_1\beta-\frac{1}{2}M_1\beta\cos(\beta L_1)^2-\frac{1}{2}\sinh(\beta L_1)M_1\beta\sin(\beta L_1)\right)M_2\beta\cos(\beta L_2)\right.$$
$$+\frac{1}{2}\cosh(\beta L_2)\left(-\frac{1}{2}\cos(\beta L_1)M_1\beta\sin(\beta L_1)+1+\frac{1}{2}\sinh(\beta L_1)M_1\beta\cos(\beta L_1)\right)M_2\beta\sin(\beta L_2)+\frac{1}{2}\cosh(\beta L_1)M_1\beta\sin(\beta L_1)-1$$
$$-\frac{1}{2}\cosh(\beta L_1)M_1\beta\sinh(\beta L_1)+\frac{1}{2}\left(-\frac{1}{2}M_1\beta-\frac{1}{2}\sinh(\beta L_1)M_1\beta\sin(\beta L_1)+\frac{1}{2}M_1\beta\cosh(\beta L_1)^2\right)M_2\beta\cosh(\beta L_2)^2$$
$$\left.+\frac{1}{2}M_2\beta\cosh(\beta L_2)\left(\frac{1}{2}\cosh(\beta L_1)M_1\beta\sin(\beta L_1)-1-\frac{1}{2}\cosh(\beta L_1)M_1\beta\sinh(\beta L_1)\right)\sinh(\beta L_2)\right)B$$

d. Constants of the eigenfunction of the third beam element: $c_{13} \sim c_{16}$

$c_{13} =$

$$\left(\frac{1}{2}\sin(\beta L_3)\left(\frac{1}{2}\sin(\beta L_2)\left(1+\frac{1}{2}\cos(\beta L_1)\,M_1\,\beta\sin(\beta L_1)-\frac{1}{2}\cosh(\beta L_1)\,M_1\,\beta\sin(\beta L_1)\right)M_2\,\beta\cos(\beta L_2)+\frac{1}{2}\left(-\frac{1}{2}M_1\,\beta\cos(\beta L_1)^2\right.\right.\right.$$
$$+\frac{1}{2}\cosh(\beta L_1)\,M_1\,\beta\cos(\beta L_1)\Big)M_2\,\beta-\frac{1}{2}\left(-\frac{1}{2}M_1\,\beta\cos(\beta L_1)^2+\frac{1}{2}\cosh(\beta L_1)\,M_1\,\beta\cos(\beta L_1)\right)M_2\,\beta\cos(\beta L_2)^2+1$$
$$+\frac{1}{2}\cos(\beta L_1)\,M_1\,\beta\sin(\beta L_1)-\frac{1}{2}\cosh(\beta L_1)\,M_1\,\beta\sin(\beta L_1)+\frac{1}{2}\sin(\beta L_2)\left(-1-\frac{1}{2}\sinh(\beta L_1)\,M_1\,\beta\cos(\beta L_1)\right.$$
$$+\frac{1}{2}\cosh(\beta L_1)\,M_1\,\beta\sinh(\beta L_1)\Big)M_2\,\beta\cosh(\beta L_2)+\frac{1}{2}M_2\,\beta\sin(\beta L_2)\left(\frac{1}{2}\cosh(\beta L_1)\,M_1\,\beta\cos(\beta L_1)\right.$$
$$\left.\left.-\frac{1}{2}M_1\,\beta\cosh(\beta L_1)^2\right)\sinh(\beta L_2)\Big)M_3\,\beta\cos(\beta L_3)+\frac{1}{2}\left(-\frac{1}{2}\cos(\beta L_2)\left(-\frac{1}{2}M_1\,\beta\cos(\beta L_1)^2\right.\right.\right.$$
$$+\frac{1}{2}\cosh(\beta L_1)\,M_1\,\beta\cos(\beta L_1)\Big)M_2\,\beta\sin(\beta L_2)-\frac{1}{2}\left(1+\frac{1}{2}\cos(\beta L_1)\,M_1\,\beta\sin(\beta L_1)-\frac{1}{2}\cosh(\beta L_1)\,M_1\,\beta\sin(\beta L_1)\right)M_2\,\beta\cos(\beta L_2)^2$$
$$-\frac{1}{2}\cos(\beta L_2)\left(-1-\frac{1}{2}\sinh(\beta L_1)\,M_1\,\beta\cos(\beta L_1)+\frac{1}{2}\cosh(\beta L_1)\,M_1\,\beta\sinh(\beta L_1)\right)M_2\,\beta\cosh(\beta L_2)-\frac{1}{2}M_1\,\beta\cos(\beta L_1)^2$$
$$+\frac{1}{2}\cosh(\beta L_1)\,M_1\,\beta\cos(\beta L_1)-\frac{1}{2}M_2\,\beta\cos(\beta L_2)\left(\frac{1}{2}\cosh(\beta L_1)\,M_1\,\beta\cos(\beta L_1)-\frac{1}{2}M_1\,\beta\cosh(\beta L_1)^2\right)\sinh(\beta L_2)\Big)M_3\,\beta-\frac{1}{2}\Big($$
$$-\frac{1}{2}\cos(\beta L_2)\left(-\frac{1}{2}M_1\,\beta\cos(\beta L_1)^2+\frac{1}{2}\cosh(\beta L_1)\,M_1\,\beta\cos(\beta L_1)\right)M_2\,\beta\sin(\beta L_2)-\frac{1}{2}\left(1+\frac{1}{2}\cos(\beta L_1)\,M_1\,\beta\sin(\beta L_1)\right.$$
$$-\frac{1}{2}\cosh(\beta L_1)\,M_1\,\beta\sin(\beta L_1)\Big)M_2\,\beta\cos(\beta L_2)^2-\frac{1}{2}\cos(\beta L_2)\left(-1-\frac{1}{2}\sinh(\beta L_1)\,M_1\,\beta\cos(\beta L_1)\right.$$
$$+\frac{1}{2}\cosh(\beta L_1)\,M_1\,\beta\sinh(\beta L_1)\Big)M_2\,\beta\cosh(\beta L_2)-\frac{1}{2}M_1\,\beta\cos(\beta L_1)^2+\frac{1}{2}\cosh(\beta L_1)\,M_1\,\beta\cos(\beta L_1)$$
$$-\frac{1}{2}M_2\,\beta\cos(\beta L_2)\left(\frac{1}{2}\cosh(\beta L_1)\,M_1\,\beta\cos(\beta L_1)-\frac{1}{2}M_1\,\beta\cosh(\beta L_1)^2\right)\sinh(\beta L_2)\Big)M_3\,\beta\cos(\beta L_3)^2+\frac{1}{2}\sin(\beta L_2)\Big(1$$
$$+\frac{1}{2}\cos(\beta L_1)\,M_1\,\beta\sin(\beta L_1)-\frac{1}{2}\cosh(\beta L_1)\,M_1\,\beta\sin(\beta L_1)\Big)M_2\,\beta\cos(\beta L_2)+\frac{1}{2}\left(-\frac{1}{2}M_1\,\beta\cos(\beta L_1)^2\right.$$
$$+\frac{1}{2}\cosh(\beta L_1)\,M_1\,\beta\cos(\beta L_1)\Big)M_2\,\beta-\frac{1}{2}\left(-\frac{1}{2}M_1\,\beta\cos(\beta L_1)^2+\frac{1}{2}\cosh(\beta L_1)\,M_1\,\beta\cos(\beta L_1)\right)M_2\,\beta\cos(\beta L_2)^2+1$$
$$+\frac{1}{2}\cos(\beta L_1)\,M_1\,\beta\sin(\beta L_1)-\frac{1}{2}\cosh(\beta L_1)\,M_1\,\beta\sin(\beta L_1)+\frac{1}{2}\sin(\beta L_2)\left(-1-\frac{1}{2}\sinh(\beta L_1)\,M_1\,\beta\cos(\beta L_1)\right.$$
$$+\frac{1}{2}\cosh(\beta L_1)\,M_1\,\beta\sinh(\beta L_1)\Big)M_2\,\beta\cosh(\beta L_2)+\frac{1}{2}M_2\,\beta\sin(\beta L_2)\left(\frac{1}{2}\cosh(\beta L_1)\,M_1\,\beta\cos(\beta L_1)-\frac{1}{2}M_1\,\beta\cosh(\beta L_1)^2\right)\sinh(\beta L_2)$$
$$+\frac{1}{2}\sin(\beta L_3)\left(-\frac{1}{2}\sinh(\beta L_2)\left(1+\frac{1}{2}\cos(\beta L_1)\,M_1\,\beta\sin(\beta L_1)-\frac{1}{2}\cosh(\beta L_1)\,M_1\,\beta\sin(\beta L_1)\right)M_2\,\beta\cos(\beta L_2)-\frac{1}{2}\sinh(\beta L_2)\Big(-1\right.$$
$$-\frac{1}{2}\sinh(\beta L_1)\,M_1\,\beta\cos(\beta L_1)+\frac{1}{2}\cosh(\beta L_1)\,M_1\,\beta\sinh(\beta L_1)\Big)M_2\,\beta\cosh(\beta L_2)-\frac{1}{2}\sinh(\beta L_2)\left(-\frac{1}{2}M_1\,\beta\cos(\beta L_1)^2\right.$$
$$+\frac{1}{2}\cosh(\beta L_1)\,M_1\,\beta\cos(\beta L_1)\Big)M_2\,\beta\sin(\beta L_2)-\frac{1}{2}M_2\,\beta\left(\frac{1}{2}\cosh(\beta L_1)\,M_1\,\beta\cos(\beta L_1)-\frac{1}{2}M_1\,\beta\cosh(\beta L_1)^2\right)\cosh(\beta L_2)^2-1$$
$$\left.-\frac{1}{2}\sinh(\beta L_1)\,M_1\,\beta\cos(\beta L_1)+\frac{1}{2}\cosh(\beta L_1)\,M_1\,\beta\sinh(\beta L_1)+\frac{1}{2}M_2\,\beta\left(\frac{1}{2}\cosh(\beta L_1)\,M_1\,\beta\cos(\beta L_1)-\frac{1}{2}M_1\,\beta\cosh(\beta L_1)^2\right)\right)$$
$$M_3\,\beta\cosh(\beta L_3)+\frac{1}{2}M_3\,\beta\sin(\beta L_3)\left(\frac{1}{2}\cosh(\beta L_2)\left(1+\frac{1}{2}\cos(\beta L_1)\,M_1\,\beta\sin(\beta L_1)-\frac{1}{2}\cosh(\beta L_1)\,M_1\,\beta\sin(\beta L_1)\right)M_2\,\beta\cos(\beta L_2)\right.$$
$$+\frac{1}{2}\left(-1-\frac{1}{2}\sinh(\beta L_1)\,M_1\,\beta\cos(\beta L_1)+\frac{1}{2}\cosh(\beta L_1)\,M_1\,\beta\sinh(\beta L_1)\right)M_2\,\beta\cosh(\beta L_2)^2+\frac{1}{2}\cosh(\beta L_1)\,M_1\,\beta\cos(\beta L_1)$$
$$-\frac{1}{2}M_1\,\beta\cosh(\beta L_1)^2+\frac{1}{2}\cosh(\beta L_2)\left(-\frac{1}{2}M_1\,\beta\cos(\beta L_1)^2+\frac{1}{2}\cosh(\beta L_1)\,M_1\,\beta\cos(\beta L_1)\right)M_2\,\beta\sin(\beta L_2)$$
$$\left.+\frac{1}{2}M_2\,\beta\cosh(\beta L_2)\left(\frac{1}{2}\cosh(\beta L_1)\,M_1\,\beta\cos(\beta L_1)-\frac{1}{2}M_1\,\beta\cosh(\beta L_1)^2\right)\sinh(\beta L_2)\right)\sinh(\beta L_3)\Big)A+\left(\frac{1}{2}\left(-\frac{1}{2}\left(\frac{1}{2}M_1\,\beta\right.\right.\right.$$
$$\left.\left.-\frac{1}{2}M_1\,\beta\cos(\beta L_1)^2-\frac{1}{2}\sinh(\beta L_1)\,M_1\,\beta\sin(\beta L_1)\right)M_2\,\beta\cos(\beta L_2)^2-\frac{1}{2}\cos(\beta L_1)\,M_1\,\beta\sin(\beta L_1)+1+\frac{1}{2}\sinh(\beta L_1)\,M_1\,\beta\cos(\beta L_1)$$

$$-\frac{1}{2}\cos(\beta L_2)\left(-\frac{1}{2}\cos(\beta L_1)\,M_1\,\beta\sin(\beta L_1)+1+\frac{1}{2}\sinh(\beta L_1)\,M_1\,\beta\cos(\beta L_1)\right)M_2\,\beta\sin(\beta L_2)$$
$$-\frac{1}{2}M_2\,\beta\cos(\beta L_2)\left(\frac{1}{2}\cosh(\beta L_1)\,M_1\,\beta\sin(\beta L_1)-1-\frac{1}{2}\cosh(\beta L_1)\,M_1\,\beta\sinh(\beta L_1)\right)\sinh(\beta L_2)-\frac{1}{2}\cos(\beta L_2)\left(-\frac{1}{2}M_1\,\beta\right.$$
$$\left.-\frac{1}{2}\sinh(\beta L_1)\,M_1\,\beta\sin(\beta L_1)+\frac{1}{2}M_1\,\beta\cosh(\beta L_1)^2\right)M_2\,\beta\cosh(\beta L_2)\Big)M_3\,\beta+\frac{1}{2}\left(-\frac{1}{2}\cos(\beta L_1)\,M_1\,\beta\sin(\beta L_1)+1\right.$$
$$\left.+\frac{1}{2}\sinh(\beta L_1)\,M_1\,\beta\cos(\beta L_1)\right)M_2\,\beta+\frac{1}{2}M_1\,\beta-\frac{1}{2}M_1\,\beta\cos(\beta L_1)^2-\frac{1}{2}\sinh(\beta L_1)\,M_1\,\beta\sin(\beta L_1)+\frac{1}{2}\sin(\beta L_2)\left(\frac{1}{2}M_1\,\beta\right.$$
$$\left.-\frac{1}{2}M_1\,\beta\cos(\beta L_1)^2-\frac{1}{2}\sinh(\beta L_1)\,M_1\,\beta\sin(\beta L_1)\right)M_2\,\beta\cos(\beta L_2)+\frac{1}{2}\sin(\beta L_2)\left(-\frac{1}{2}M_1\,\beta-\frac{1}{2}\sinh(\beta L_1)\,M_1\,\beta\sin(\beta L_1)\right.$$
$$\left.+\frac{1}{2}M_1\,\beta\cosh(\beta L_1)^2\right)M_2\,\beta\cosh(\beta L_2)-\frac{1}{2}\left(-\frac{1}{2}\cos(\beta L_1)\,M_1\,\beta\sin(\beta L_1)+1+\frac{1}{2}\sinh(\beta L_1)\,M_1\,\beta\cos(\beta L_1)\right)M_2\,\beta\cos(\beta L_2)^2$$
$$+\frac{1}{2}M_2\,\beta\sin(\beta L_2)\left(\frac{1}{2}\cosh(\beta L_1)\,M_1\,\beta\sin(\beta L_1)-1-\frac{1}{2}\cosh(\beta L_1)\,M_1\,\beta\sinh(\beta L_1)\right)\sinh(\beta L_2)+\frac{1}{2}\sin(\beta L_3)\left(\frac{1}{2}\right.$$
$$\left.-\frac{1}{2}\cos(\beta L_1)\,M_1\,\beta\sin(\beta L_1)+1+\frac{1}{2}\sinh(\beta L_1)\,M_1\,\beta\cos(\beta L_1)\right)M_2\,\beta+\frac{1}{2}M_1\,\beta-\frac{1}{2}M_1\,\beta\cos(\beta L_1)^2-\frac{1}{2}\sinh(\beta L_1)\,M_1\,\beta\sin(\beta L_1)$$
$$+\frac{1}{2}\sin(\beta L_2)\left(\frac{1}{2}M_1\,\beta-\frac{1}{2}M_1\,\beta\cos(\beta L_1)^2-\frac{1}{2}\sinh(\beta L_1)\,M_1\,\beta\sin(\beta L_1)\right)M_2\,\beta\cos(\beta L_2)+\frac{1}{2}\sin(\beta L_2)\left(-\frac{1}{2}M_1\,\beta\right.$$
$$\left.-\frac{1}{2}\sinh(\beta L_1)\,M_1\,\beta\sin(\beta L_1)+\frac{1}{2}M_1\,\beta\cosh(\beta L_1)^2\right)M_2\,\beta\cosh(\beta L_2)-\frac{1}{2}\left(-\frac{1}{2}\cos(\beta L_1)\,M_1\,\beta\sin(\beta L_1)+1\right.$$
$$\left.+\frac{1}{2}\sinh(\beta L_1)\,M_1\,\beta\cos(\beta L_1)\right)M_2\,\beta\cos(\beta L_2)^2+\frac{1}{2}M_2\,\beta\sin(\beta L_2)\left(\frac{1}{2}\cosh(\beta L_1)\,M_1\,\beta\sin(\beta L_1)-1\right.$$
$$\left.-\frac{1}{2}\cosh(\beta L_1)\,M_1\,\beta\sinh(\beta L_1)\right)\sinh(\beta L_2)\Big)M_3\,\beta\cos(\beta L_3)+\frac{1}{2}\sin(\beta L_3)\left(-\frac{1}{2}\sinh(\beta L_2)\left(\frac{1}{2}M_1\,\beta-\frac{1}{2}M_1\,\beta\cos(\beta L_1)^2\right.\right.$$
$$\left.-\frac{1}{2}\sinh(\beta L_1)\,M_1\,\beta\sin(\beta L_1)\right)M_2\,\beta\cos(\beta L_2)-\frac{1}{2}\sinh(\beta L_2)\left(-\frac{1}{2}\cos(\beta L_1)\,M_1\,\beta\sin(\beta L_1)+1\right.$$
$$\left.+\frac{1}{2}\sinh(\beta L_1)\,M_1\,\beta\cos(\beta L_1)\right)M_2\,\beta\sin(\beta L_2)-\frac{1}{2}M_1\,\beta-\frac{1}{2}\sinh(\beta L_1)\,M_1\,\beta\sin(\beta L_1)+\frac{1}{2}M_1\,\beta\cosh(\beta L_1)^2-\frac{1}{2}\sinh(\beta L_2)\left(\right.$$
$$\left.-\frac{1}{2}M_1\,\beta-\frac{1}{2}\sinh(\beta L_1)\,M_1\,\beta\sin(\beta L_1)+\frac{1}{2}M_1\,\beta\cosh(\beta L_1)^2\right)M_2\,\beta\cosh(\beta L_2)+\frac{1}{2}M_2\,\beta\left(\frac{1}{2}\cosh(\beta L_1)\,M_1\,\beta\sin(\beta L_1)-1\right.$$
$$\left.-\frac{1}{2}\cosh(\beta L_1)\,M_1\,\beta\sinh(\beta L_1)\right)-\frac{1}{2}M_2\,\beta\left(\frac{1}{2}\cosh(\beta L_1)\,M_1\,\beta\sin(\beta L_1)-1-\frac{1}{2}\cosh(\beta L_1)\,M_1\,\beta\sinh(\beta L_1)\right)\cosh(\beta L_2)^2\Big)$$
$$M_3\,\beta\cosh(\beta L_3)-\frac{1}{2}\left(-\frac{1}{2}\left(\frac{1}{2}M_1\,\beta-\frac{1}{2}M_1\,\beta\cos(\beta L_1)^2-\frac{1}{2}\sinh(\beta L_1)\,M_1\,\beta\sin(\beta L_1)\right)M_2\,\beta\cos(\beta L_2)^2-\frac{1}{2}\cos(\beta L_1)\,M_1\,\beta\sin(\beta L_1)\right.$$
$$\left.+1+\frac{1}{2}\sinh(\beta L_1)\,M_1\,\beta\cos(\beta L_1)-\frac{1}{2}\cos(\beta L_2)\left(-\frac{1}{2}\cos(\beta L_1)\,M_1\,\beta\sin(\beta L_1)+1+\frac{1}{2}\sinh(\beta L_1)\,M_1\,\beta\cos(\beta L_1)\right)M_2\,\beta\sin(\beta L_2)\right.$$
$$\left.-\frac{1}{2}M_2\,\beta\cos(\beta L_2)\left(\frac{1}{2}\cosh(\beta L_1)\,M_1\,\beta\sin(\beta L_1)-1-\frac{1}{2}\cosh(\beta L_1)\,M_1\,\beta\sinh(\beta L_1)\right)\sinh(\beta L_2)-\frac{1}{2}\cos(\beta L_2)\left(-\frac{1}{2}M_1\,\beta\right.\right.$$
$$\left.-\frac{1}{2}\sinh(\beta L_1)\,M_1\,\beta\sin(\beta L_1)+\frac{1}{2}M_1\,\beta\cosh(\beta L_1)^2\right)M_2\,\beta\cosh(\beta L_2)\Big)M_3\,\beta\cos(\beta L_3)^2+\frac{1}{2}M_3\,\beta\sin(\beta L_3)\left(\frac{1}{2}\cosh(\beta L_2)\left(\frac{1}{2}M_1\,\beta\right.\right.$$
$$\left.-\frac{1}{2}M_1\,\beta\cos(\beta L_1)^2-\frac{1}{2}\sinh(\beta L_1)\,M_1\,\beta\sin(\beta L_1)\right)M_2\,\beta\cos(\beta L_2)+\frac{1}{2}\cosh(\beta L_2)\left(-\frac{1}{2}\cos(\beta L_1)\,M_1\,\beta\sin(\beta L_1)+1\right.$$
$$\left.+\frac{1}{2}\sinh(\beta L_1)\,M_1\,\beta\cos(\beta L_1)\right)M_2\,\beta\sin(\beta L_2)+\frac{1}{2}\cosh(\beta L_1)\,M_1\,\beta\sin(\beta L_1)-1-\frac{1}{2}\cosh(\beta L_1)\,M_1\,\beta\sinh(\beta L_1)+\frac{1}{2}\left(-\frac{1}{2}M_1\,\beta\right.$$
$$\left.-\frac{1}{2}\sinh(\beta L_1)\,M_1\,\beta\sin(\beta L_1)+\frac{1}{2}M_1\,\beta\cosh(\beta L_1)^2\right)M_2\,\beta\cosh(\beta L_2)^2+\frac{1}{2}M_2\,\beta\cosh(\beta L_2)\left(\frac{1}{2}\cosh(\beta L_1)\,M_1\,\beta\sin(\beta L_1)-1\right.$$
$$\left.-\frac{1}{2}\cosh(\beta L_1)\,M_1\,\beta\sinh(\beta L_1)\right)\sinh(\beta L_2)\Big)\sinh(\beta L_3)\Big)B$$

$c_{14} =$

$$\left(-\frac{1}{2}\cos(\beta L_3)\left(-\frac{1}{2}\cos(\beta L_2)\left(-\frac{1}{2}M_1\beta\cos(\beta L_1)^2+\frac{1}{2}\cosh(\beta L_1)M_1\beta\cos(\beta L_1)\right)M_2\beta\sin(\beta L_2)-\frac{1}{2}\left(1+\frac{1}{2}\cos(\beta L_1)M_1\beta\sin(\beta L_1)\right.\right.\right.$$
$$\left.\left.-\frac{1}{2}\cosh(\beta L_1)M_1\beta\sin(\beta L_1)\right)M_2\beta\cos(\beta L_2)^2-\frac{1}{2}\cos(\beta L_2)\left(-1-\frac{1}{2}\sinh(\beta L_1)M_1\beta\cos(\beta L_1)\right.\right.$$
$$\left.\left.+\frac{1}{2}\cosh(\beta L_1)M_1\beta\sinh(\beta L_1)\right)M_2\beta\cosh(\beta L_2)-\frac{1}{2}M_1\beta\cos(\beta L_1)^2+\frac{1}{2}\cosh(\beta L_1)M_1\beta\cos(\beta L_1)\right.$$
$$\left.-\frac{1}{2}M_2\beta\cos(\beta L_2)\left(\frac{1}{2}\cosh(\beta L_1)M_1\beta\cos(\beta L_1)-\frac{1}{2}M_1\beta\cosh(\beta L_1)^2\right)\sinh(\beta L_2)\right)M_3\beta\sin(\beta L_3)-\frac{1}{2}\left(\frac{1}{2}\sin(\beta L_2)\left(1\right.\right.$$
$$\left.\left.+\frac{1}{2}\cos(\beta L_1)M_1\beta\sin(\beta L_1)-\frac{1}{2}\cosh(\beta L_1)M_1\beta\sin(\beta L_1)\right)M_2\beta\cos(\beta L_2)+\frac{1}{2}\left(-\frac{1}{2}M_1\beta\cos(\beta L_1)^2\right.\right.$$
$$\left.\left.+\frac{1}{2}\cosh(\beta L_1)M_1\beta\cos(\beta L_1)\right)M_2\beta-\frac{1}{2}\left(-\frac{1}{2}M_1\beta\cos(\beta L_1)^2+\frac{1}{2}\cosh(\beta L_1)M_1\beta\cos(\beta L_1)\right)M_2\beta\cos(\beta L_2)^2+1\right.$$
$$\left.+\frac{1}{2}\cos(\beta L_1)M_1\beta\sin(\beta L_1)-\frac{1}{2}\cosh(\beta L_1)M_1\beta\sin(\beta L_1)+\frac{1}{2}\sin(\beta L_2)\left(-1-\frac{1}{2}\sinh(\beta L_1)M_1\beta\cos(\beta L_1)\right.\right.$$
$$\left.\left.+\frac{1}{2}\cosh(\beta L_1)M_1\beta\sinh(\beta L_1)\right)M_2\beta\cosh(\beta L_2)+\frac{1}{2}M_2\beta\sin(\beta L_2)\left(\frac{1}{2}\cosh(\beta L_1)M_1\beta\cos(\beta L_1)\right.\right.$$
$$\left.\left.-\frac{1}{2}M_1\beta\cosh(\beta L_1)^2\right)\sinh(\beta L_2)\right)M_3\beta\cos(\beta L_3)^2-\frac{1}{2}\cos(\beta L_3)\left(-\frac{1}{2}\sinh(\beta L_2)\left(1+\frac{1}{2}\cos(\beta L_1)M_1\beta\sin(\beta L_1)\right.\right.$$
$$\left.\left.-\frac{1}{2}\cosh(\beta L_1)M_1\beta\sin(\beta L_1)\right)M_2\beta\cos(\beta L_2)-\frac{1}{2}\sinh(\beta L_2)\left(-1-\frac{1}{2}\sinh(\beta L_1)M_1\beta\cos(\beta L_1)\right.\right.$$
$$\left.\left.+\frac{1}{2}\cosh(\beta L_1)M_1\beta\sinh(\beta L_1)\right)M_2\beta\cosh(\beta L_2)-\frac{1}{2}\sinh(\beta L_2)\left(-\frac{1}{2}M_1\beta\cos(\beta L_1)^2+\frac{1}{2}\cosh(\beta L_1)M_1\beta\cos(\beta L_1)\right)M_2\beta\sin(\beta L_2)\right.$$
$$\left.-\frac{1}{2}M_2\beta\left(\frac{1}{2}\cosh(\beta L_1)M_1\beta\cos(\beta L_1)-\frac{1}{2}M_1\beta\cosh(\beta L_1)^2\right)\cosh(\beta L_2)^2-1-\frac{1}{2}\sinh(\beta L_1)M_1\beta\cos(\beta L_1)\right.$$
$$\left.+\frac{1}{2}\cosh(\beta L_1)M_1\beta\sinh(\beta L_1)+\frac{1}{2}M_2\beta\left(\frac{1}{2}\cosh(\beta L_1)M_1\beta\cos(\beta L_1)-\frac{1}{2}M_1\beta\cosh(\beta L_1)^2\right)\right)M_3\beta\cosh(\beta L_3)-\frac{1}{2}\cos(\beta L_2)\left(\right.$$
$$-\frac{1}{2}M_1\beta\cos(\beta L_1)^2+\frac{1}{2}\cosh(\beta L_1)M_1\beta\cos(\beta L_1)\Big)M_2\beta\sin(\beta L_2)-\frac{1}{2}\left(1+\frac{1}{2}\cos(\beta L_1)M_1\beta\sin(\beta L_1)\right.$$
$$\left.-\frac{1}{2}\cosh(\beta L_1)M_1\beta\sin(\beta L_1)\right)M_2\beta\cos(\beta L_2)^2-\frac{1}{2}\cos(\beta L_2)\left(-1-\frac{1}{2}\sinh(\beta L_1)M_1\beta\cos(\beta L_1)\right.$$
$$\left.+\frac{1}{2}\cosh(\beta L_1)M_1\beta\sinh(\beta L_1)\right)M_2\beta\cosh(\beta L_2)-\frac{1}{2}M_1\beta\cos(\beta L_1)^2+\frac{1}{2}\cosh(\beta L_1)M_1\beta\cos(\beta L_1)$$
$$-\frac{1}{2}M_2\beta\cos(\beta L_2)\left(\frac{1}{2}\cosh(\beta L_1)M_1\beta\cos(\beta L_1)-\frac{1}{2}M_1\beta\cosh(\beta L_1)^2\right)\sinh(\beta L_2)-\frac{1}{2}M_3\beta\cos(\beta L_3)\left(\frac{1}{2}\cosh(\beta L_2)\left(1\right.\right.$$
$$\left.\left.+\frac{1}{2}\cos(\beta L_1)M_1\beta\sin(\beta L_1)-\frac{1}{2}\cosh(\beta L_1)M_1\beta\sin(\beta L_1)\right)M_2\beta\cos(\beta L_2)+\frac{1}{2}\left(-1-\frac{1}{2}\sinh(\beta L_1)M_1\beta\cos(\beta L_1)\right)\right.$$
$$\left.+\frac{1}{2}\cosh(\beta L_1)M_1\beta\sinh(\beta L_1)\right)M_2\beta\cosh(\beta L_2)^2+\frac{1}{2}\cosh(\beta L_1)M_1\beta\cos(\beta L_1)-\frac{1}{2}M_1\beta\cosh(\beta L_1)^2+\frac{1}{2}\cosh(\beta L_2)\left(\right.$$
$$-\frac{1}{2}M_1\beta\cos(\beta L_1)^2+\frac{1}{2}\cosh(\beta L_1)M_1\beta\cos(\beta L_1)\Big)M_2\beta\sin(\beta L_2)+\frac{1}{2}M_2\beta\cosh(\beta L_2)\left(\frac{1}{2}\cosh(\beta L_1)M_1\beta\cos(\beta L_1)\right.$$
$$\left.-\frac{1}{2}M_1\beta\cosh(\beta L_1)^2\right)\sinh(\beta L_2)\Big)\sinh(\beta L_3)\Big)A+\left(-\frac{1}{2}\left(\frac{1}{2}\left(-\frac{1}{2}\cos(\beta L_1)M_1\beta\sin(\beta L_1)+1+\frac{1}{2}\sinh(\beta L_1)M_1\beta\cos(\beta L_1)\right)M_2\beta\right.\right.$$
$$\left.\left.+\frac{1}{2}M_1\beta-\frac{1}{2}M_1\beta\cos(\beta L_1)^2-\frac{1}{2}\sinh(\beta L_1)M_1\beta\sin(\beta L_1)+\frac{1}{2}\sin(\beta L_2)\left(\frac{1}{2}M_1\beta-\frac{1}{2}M_1\beta\cos(\beta L_1)^2\right.\right.\right.$$
$$\left.\left.\left.-\frac{1}{2}\sinh(\beta L_1)M_1\beta\sin(\beta L_1)\right)M_2\beta\cos(\beta L_2)+\frac{1}{2}\sin(\beta L_2)\left(-\frac{1}{2}M_1\beta-\frac{1}{2}\sinh(\beta L_1)M_1\beta\sin(\beta L_1)\right.\right.\right.$$
$$\left.\left.\left.+\frac{1}{2}M_1\beta\cosh(\beta L_1)^2\right)M_2\beta\cosh(\beta L_2)-\frac{1}{2}\left(-\frac{1}{2}\cos(\beta L_1)M_1\beta\sin(\beta L_1)+1+\frac{1}{2}\sinh(\beta L_1)M_1\beta\cos(\beta L_1)\right)M_2\beta\cos(\beta L_2)^2\right.\right.$$

$$+\frac{1}{2}\,M_2\,\beta\,\sin(\beta\,L_2)\left(\frac{1}{2}\cosh(\beta\,L_1)\,M_1\,\beta\,\sin(\beta\,L_1)-1-\frac{1}{2}\cosh(\beta\,L_1)\,M_1\,\beta\,\sinh(\beta\,L_1)\right)\sinh(\beta\,L_2)\Bigg)\,M_3\,\beta\,\cos(\beta\,L_3)^2-\frac{1}{2}\Bigg(\frac{1}{2}\,M_1\,\beta$$
$$-\frac{1}{2}\,M_1\,\beta\,\cos(\beta\,L_1)^2-\frac{1}{2}\sinh(\beta\,L_1)\,M_1\,\beta\,\sin(\beta\,L_1)\Bigg)\,M_2\,\beta\,\cos(\beta\,L_2)^2-\frac{1}{2}\cos(\beta\,L_1)\,M_1\,\beta\,\sin(\beta\,L_1)+1+\frac{1}{2}\sinh(\beta\,L_1)\,M_1\,\beta\,\cos(\beta\,L_1)$$
$$-\frac{1}{2}\cos(\beta\,L_2)\left(-\frac{1}{2}\cos(\beta\,L_1)\,M_1\,\beta\,\sin(\beta\,L_1)+1+\frac{1}{2}\sinh(\beta\,L_1)\,M_1\,\beta\,\cos(\beta\,L_1)\right)M_2\,\beta\,\sin(\beta\,L_2)$$
$$-\frac{1}{2}\,M_2\,\beta\,\cos(\beta\,L_2)\left(\frac{1}{2}\cosh(\beta\,L_1)\,M_1\,\beta\,\sin(\beta\,L_1)-1-\frac{1}{2}\cosh(\beta\,L_1)\,M_1\,\beta\,\sinh(\beta\,L_1)\right)\sinh(\beta\,L_2)-\frac{1}{2}\cos(\beta\,L_2)\left(-\frac{1}{2}\,M_1\,\beta\right.$$
$$\left.-\frac{1}{2}\sinh(\beta\,L_1)\,M_1\,\beta\,\sin(\beta\,L_1)+\frac{1}{2}\,M_1\,\beta\,\cosh(\beta\,L_1)^2\right)M_2\,\beta\,\cosh(\beta\,L_2)-\frac{1}{2}\cos(\beta\,L_3)\left(-\frac{1}{2}\left(\frac{1}{2}\,M_1\,\beta-\frac{1}{2}\,M_1\,\beta\,\cos(\beta\,L_1)^2\right.\right.$$
$$\left.-\frac{1}{2}\sinh(\beta\,L_1)\,M_1\,\beta\,\sin(\beta\,L_1)\right)M_2\,\beta\,\cos(\beta\,L_2)^2-\frac{1}{2}\cos(\beta\,L_1)\,M_1\,\beta\,\sin(\beta\,L_1)+1+\frac{1}{2}\sinh(\beta\,L_1)\,M_1\,\beta\,\cos(\beta\,L_1)-\frac{1}{2}\cos(\beta\,L_2)\left(\right.$$
$$\left.-\frac{1}{2}\cos(\beta\,L_1)\,M_1\,\beta\,\sin(\beta\,L_1)+1+\frac{1}{2}\sinh(\beta\,L_1)\,M_1\,\beta\,\cos(\beta\,L_1)\right)M_2\,\beta\,\sin(\beta\,L_2)-\frac{1}{2}\,M_2\,\beta\,\cos(\beta\,L_2)\left(\frac{1}{2}\cosh(\beta\,L_1)\,M_1\,\beta\,\sin(\beta\,L_1)-1\right.$$
$$\left.-\frac{1}{2}\cosh(\beta\,L_1)\,M_1\,\beta\,\sinh(\beta\,L_1)\right)\sinh(\beta\,L_2)-\frac{1}{2}\cos(\beta\,L_2)\left(-\frac{1}{2}\,M_1\,\beta-\frac{1}{2}\sinh(\beta\,L_1)\,M_1\,\beta\,\sin(\beta\,L_1)\right.$$
$$\left.+\frac{1}{2}\,M_1\,\beta\,\cosh(\beta\,L_1)^2\right)M_2\,\beta\,\cosh(\beta\,L_2)\Bigg)\,M_3\,\beta\,\sin(\beta\,L_3)-\frac{1}{2}\,M_3\,\beta\,\cos(\beta\,L_3)\left(\frac{1}{2}\cosh(\beta\,L_2)\left(\frac{1}{2}\,M_1\,\beta-\frac{1}{2}\,M_1\,\beta\,\cos(\beta\,L_1)^2\right.\right.$$
$$\left.-\frac{1}{2}\sinh(\beta\,L_1)\,M_1\,\beta\,\sin(\beta\,L_1)\right)M_2\,\beta\,\cos(\beta\,L_2)+\frac{1}{2}\cosh(\beta\,L_2)\left(-\frac{1}{2}\cos(\beta\,L_1)\,M_1\,\beta\,\sin(\beta\,L_1)+1\right.$$
$$\left.+\frac{1}{2}\sinh(\beta\,L_1)\,M_1\,\beta\,\cos(\beta\,L_1)\right)M_2\,\beta\,\sin(\beta\,L_2)+\frac{1}{2}\cosh(\beta\,L_1)\,M_1\,\beta\,\sin(\beta\,L_1)-1-\frac{1}{2}\cosh(\beta\,L_1)\,M_1\,\beta\,\sinh(\beta\,L_1)+\frac{1}{2}\left(-\frac{1}{2}\,M_1\,\beta\right.$$
$$\left.-\frac{1}{2}\sinh(\beta\,L_1)\,M_1\,\beta\,\sin(\beta\,L_1)+\frac{1}{2}\,M_1\,\beta\,\cosh(\beta\,L_1)^2\right)M_2\,\beta\,\cosh(\beta\,L_2)^2+\frac{1}{2}\,M_2\,\beta\,\cosh(\beta\,L_2)\left(\frac{1}{2}\cosh(\beta\,L_1)\,M_1\,\beta\,\sin(\beta\,L_1)-1\right.$$
$$\left.-\frac{1}{2}\cosh(\beta\,L_1)\,M_1\,\beta\,\sinh(\beta\,L_1)\right)\sinh(\beta\,L_2)\Bigg)\sinh(\beta\,L_3)-\frac{1}{2}\cos(\beta\,L_3)\left(-\frac{1}{2}\sinh(\beta\,L_2)\left(\frac{1}{2}\,M_1\,\beta-\frac{1}{2}\,M_1\,\beta\,\cos(\beta\,L_1)^2\right.\right.$$
$$\left.-\frac{1}{2}\sinh(\beta\,L_1)\,M_1\,\beta\,\sin(\beta\,L_1)\right)M_2\,\beta\,\cos(\beta\,L_2)-\frac{1}{2}\sinh(\beta\,L_2)\left(-\frac{1}{2}\cos(\beta\,L_1)\,M_1\,\beta\,\sin(\beta\,L_1)+1\right.$$
$$\left.+\frac{1}{2}\sinh(\beta\,L_1)\,M_1\,\beta\,\cos(\beta\,L_1)\right)M_2\,\beta\,\sin(\beta\,L_2)-\frac{1}{2}\,M_1\,\beta-\frac{1}{2}\sinh(\beta\,L_1)\,M_1\,\beta\,\sin(\beta\,L_1)+\frac{1}{2}\,M_1\,\beta\,\cosh(\beta\,L_1)^2-\frac{1}{2}\sinh(\beta\,L_2)\left(\right.$$
$$\left.-\frac{1}{2}\,M_1\,\beta-\frac{1}{2}\sinh(\beta\,L_1)\,M_1\,\beta\,\sin(\beta\,L_1)+\frac{1}{2}\,M_1\,\beta\,\cosh(\beta\,L_1)^2\right)M_2\,\beta\,\cosh(\beta\,L_2)+\frac{1}{2}\,M_2\,\beta\left(\frac{1}{2}\cosh(\beta\,L_1)\,M_1\,\beta\,\sin(\beta\,L_1)-1\right.$$
$$\left.-\frac{1}{2}\cosh(\beta\,L_1)\,M_1\,\beta\,\sinh(\beta\,L_1)\right)-\frac{1}{2}\,M_2\,\beta\left(\frac{1}{2}\cosh(\beta\,L_1)\,M_1\,\beta\,\sin(\beta\,L_1)-1-\frac{1}{2}\cosh(\beta\,L_1)\,M_1\,\beta\,\sinh(\beta\,L_1)\right)\cosh(\beta\,L_2)^2\Bigg)$$
$$M_3\,\beta\,\cosh(\beta\,L_3)\Bigg)\,B$$

$c_{15} =$

$$\left(-\frac{1}{2}\,M_3\,\beta\,\cos(\beta\,L_3)\left(\frac{1}{2}\sin(\beta\,L_2)\left(1+\frac{1}{2}\cos(\beta\,L_1)\,M_1\,\beta\,\sin(\beta\,L_1)-\frac{1}{2}\cosh(\beta\,L_1)\,M_1\,\beta\,\sin(\beta\,L_1)\right)M_2\,\beta\,\cos(\beta\,L_2)+\frac{1}{2}\left(\right.\right.$$
$$\left.-\frac{1}{2}\,M_1\,\beta\,\cos(\beta\,L_1)^2+\frac{1}{2}\cosh(\beta\,L_1)\,M_1\,\beta\,\cos(\beta\,L_1)\right)M_2\,\beta-\frac{1}{2}\left(-\frac{1}{2}\,M_1\,\beta\,\cos(\beta\,L_1)^2+\frac{1}{2}\cosh(\beta\,L_1)\,M_1\,\beta\,\cos(\beta\,L_1)\right)M_2\,\beta\,\cos(\beta\,L_2)^2+1$$
$$+\frac{1}{2}\cos(\beta\,L_1)\,M_1\,\beta\,\sin(\beta\,L_1)-\frac{1}{2}\cosh(\beta\,L_1)\,M_1\,\beta\,\sin(\beta\,L_1)+\frac{1}{2}\sin(\beta\,L_2)\left(-1-\frac{1}{2}\sinh(\beta\,L_1)\,M_1\,\beta\,\cos(\beta\,L_1)\right.$$
$$\left.+\frac{1}{2}\cosh(\beta\,L_1)\,M_1\,\beta\,\sinh(\beta\,L_1)\right)M_2\,\beta\,\cosh(\beta\,L_2)+\frac{1}{2}\,M_2\,\beta\sin(\beta\,L_2)\left(\frac{1}{2}\cosh(\beta\,L_1)\,M_1\,\beta\,\cos(\beta\,L_1)\right.$$
$$\left.-\frac{1}{2}\,M_1\,\beta\,\cosh(\beta\,L_1)^2\right)\sinh(\beta\,L_2)\Bigg)\sinh(\beta\,L_3)-\frac{1}{2}\left(-\frac{1}{2}\sinh(\beta\,L_2)\left(1+\frac{1}{2}\cos(\beta\,L_1)\,M_1\,\beta\,\sin(\beta\,L_1)\right.\right.$$

$$+\frac{1}{2}\cosh(\beta L_1)\,M_1\beta\sinh(\beta L_1)\Big)M_2\beta\cosh(\beta L_2)-\frac{1}{2}\sinh(\beta L_2)\left(-\frac{1}{2}M_1\beta\cos(\beta L_1)^2+\frac{1}{2}\cosh(\beta L_1)\,M_1\beta\cos(\beta L_1)\right)M_2\beta\sin(\beta L_2)$$
$$-\frac{1}{2}M_2\beta\left(\frac{1}{2}\cosh(\beta L_1)\,M_1\beta\cos(\beta L_1)-\frac{1}{2}M_1\beta\cosh(\beta L_1)^2\right)\cosh(\beta L_2)^2-1-\frac{1}{2}\sinh(\beta L_1)\,M_1\beta\cos(\beta L_1)$$
$$+\frac{1}{2}\cosh(\beta L_1)\,M_1\beta\sinh(\beta L_1)+\frac{1}{2}M_2\beta\left(\frac{1}{2}\cosh(\beta L_1)\,M_1\beta\cos(\beta L_1)-\frac{1}{2}M_1\beta\cosh(\beta L_1)^2\right)\Big)\cosh(\beta L_3)\,M_3\beta\sinh(\beta L_3)$$
$$-\frac{1}{2}M_3\beta\sin(\beta L_3)\left(-\frac{1}{2}\cos(\beta L_2)\left(-\frac{1}{2}M_1\beta\cos(\beta L_1)^2+\frac{1}{2}\cosh(\beta L_1)\,M_1\beta\cos(\beta L_1)\right)M_2\beta\sin(\beta L_2)-\frac{1}{2}\Big(1$$
$$+\frac{1}{2}\cos(\beta L_1)\,M_1\beta\sin(\beta L_1)-\frac{1}{2}\cosh(\beta L_1)\,M_1\beta\sin(\beta L_1)\Big)M_2\beta\cos(\beta L_2)^2-\frac{1}{2}\cos(\beta L_2)\left(-1-\frac{1}{2}\sinh(\beta L_1)\,M_1\beta\cos(\beta L_1)\right.$$
$$+\frac{1}{2}\cosh(\beta L_1)\,M_1\beta\sinh(\beta L_1)\Big)M_2\beta\cosh(\beta L_2)-\frac{1}{2}M_1\beta\cos(\beta L_1)^2+\frac{1}{2}\cosh(\beta L_1)\,M_1\beta\cos(\beta L_1)$$
$$-\frac{1}{2}M_2\beta\cos(\beta L_2)\left(\frac{1}{2}\cosh(\beta L_1)\,M_1\beta\cos(\beta L_1)-\frac{1}{2}M_1\beta\cosh(\beta L_1)^2\right)\sinh(\beta L_2)\Big)\sinh(\beta L_3)-\frac{1}{2}M_3\beta\left(\frac{1}{2}\cosh(\beta L_2)\left(1\right.\right.$$
$$+\frac{1}{2}\cos(\beta L_1)\,M_1\beta\sin(\beta L_1)-\frac{1}{2}\cosh(\beta L_1)\,M_1\beta\sin(\beta L_1)\Big)M_2\beta\cos(\beta L_2)+\frac{1}{2}\left(-1-\frac{1}{2}\sinh(\beta L_1)\,M_1\beta\cos(\beta L_1)\right.$$
$$+\frac{1}{2}\cosh(\beta L_1)\,M_1\beta\sinh(\beta L_1)\Big)M_2\beta\cosh(\beta L_2)^2+\frac{1}{2}\cosh(\beta L_1)\,M_1\beta\cos(\beta L_1)-\frac{1}{2}M_1\beta\cosh(\beta L_1)^2+\frac{1}{2}\cosh(\beta L_2)\left(\right.$$
$$-\frac{1}{2}M_1\beta\cos(\beta L_1)^2+\frac{1}{2}\cosh(\beta L_1)\,M_1\beta\cos(\beta L_1)\Big)M_2\beta\sin(\beta L_2)+\frac{1}{2}M_2\beta\cosh(\beta L_2)\left(\frac{1}{2}\cosh(\beta L_1)\,M_1\beta\cos(\beta L_1)\right.$$
$$-\frac{1}{2}M_1\beta\cosh(\beta L_1)^2\Big)\sinh(\beta L_2)\Big)\cosh(\beta L_3)^2-\frac{1}{2}\sinh(\beta L_2)\left(1+\frac{1}{2}\cos(\beta L_1)\,M_1\beta\sin(\beta L_1)\right.$$
$$-\frac{1}{2}\cosh(\beta L_1)\,M_1\beta\sin(\beta L_1)\Big)M_2\beta\cos(\beta L_2)-\frac{1}{2}\sinh(\beta L_2)\left(-1-\frac{1}{2}\sinh(\beta L_1)\,M_1\beta\cos(\beta L_1)\right.$$
$$+\frac{1}{2}\cosh(\beta L_1)\,M_1\beta\sinh(\beta L_1)\Big)M_2\beta\cosh(\beta L_2)-\frac{1}{2}\sinh(\beta L_2)\left(-\frac{1}{2}M_1\beta\cos(\beta L_1)^2+\frac{1}{2}\cosh(\beta L_1)\,M_1\beta\cos(\beta L_1)\right)\Big)M_2\beta\sin(\beta L_2)$$
$$-\frac{1}{2}M_2\beta\left(\frac{1}{2}\cosh(\beta L_1)\,M_1\beta\cos(\beta L_1)-\frac{1}{2}M_1\beta\cosh(\beta L_1)^2\right)\cosh(\beta L_2)^2-1-\frac{1}{2}\sinh(\beta L_1)\,M_1\beta\cos(\beta L_1)$$
$$+\frac{1}{2}\cosh(\beta L_1)\,M_1\beta\sinh(\beta L_1)+\frac{1}{2}M_2\beta\left(\frac{1}{2}\cosh(\beta L_1)\,M_1\beta\cos(\beta L_1)-\frac{1}{2}M_1\beta\cosh(\beta L_1)^2\right)+\frac{1}{2}M_3\beta\left(\frac{1}{2}\cosh(\beta L_2)\left(1\right.\right.$$
$$+\frac{1}{2}\cos(\beta L_1)\,M_1\beta\sin(\beta L_1)-\frac{1}{2}\cosh(\beta L_1)\,M_1\beta\sin(\beta L_1)\Big)M_2\beta\cos(\beta L_2)+\frac{1}{2}\left(-1-\frac{1}{2}\sinh(\beta L_1)\,M_1\beta\cos(\beta L_1)\right.$$
$$+\frac{1}{2}\cosh(\beta L_1)\,M_1\beta\sinh(\beta L_1)\Big)M_2\beta\cosh(\beta L_2)^2+\frac{1}{2}\cosh(\beta L_1)\,M_1\beta\cos(\beta L_1)-\frac{1}{2}M_1\beta\cosh(\beta L_1)^2+\frac{1}{2}\cosh(\beta L_2)\left(\right.$$
$$-\frac{1}{2}M_1\beta\cos(\beta L_1)^2+\frac{1}{2}\cosh(\beta L_1)\,M_1\beta\cos(\beta L_1)\Big)M_2\beta\sin(\beta L_2)+\frac{1}{2}M_2\beta\cosh(\beta L_2)\left(\frac{1}{2}\cosh(\beta L_1)\,M_1\beta\cos(\beta L_1)\right.$$
$$-\frac{1}{2}M_1\beta\cosh(\beta L_1)^2\Big)\sinh(\beta L_2)\Big)\Big)A+\left(-\frac{1}{2}M_3\beta\cos(\beta L_3)\left(\frac{1}{2}\left(-\frac{1}{2}\cos(\beta L_1)\,M_1\beta\sin(\beta L_1)+1\right.\right.\right.$$
$$+\frac{1}{2}\sinh(\beta L_1)\,M_1\beta\cos(\beta L_1)\Big)M_2\beta+\frac{1}{2}M_1\beta-\frac{1}{2}M_1\beta\cos(\beta L_1)^2-\frac{1}{2}\sinh(\beta L_1)\,M_1\beta\sin(\beta L_1)+\frac{1}{2}\sin(\beta L_2)\left(\frac{1}{2}M_1\beta\right.$$
$$-\frac{1}{2}M_1\beta\cos(\beta L_1)^2-\frac{1}{2}\sinh(\beta L_1)\,M_1\beta\sin(\beta L_1)\Big)M_2\beta\cos(\beta L_2)+\frac{1}{2}\sin(\beta L_2)\left(-\frac{1}{2}M_1\beta-\frac{1}{2}\sinh(\beta L_1)\,M_1\beta\sin(\beta L_1)\right.$$
$$+\frac{1}{2}M_1\beta\cosh(\beta L_1)^2\Big)M_2\beta\cosh(\beta L_2)-\frac{1}{2}\left(-\frac{1}{2}\cos(\beta L_1)\,M_1\beta\sin(\beta L_1)+1+\frac{1}{2}\sinh(\beta L_1)\,M_1\beta\cos(\beta L_1)\right)M_2\beta\cos(\beta L_2)^2$$
$$+\frac{1}{2}M_2\beta\sin(\beta L_2)\left(\frac{1}{2}\cosh(\beta L_1)\,M_1\beta\sin(\beta L_1)-1-\frac{1}{2}\cosh(\beta L_1)\,M_1\beta\sinh(\beta L_1)\right)\sinh(\beta L_2)\Big)\sinh(\beta L_3)-\frac{1}{2}M_3\beta\sin(\beta L_3)\left(\right.$$
$$-\frac{1}{2}\left(\frac{1}{2}M_1\beta-\frac{1}{2}M_1\beta\cos(\beta L_1)^2-\frac{1}{2}\sinh(\beta L_1)\,M_1\beta\sin(\beta L_1)\right)M_2\beta\cos(\beta L_2)^2-\frac{1}{2}\cos(\beta L_1)\,M_1\beta\sin(\beta L_1)+1$$
$$+\frac{1}{2}\sinh(\beta L_1)\,M_1\beta\cos(\beta L_1)-\frac{1}{2}\cos(\beta L_2)\left(-\frac{1}{2}\cos(\beta L_1)\,M_1\beta\sin(\beta L_1)+1+\frac{1}{2}\sinh(\beta L_1)\,M_1\beta\cos(\beta L_1)\right)M_2\beta\sin(\beta L_2)$$
$$-\frac{1}{2}M_2\beta\cos(\beta L_2)\left(\frac{1}{2}\cosh(\beta L_1)\,M_1\beta\sin(\beta L_1)-1-\frac{1}{2}\cosh(\beta L_1)\,M_1\beta\sinh(\beta L_1)\right)\sinh(\beta L_2)-\frac{1}{2}\cos(\beta L_2)\left(-\frac{1}{2}M_1\beta\right.$$
$$-\frac{1}{2}\sinh(\beta L_1)\,M_1\beta\sin(\beta L_1)+\frac{1}{2}M_1\beta\cosh(\beta L_1)^2\Big)M_2\beta\cosh(\beta L_2)\Big)\sinh(\beta L_3)-\frac{1}{2}\sinh(\beta L_2)\left(\frac{1}{2}M_1\beta-\frac{1}{2}M_1\beta\cos(\beta L_1)^2\right.$$
$$-\frac{1}{2}\sinh(\beta L_1)\,M_1\beta\sin(\beta L_1)\Big)M_2\beta\cos(\beta L_2)-\frac{1}{2}\sinh(\beta L_2)\left(-\frac{1}{2}\cos(\beta L_1)\,M_1\beta\sin(\beta L_1)+1\right.$$

$$+\frac{1}{2}\sinh(\beta L_1)\,M_1\beta\cos(\beta L_1)\Big)M_2\beta\sin(\beta L_2)-\frac{1}{2}M_1\beta-\frac{1}{2}\sinh(\beta L_1)\,M_1\beta\sin(\beta L_1)+\frac{1}{2}M_1\beta\cosh(\beta L_1)^2-\frac{1}{2}\sinh(\beta L_2)\Big($$
$$-\frac{1}{2}M_1\beta-\frac{1}{2}\sinh(\beta L_1)\,M_1\beta\sin(\beta L_1)+\frac{1}{2}M_1\beta\cosh(\beta L_1)^2\Big)M_2\beta\cosh(\beta L_2)+\frac{1}{2}M_2\beta\Big(\frac{1}{2}\cosh(\beta L_1)\,M_1\beta\sin(\beta L_1)-1$$
$$-\frac{1}{2}\cosh(\beta L_1)\,M_1\beta\sinh(\beta L_1)\Big)-\frac{1}{2}M_2\beta\Big(\frac{1}{2}\cosh(\beta L_1)\,M_1\beta\sin(\beta L_1)-1-\frac{1}{2}\cosh(\beta L_1)\,M_1\beta\sinh(\beta L_1)\Big)\cosh(\beta L_2)^2-\frac{1}{2}\Big($$
$$-\frac{1}{2}\sinh(\beta L_2)\Big(\frac{1}{2}M_1\beta-\frac{1}{2}M_1\beta\cos(\beta L_1)^2-\frac{1}{2}\sinh(\beta L_1)\,M_1\beta\sin(\beta L_1)\Big)M_2\beta\cos(\beta L_2)-\frac{1}{2}\sinh(\beta L_2)\Big($$
$$-\frac{1}{2}\cos(\beta L_1)\,M_1\beta\sin(\beta L_1)+1+\frac{1}{2}\sinh(\beta L_1)\,M_1\beta\cos(\beta L_1)\Big)M_2\beta\sin(\beta L_2)-\frac{1}{2}M_1\beta-\frac{1}{2}\sinh(\beta L_1)\,M_1\beta\sin(\beta L_1)$$
$$+\frac{1}{2}M_1\beta\cosh(\beta L_1)^2-\frac{1}{2}\sinh(\beta L_2)\Big(-\frac{1}{2}M_1\beta-\frac{1}{2}\sinh(\beta L_1)\,M_1\beta\sin(\beta L_1)+\frac{1}{2}M_1\beta\cosh(\beta L_1)^2\Big)M_2\beta\cosh(\beta L_2)$$
$$+\frac{1}{2}M_2\beta\Big(\frac{1}{2}\cosh(\beta L_1)\,M_1\beta\sin(\beta L_1)-1-\frac{1}{2}\cosh(\beta L_1)\,M_1\beta\sinh(\beta L_1)\Big)-\frac{1}{2}M_2\beta\Big(\frac{1}{2}\cosh(\beta L_1)\,M_1\beta\sin(\beta L_1)-1$$
$$-\frac{1}{2}\cosh(\beta L_1)\,M_1\beta\sinh(\beta L_1)\Big)\cosh(\beta L_2)^2\Big)\cosh(\beta L_3)\,M_3\beta\sinh(\beta L_3)+\frac{1}{2}M_3\beta\Big(\frac{1}{2}\cosh(\beta L_2)\Big(\frac{1}{2}M_1\beta-\frac{1}{2}M_1\beta\cos(\beta L_1)^2$$
$$-\frac{1}{2}\sinh(\beta L_1)\,M_1\beta\sin(\beta L_1)\Big)M_2\beta\cos(\beta L_2)+\frac{1}{2}\cosh(\beta L_2)\Big(-\frac{1}{2}\cos(\beta L_1)\,M_1\beta\sin(\beta L_1)+1$$
$$+\frac{1}{2}\sinh(\beta L_1)\,M_1\beta\cos(\beta L_1)\Big)M_2\beta\sin(\beta L_2)+\frac{1}{2}\cosh(\beta L_1)\,M_1\beta\sin(\beta L_1)-1-\frac{1}{2}\cosh(\beta L_1)\,M_1\beta\sinh(\beta L_1)+\frac{1}{2}\Big(-\frac{1}{2}M_1\beta$$
$$-\frac{1}{2}\sinh(\beta L_1)\,M_1\beta\sin(\beta L_1)+\frac{1}{2}M_1\beta\cosh(\beta L_1)^2\Big)M_2\beta\cosh(\beta L_2)^2+\frac{1}{2}M_2\beta\cosh(\beta L_2)\Big(\frac{1}{2}\cosh(\beta L_1)\,M_1\beta\sin(\beta L_1)-1$$
$$-\frac{1}{2}\cosh(\beta L_1)\,M_1\beta\sinh(\beta L_1)\Big)\sinh(\beta L_2)\Big)-\frac{1}{2}M_3\beta\Big(\frac{1}{2}\cosh(\beta L_2)\Big(\frac{1}{2}M_1\beta-\frac{1}{2}M_1\beta\cos(\beta L_1)^2$$
$$-\frac{1}{2}\sinh(\beta L_1)\,M_1\beta\sin(\beta L_1)\Big)M_2\beta\cos(\beta L_2)+\frac{1}{2}\cosh(\beta L_2)\Big(-\frac{1}{2}\cos(\beta L_1)\,M_1\beta\sin(\beta L_1)+1$$
$$+\frac{1}{2}\sinh(\beta L_1)\,M_1\beta\cos(\beta L_1)\Big)M_2\beta\sin(\beta L_2)+\frac{1}{2}\cosh(\beta L_1)\,M_1\beta\sin(\beta L_1)-1-\frac{1}{2}\cosh(\beta L_1)\,M_1\beta\sinh(\beta L_1)+\frac{1}{2}\Big(-\frac{1}{2}M_1\beta$$
$$-\frac{1}{2}\sinh(\beta L_1)\,M_1\beta\sin(\beta L_1)+\frac{1}{2}M_1\beta\cosh(\beta L_1)^2\Big)M_2\beta\cosh(\beta L_2)^2+\frac{1}{2}M_2\beta\cosh(\beta L_2)\Big(\frac{1}{2}\cosh(\beta L_1)\,M_1\beta\sin(\beta L_1)-1$$
$$-\frac{1}{2}\cosh(\beta L_1)\,M_1\beta\sinh(\beta L_1)\Big)\sinh(\beta L_2)\Big)\cosh(\beta L_3)^2\Big)B$$

$c_{16} =$

$$\left(\frac{1}{2} M_3 \beta \cos(\beta L_3) \left(\frac{1}{2} \sin(\beta L_2) \left(1+\frac{1}{2} \cos(\beta L_1) M_1 \beta \sin(\beta L_1)-\frac{1}{2} \cosh(\beta L_1) M_1 \beta \sin(\beta L_1)\right) M_2 \beta \cos(\beta L_2)+\frac{1}{2} \left(\right.\right.\right.$$
$$\left.\left.-\frac{1}{2} M_1 \beta \cos(\beta L_1)^2+\frac{1}{2} \cosh(\beta L_1) M_1 \beta \cos(\beta L_1)\right) M_2 \beta-\frac{1}{2} \left(-\frac{1}{2} M_1 \beta \cos(\beta L_1)^2+\frac{1}{2} \cosh(\beta L_1) M_1 \beta \cos(\beta L_1)\right) M_2 \beta \cos(\beta L_2)^2+1$$
$$+\frac{1}{2} \cos(\beta L_1) M_1 \beta \sin(\beta L_1)-\frac{1}{2} \cosh(\beta L_1) M_1 \beta \sin(\beta L_1)+\frac{1}{2} \sin(\beta L_2) \left(-1-\frac{1}{2} \sinh(\beta L_1) M_1 \beta \cos(\beta L_1)\right.$$
$$\left.+\frac{1}{2} \cosh(\beta L_1) M_1 \beta \sinh(\beta L_1)\right) M_2 \beta \cosh(\beta L_2)+\frac{1}{2} M_2 \beta \sin(\beta L_2) \left(\frac{1}{2} \cosh(\beta L_1) M_1 \beta \cos(\beta L_1)\right.$$
$$\left.-\frac{1}{2} M_1 \beta \cosh(\beta L_1)^2\right) \sinh(\beta L_2)\Big) \cosh(\beta L_3)+\frac{1}{2} M_3 \beta \cosh(\beta L_3)^2 \left(-\frac{1}{2} \sinh(\beta L_2) \left(1+\frac{1}{2} \cos(\beta L_1) M_1 \beta \sin(\beta L_1)\right.\right.$$
$$\left.-\frac{1}{2} \cosh(\beta L_1) M_1 \beta \sin(\beta L_1)\right) M_2 \beta \cos(\beta L_2)-\frac{1}{2} \sinh(\beta L_2) \left(-1-\frac{1}{2} \sinh(\beta L_1) M_1 \beta \cos(\beta L_1)\right.$$
$$\left.+\frac{1}{2} \cosh(\beta L_1) M_1 \beta \sinh(\beta L_1)\right) M_2 \beta \cosh(\beta L_2)-\frac{1}{2} \sinh(\beta L_2) \left(-\frac{1}{2} M_1 \beta \cos(\beta L_1)^2+\frac{1}{2} \cosh(\beta L_1) M_1 \beta \cos(\beta L_1)\right) M_2 \beta \sin(\beta L_2)$$
$$-\frac{1}{2} M_2 \beta \left(\frac{1}{2} \cosh(\beta L_1) M_1 \beta \cos(\beta L_1)-\frac{1}{2} M_1 \beta \cosh(\beta L_1)^2\right) \cosh(\beta L_2)^2-1-\frac{1}{2} \sinh(\beta L_1) M_1 \beta \cos(\beta L_1)$$
$$+\frac{1}{2} \cosh(\beta L_1) M_1 \beta \sinh(\beta L_1)+\frac{1}{2} M_2 \beta \left(\frac{1}{2} \cosh(\beta L_1) M_1 \beta \cos(\beta L_1)-\frac{1}{2} M_1 \beta \cosh(\beta L_1)^2\right)\Big)+\frac{1}{2} \cosh(\beta L_2) \left(1\right.$$
$$+\frac{1}{2} \cos(\beta L_1) M_1 \beta \sin(\beta L_1)-\frac{1}{2} \cosh(\beta L_1) M_1 \beta \sin(\beta L_1)\Big) M_2 \beta \cos(\beta L_2)+\frac{1}{2} \left(-1-\frac{1}{2} \sinh(\beta L_1) M_1 \beta \cos(\beta L_1)\right.$$
$$\left.+\frac{1}{2} \cosh(\beta L_1) M_1 \beta \sinh(\beta L_1)\right) M_2 \beta \cosh(\beta L_2)^2+\frac{1}{2} \cosh(\beta L_1) M_1 \beta \cos(\beta L_1)-\frac{1}{2} M_1 \beta \cosh(\beta L_1)^2+\frac{1}{2} \cosh(\beta L_2) \left(\right.$$
$$\left.-\frac{1}{2} M_1 \beta \cos(\beta L_1)^2+\frac{1}{2} \cosh(\beta L_1) M_1 \beta \cos(\beta L_1)\right) M_2 \beta \sin(\beta L_2)+\frac{1}{2} M_2 \beta \cosh(\beta L_2) \left(\frac{1}{2} \cosh(\beta L_1) M_1 \beta \cos(\beta L_1)\right.$$
$$\left.-\frac{1}{2} M_1 \beta \cosh(\beta L_1)^2\right) \sinh(\beta L_2)+\frac{1}{2} M_3 \beta \sin(\beta L_3) \left(-\frac{1}{2} \cos(\beta L_2) \left(-\frac{1}{2} M_1 \beta \cos(\beta L_1)^2\right.\right.$$
$$\left.+\frac{1}{2} \cosh(\beta L_1) M_1 \beta \cos(\beta L_1)\right) M_2 \beta \sin(\beta L_2)-\frac{1}{2} \left(1+\frac{1}{2} \cos(\beta L_1) M_1 \beta \sin(\beta L_1)-\frac{1}{2} \cosh(\beta L_1) M_1 \beta \sin(\beta L_1)\right) M_2 \beta \cos(\beta L_2)^2$$
$$-\frac{1}{2} \cos(\beta L_2) \left(-1-\frac{1}{2} \sinh(\beta L_1) M_1 \beta \cos(\beta L_1)+\frac{1}{2} \cosh(\beta L_1) M_1 \beta \sinh(\beta L_1)\right) M_2 \beta \cosh(\beta L_2)-\frac{1}{2} M_1 \beta \cos(\beta L_1)^2$$
$$+\frac{1}{2} \cosh(\beta L_1) M_1 \beta \cos(\beta L_1)-\frac{1}{2} M_2 \beta \cos(\beta L_2) \left(\frac{1}{2} \cosh(\beta L_1) M_1 \beta \cos(\beta L_1)-\frac{1}{2} M_1 \beta \cosh(\beta L_1)^2\right) \sinh(\beta L_2)\Big) \cosh(\beta L_3)$$
$$+\frac{1}{2} \left(\frac{1}{2} \cosh(\beta L_2) \left(1+\frac{1}{2} \cos(\beta L_1) M_1 \beta \sin(\beta L_1)-\frac{1}{2} \cosh(\beta L_1) M_1 \beta \sin(\beta L_1)\right) M_2 \beta \cos(\beta L_2)+\frac{1}{2} \left(-1\right.\right.$$
$$\left.-\frac{1}{2} \sinh(\beta L_1) M_1 \beta \cos(\beta L_1)+\frac{1}{2} \cosh(\beta L_1) M_1 \beta \sinh(\beta L_1)\right) M_2 \beta \cosh(\beta L_2)^2+\frac{1}{2} \cosh(\beta L_1) M_1 \beta \cos(\beta L_1)-\frac{1}{2} M_1 \beta \cosh(\beta L_1)^2$$
$$+\frac{1}{2} \cosh(\beta L_2) \left(-\frac{1}{2} M_1 \beta \cos(\beta L_1)^2+\frac{1}{2} \cosh(\beta L_1) M_1 \beta \cos(\beta L_1)\right) M_2 \beta \sin(\beta L_2)$$
$$\left.+\frac{1}{2} M_2 \beta \cosh(\beta L_2) \left(\frac{1}{2} \cosh(\beta L_1) M_1 \beta \cos(\beta L_1)-\frac{1}{2} M_1 \beta \cosh(\beta L_1)^2\right) \sinh(\beta L_2)\right) \cosh(\beta L_3) M_3 \beta \sinh(\beta L_3)\Big) A$$
$$+\left(\frac{1}{2} M_3 \beta \cos(\beta L_3) \left(\frac{1}{2} \left(-\frac{1}{2} \cos(\beta L_1) M_1 \beta \sin(\beta L_1)+1+\frac{1}{2} \sinh(\beta L_1) M_1 \beta \cos(\beta L_1)\right) M_2 \beta+\frac{1}{2} M_1 \beta-\frac{1}{2} M_1 \beta \cos(\beta L_1)^2\right.\right.$$
$$\left.-\frac{1}{2} \sinh(\beta L_1) M_1 \beta \sin(\beta L_1)+\frac{1}{2} \sin(\beta L_2) \left(\frac{1}{2} M_1 \beta-\frac{1}{2} M_1 \beta \cos(\beta L_1)^2-\frac{1}{2} \sinh(\beta L_1) M_1 \beta \sin(\beta L_1)\right) M_2 \beta \cos(\beta L_2)$$
$$+\frac{1}{2} \sin(\beta L_2) \left(-\frac{1}{2} M_1 \beta-\frac{1}{2} \sinh(\beta L_1) M_1 \beta \sin(\beta L_1)+\frac{1}{2} M_1 \beta \cosh(\beta L_1)^2\right) M_2 \beta \cosh(\beta L_2)-\frac{1}{2} \left(-\frac{1}{2} \cos(\beta L_1) M_1 \beta \sin(\beta L_1)+1\right.$$
$$\left.+\frac{1}{2} \sinh(\beta L_1) M_1 \beta \cos(\beta L_1)\right) M_2 \beta \cos(\beta L_2)^2+\frac{1}{2} M_2 \beta \sin(\beta L_2) \left(\frac{1}{2} \cosh(\beta L_1) M_1 \beta \sin(\beta L_1)-1\right.$$

$$-\frac{1}{2}\cosh(\beta L_1)\,M_1\,\beta\,\sinh(\beta L_1)\Big)\sinh(\beta L_2)\Big)\cosh(\beta L_3)+\frac{1}{2}M_3\,\beta\,\sin(\beta L_3)\left(-\frac{1}{2}\left(\frac{1}{2}M_1\,\beta-\frac{1}{2}M_1\,\beta\cos(\beta L_1)^2\right.\right.$$
$$-\frac{1}{2}\sinh(\beta L_1)\,M_1\,\beta\,\sin(\beta L_1)\Big)M_2\,\beta\cos(\beta L_2)^2-\frac{1}{2}\cos(\beta L_1)\,M_1\,\beta\,\sin(\beta L_1)+1+\frac{1}{2}\sinh(\beta L_1)\,M_1\,\beta\cos(\beta L_1)-\frac{1}{2}\cos(\beta L_2)\left(\right.$$
$$-\frac{1}{2}\cos(\beta L_1)\,M_1\,\beta\,\sin(\beta L_1)+1+\frac{1}{2}\sinh(\beta L_1)\,M_1\,\beta\cos(\beta L_1)\Big)M_2\,\beta\,\sin(\beta L_2)-\frac{1}{2}M_2\,\beta\cos(\beta L_2)\left(\frac{1}{2}\cosh(\beta L_1)\,M_1\,\beta\,\sin(\beta L_1)-1\right.$$
$$-\frac{1}{2}\cosh(\beta L_1)\,M_1\,\beta\,\sinh(\beta L_1)\Big)\sinh(\beta L_2)-\frac{1}{2}\cos(\beta L_2)\left(-\frac{1}{2}M_1\,\beta-\frac{1}{2}\sinh(\beta L_1)\,M_1\,\beta\,\sin(\beta L_1)\right.$$
$$+\frac{1}{2}M_1\,\beta\cosh(\beta L_1)^2\Big)M_2\,\beta\cosh(\beta L_2)\Big)\cosh(\beta L_3)+\frac{1}{2}\cosh(\beta L_2)\left(\frac{1}{2}M_1\,\beta-\frac{1}{2}M_1\,\beta\cos(\beta L_1)^2\right.$$
$$-\frac{1}{2}\sinh(\beta L_1)\,M_1\,\beta\,\sin(\beta L_1)\Big)M_2\,\beta\cos(\beta L_2)+\frac{1}{2}\cosh(\beta L_2)\left(-\frac{1}{2}\cos(\beta L_1)\,M_1\,\beta\,\sin(\beta L_1)+1\right.$$
$$+\frac{1}{2}\sinh(\beta L_1)\,M_1\,\beta\cos(\beta L_1)\Big)M_2\,\beta\,\sin(\beta L_2)+\frac{1}{2}\cosh(\beta L_1)\,M_1\,\beta\,\sin(\beta L_1)-1-\frac{1}{2}\cosh(\beta L_1)\,M_1\,\beta\,\sinh(\beta L_1)+\frac{1}{2}\left(-\frac{1}{2}M_1\,\beta\right.$$
$$-\frac{1}{2}\sinh(\beta L_1)\,M_1\,\beta\,\sin(\beta L_1)+\frac{1}{2}M_1\,\beta\cosh(\beta L_1)^2\Big)M_2\,\beta\cosh(\beta L_2)^2+\frac{1}{2}M_2\,\beta\cosh(\beta L_2)\left(\frac{1}{2}\cosh(\beta L_1)\,M_1\,\beta\,\sin(\beta L_1)-1\right.$$
$$-\frac{1}{2}\cosh(\beta L_1)\,M_1\,\beta\,\sinh(\beta L_1)\Big)\sinh(\beta L_2)+\frac{1}{2}M_3\,\beta\cosh(\beta L_3)^2\left(-\frac{1}{2}\sinh(\beta L_2)\left(\frac{1}{2}M_1\,\beta-\frac{1}{2}M_1\,\beta\cos(\beta L_1)^2\right.\right.$$
$$-\frac{1}{2}\sinh(\beta L_1)\,M_1\,\beta\,\sin(\beta L_1)\Big)M_2\,\beta\cos(\beta L_2)-\frac{1}{2}\sinh(\beta L_2)\left(-\frac{1}{2}\cos(\beta L_1)\,M_1\,\beta\,\sin(\beta L_1)+1\right.$$
$$+\frac{1}{2}\sinh(\beta L_1)\,M_1\,\beta\cos(\beta L_1)\Big)M_2\,\beta\,\sin(\beta L_2)-\frac{1}{2}M_1\,\beta-\frac{1}{2}\sinh(\beta L_1)\,M_1\,\beta\,\sin(\beta L_1)+\frac{1}{2}M_1\,\beta\cosh(\beta L_1)^2-\frac{1}{2}\sinh(\beta L_2)\left(\right.$$
$$-\frac{1}{2}M_1\,\beta-\frac{1}{2}\sinh(\beta L_1)\,M_1\,\beta\,\sin(\beta L_1)+\frac{1}{2}M_1\,\beta\cosh(\beta L_1)^2\Big)M_2\,\beta\cosh(\beta L_2)+\frac{1}{2}M_2\,\beta\left(\frac{1}{2}\cosh(\beta L_1)\,M_1\,\beta\,\sin(\beta L_1)-1\right.$$
$$-\frac{1}{2}\cosh(\beta L_1)\,M_1\,\beta\,\sinh(\beta L_1)\Big)-\frac{1}{2}M_2\,\beta\left(\frac{1}{2}\cosh(\beta L_1)\,M_1\,\beta\,\sin(\beta L_1)-1-\frac{1}{2}\cosh(\beta L_1)\,M_1\,\beta\,\sinh(\beta L_1)\right)\cosh(\beta L_2)^2\Big)$$
$$+\frac{1}{2}\left(\frac{1}{2}\cosh(\beta L_2)\left(\frac{1}{2}M_1\,\beta-\frac{1}{2}M_1\,\beta\cos(\beta L_1)^2-\frac{1}{2}\sinh(\beta L_1)\,M_1\,\beta\,\sin(\beta L_1)\right)M_2\,\beta\cos(\beta L_2)+\frac{1}{2}\cosh(\beta L_2)\left(\right.\right.$$
$$-\frac{1}{2}\cos(\beta L_1)\,M_1\,\beta\,\sin(\beta L_1)+1+\frac{1}{2}\sinh(\beta L_1)\,M_1\,\beta\cos(\beta L_1)\Big)M_2\,\beta\,\sin(\beta L_2)+\frac{1}{2}\cosh(\beta L_1)\,M_1\,\beta\,\sin(\beta L_1)-1$$
$$-\frac{1}{2}\cosh(\beta L_1)\,M_1\,\beta\,\sinh(\beta L_1)+\frac{1}{2}\left(-\frac{1}{2}M_1\,\beta-\frac{1}{2}\sinh(\beta L_1)\,M_1\,\beta\,\sin(\beta L_1)+\frac{1}{2}M_1\,\beta\cosh(\beta L_1)^2\right)M_2\,\beta\cosh(\beta L_2)^2$$
$$+\frac{1}{2}M_2\,\beta\cosh(\beta L_2)\left(\frac{1}{2}\cosh(\beta L_1)\,M_1\,\beta\,\sin(\beta L_1)-1-\frac{1}{2}\cosh(\beta L_1)\,M_1\,\beta\,\sinh(\beta L_1)\right)\sinh(\beta L_2)\Big)\cosh(\beta L_3)\,M_3\,\beta\,\sinh(\beta L_3)\Big)\,B$$

VITA

Name:	Yoon Mo Kim
Address:	Department of Civil Engineering Texas A&M University 3136 TAMU College Station, Texas 77843-3136
Email Address:	buffering98@gmail.com
Education:	B.S., Civil Engineering, Myong-ji University, Yong-in, Republic of Korea 2006 M.S., Civil Engineering, Texas A&M University, 2011